Confined Synthesis of Silicalite-1 in Nanoporous Polymer Templates

A THESIS

SUBMITTED TO THE FACULTY OF THE GRADUATE SCHOOL

OF THE UNIVERSITY OF MINNESOTA

BY

Aruna Ramkrishnan

IN PARTIAL FULFILLMENT OF THE REQUIREMENTS

FOR THE DEGREE OF

MASTER OF SCIENCE

Adviser: Prof. Michael Tsapatsis

Co-adviser: Prof. Marc Hillmyer

March, 2011

Acknowledgements

I sincerely thank my advisers Prof. Michael Tsapatsis and Prof. Marc Hillmyer for their guidance throughout this project. Their patience, encouragement and mentorship have taught me a lot. I am grateful to them for their inputs and support.

My colleagues in the Tsapatsis group have helped me immensely over the last two years. Rajiv, Sandeep, ChunYi, Bahman, Liz, Dongxia, Wei Fan, Jikku, Nafiseh and many other office and lab mates have made my research experience lively and enjoyable. Special thanks go to Sandeep Kumar and Xueyi Zhang for carrying out TEM imaging for my project. I would also like to thank the people who have collaborated with me at various points in this project – Brad Jones from the Lodge group and Louis Pitet from the Hillmyer group. Working with them has been an enriching experience. I would like to thank the NIRT team for technical inputs and suggestions and acknowledge NSF for the funding for this project.

I cannot thank my friends and family enough for their unconditional love and care. It is to them that I dedicate this work.

Dedication

To my family and friends

Abstract

The project goal is to achieve confined synthesis of zeolites in nanoporous polymers. Different research directions have been explored towards this goal in terms of both choice of a suitable polymer template and choice of a suitable zeolite synthesis method, until the correct conditions for confined synthesis of zeolite in nanoporous polymers were found. The main contributions of this body of work are:

(i) The stability of polymer thin films has been studied under zeolite synthesis conditions and the formation of sub-monolayers of a,b oriented Silicalite-1 crystals on a polymer thin film has been reported.

(ii) Confined synthesis of disordered, mesoporous Silicalite-1 has been demonstrated in a nanoporous linear polyethylene template.

(iii) Solvothermal synthesis methods have been explored using ethanol as a medium to synthesize Silicalite-1 for potential application to confined synthesis.

TABLE OF CONTENTS

List of Tables

List of Figures

1. INTRODUCTION

1.1 Overview and motivation

Zeolites are microporous aluminosilicates which have complex structures consisting of pore networks. Zeolites, by virtue of their ordered micropores, enable shape selective transformations in chemical reactions and consequently find application as catalysts for industrial reactions like cracking, oxidation, hydroisomerization, alkyation and esterification. Ordered microporosity also leads to very high surface areas for zeolites, increasing their effectiveness as catalysts. However, the micropores impose severe mass transfer constraints on the species involved in the reaction, decreasing the overall rate of catalysis.[1, 2] Therefore, it is important to develop ways to improve catalyst utilization during the chemical reactions. The degree of utilization of a catalyst can be characterized in terms of the effectiveness factor η, defined as the ratio of observed reaction rate to the theoretical rate in the absence of diffusion limitations. $\eta \rightarrow 1$ corresponds to maximum utilization of the catalyst. This can be achieved by decreasing the mass transfer limitation, i.e. by increasing the accessibility of the micropores and has been done in the past either by increasing the width of micropores or decreasing the diffusion path lengths.[1] However, wide pore zeolites are not a solution for those systems where specific microporosity is desired in the catalyst. 'Hierarchical' systems, on the other hand, aim to shorten diffusion path lengths by introducing additional mesopores within zeolite crystals while retaining the original micropores. Previous studies have experimentally established that mesoporosity causes significant improvement of diffusion

within catalysts, substantially increasing catalytic performance.[3] Figure 1 shows how mesopores affect the concentration profile of reactants and hence the overall reaction rate in zeolites. Mesoporous zeolites can be synthesized in a number of ways. Conventionally, dealumination has been done to introduce mesopores into zeolites. It involves treating the zeolite with steam at elevated temperatures to break aluminum-oxygen bonds and expel aluminum from the framework.[4] Newer methods that have developed are carbon templating[5] with carbon black, carbon fibers, nanotubes, and aerogels, desilication,[6] zeolite seed assembly, polymer templating,[7] etc. Currently, carbon templating appears to be the most practical and controllable method for making mesoporous zeolites. It also gives the highest pore volume (>1.0 mL/g).[3] Polymers are attractive choices as templates to synthesize mesoporous zeolite, primarily because they are industrially friendly materials in terms of processing and scale-up. Potentially, they can also be easily separated from zeolites by dissolution in organic solvents at low temperatures. This project aims to explore the potential of polymers for templating zeolites.

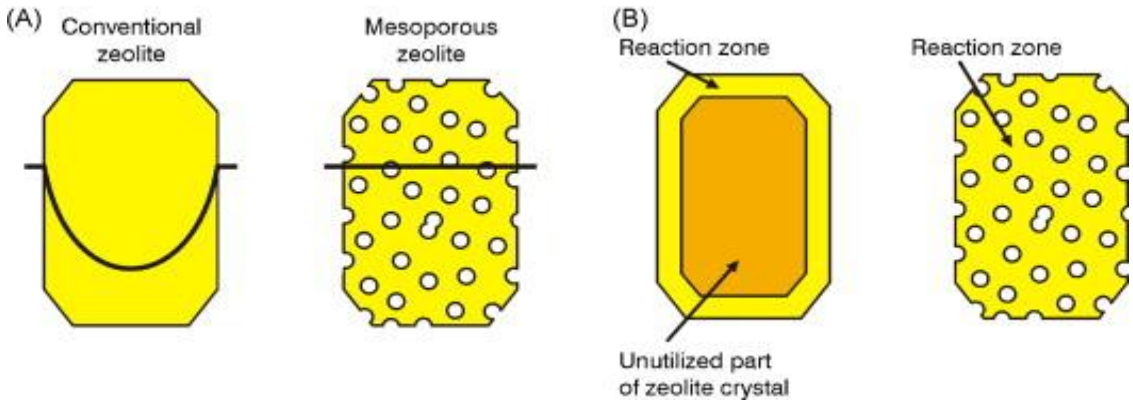

Figure 1: (a) Concentration profile of reactant and (b) Catalyst utilization for conventional vs mesoporous zeolites[8]

Zeolites are also called ‘molecular sieves’ due to their ability to sort molecules by physical size exclusion processes.[9] Therefore, apart from being used as catalysts, zeolite crystals have also been assembled into membranes in the industry, as they offer significant savings in energy expenditure for separation processes compared to alternative options like distillation, evaporation and crystallization, although their current use is limited.[10] Zeolite membranes were commercialized in the late 90’s, but for small-scale applications that utilized little membrane area.[11] Scale-up has been difficult due to high cost and low performance of membranes. Thus, it is important to overcome both performance and cost barriers in order to aid their commercialization. Selectivity and permeability of membranes can be improved by lowering membrane defects, improving pore orientation and decreasing membrane thickness. One way to satisfy these conditions is to synthesize well-faceted nano-sized zeolite crystals by confined synthesis and assemble them precisely in a way that preserves uniform orientation to form a seed layer that can be grown into ultra thin zeolite membranes, with thickness of the order of one hundred nanometers. Reduction in the size of zeolite crystals also increases the surface area to volume ratio, which improves zeolite activity for catalysis applications apart from decreasing diffusion path lengths which speed up separations processes.[12] Confined synthesis allows us to control both the size and shape of zeolite crystals. This means that there exist potential advantages from both catalysis and separations points of view for confined synthesis.

The primary goal of the project is to grow mesoporous zeolite with pores in the size range of 2-50 nm for use as catalysts. Mesopores enhance the transport of molecules to and from the active sites in the micropores of the zeolite, consequently improving the

speed of catalysis. Thus, a single material can couple the enhanced transport features of mesopores with the catalytic features of micropores. This makes mesoporous zeolites attractive catalysts for the industry. Confined synthesis is a route to synthesize well developed zeolite crystals of controlled size and porosity. Various templates have been used in the past for growing nanomaterials – carbon,[13, 14] inefficiently packed polymers,[15] surfactants,[16] colloids,[17] nanocasted porous metals, etc. These methods have been explained and compared in Table 1. A more detailed analysis of the choice of polymer template has been done later. Of these templates, carbon is the only one that has successfully been used to synthesize both monodisperse and nanosized zeolites. However, industrial scale-up of the carbon templating method might be infeasible because of high costs of processing and difficulty in attaining the correct morphology and purity. Hence, alternative templates should be explored to overcome these disadvantages. For this project, polymeric materials have been chosen to aid the process of nanozeolite synthesis by acting as an inert matrix or templating material due to the following advantages– (i) Chemical inertness at zeolite synthesis conditions, (ii) Better recoverability and recycling potential compared to materials like carbon (e.g., one can use a solvent to dissolve away the polymer matrix and recover the polymer from the solvent for reuse) and (iii) Low processing costs.

Table 4: Confined synthesis inside porous materials

Template Used	Material Synthesized	Advantages	Disadvantages
Three dimensionally ordered mesoporous carbon[18] 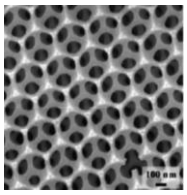	Inorganic crystals like zinc oxide, zeolites.	Very monodisperse particles obtained. Sizes are tunable by selection of appropriate colloidal crystal template.	Template synthesis scale-up issues. Chemical treatment of carbon is required to make it hydrophilic.
Surfactants[16] 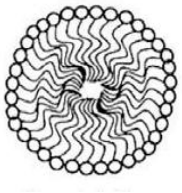	Ordered inorganic mesoporous materials like MCM-41.	Low mesopore sizes (5-20 nm) can be attained. Sizes are tunable.	Thin pore walls in decrease overall stability.
Colloids[17] 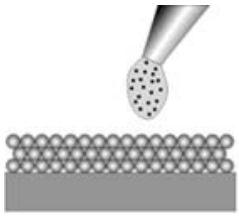	Nanoporous materials including organic, inorganic, and metallic compounds.	High, ordered porosity can be achieved. Porosity can be tuned by changing crystal size.	Low chemical and hydrothermal stability due to thin pore walls.

Inefficiently packed polymers[19] 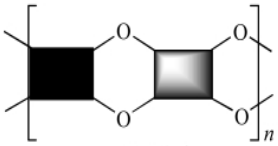 PIM 1-6	Polymers of intrinsic microporosity (PIMs) have been used to template organic nanoporous materials.	Robust, solution processable.	Only micropores can be obtained by this method.
Ordered block copolymers[20] 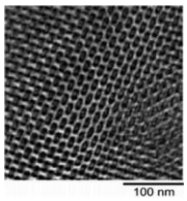	Polymers, organics, inorganic crystals like zinc oxide.	Controllable, monodisperse pores can be obtained.	Pores are often isolated, not interconnected.
Gyroid[21] 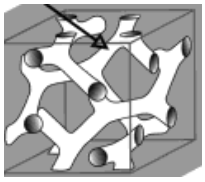	Inorganic nanoparticles.	Pores are reasonably monodisperse and bicontinuous and are tunable in the mesoporous range.	Gyroid morphology is obtained in a small composition window that's experimentally challenging to achieve.
Polymer aerogels[22] 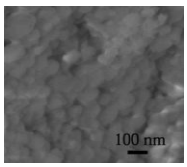	Zeolites and other inorganic materials.	Pores are in the mesoporous range. Aerogel is easy to synthesize.	Has bimodal pore size distribution.

Polymeric bicontinuous microemulsions[20] 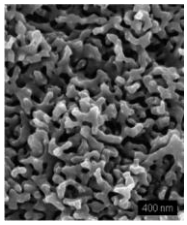	Nanoporous ceramics, inverse polymer templates.	Very high degree of bicontinuity present. Pore sizes tunable from 10-100 nm.	Narrow composition window for this morphology.

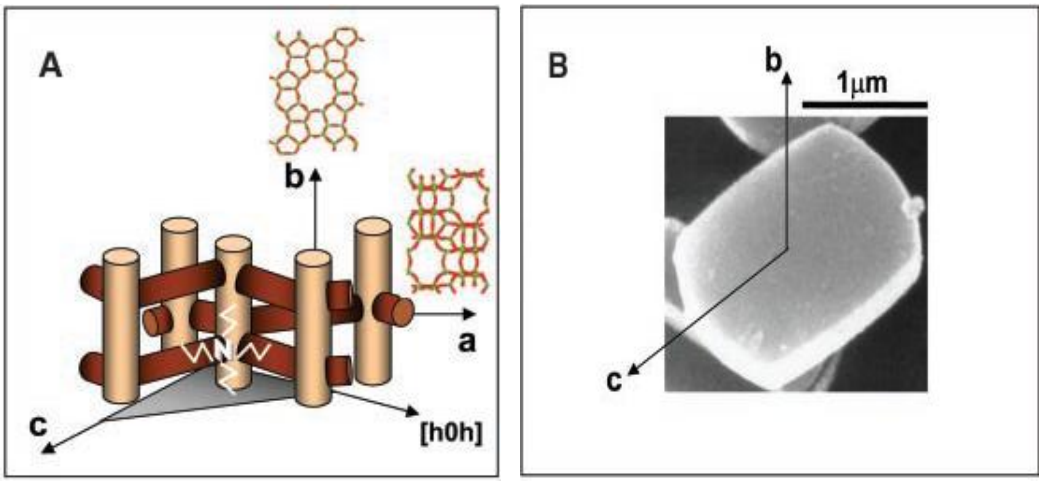

Figure 2: (a) MFI framework (b) Typical MFI crystal[23]

Different zeolites have different pore and channel structures collectively called 'frameworks'. Of these, the MFI framework (Figure 2) is important because the pore size is close to that of important organic molecules like xylene, which is used as a solvent and starting material for the synthesis of a wide range of chemicals.[23] The all-silica zeolite with an MFI framework, Siliceous ZSM-5, also called Silicalite-1, has been chosen as the zeolite to be synthesized and studied. This is because Silicalite-1 is of immense importance both as a model system and in the industry. For example, it is used in the separation of *p*-xylene from its *o*- and *m*- isomers (which have large kinetic diameters and

are rejected by the zeolite pores).[24] In addition, it is a chemically and structurally robust zeolite and is stable under many harsh conditions. Once confined synthesis methods are successfully developed for Silicalite-1, they can subsequently be extended to synthesize other zeolites.

1.2 Previous Work

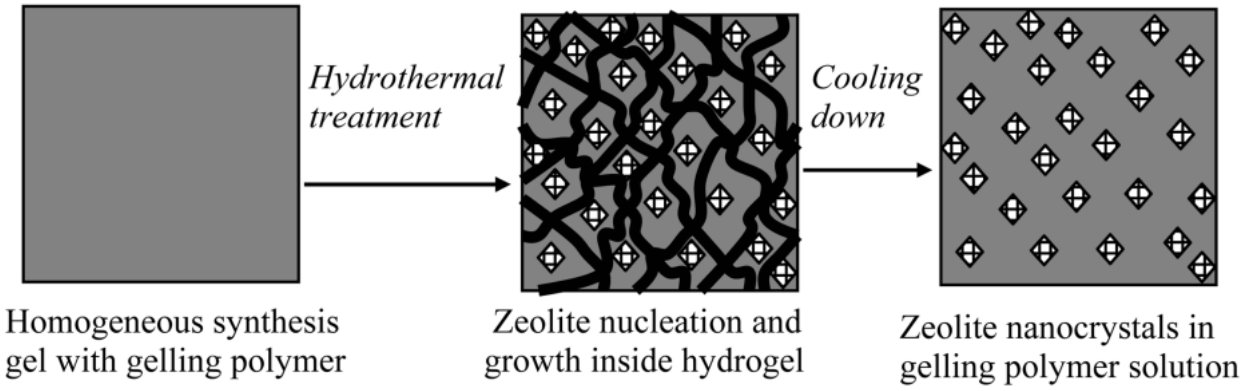

Figure 3: Schematic of confined synthesis of zeolite inside hydrogel[25]

In 2003, Wang et al.[25] developed a route to synthesize zeolite nanocrystals using crosslinked thermoreversible polymer hydrogels as space confining nanoreactors. The hydrogel, being temperature sensitive, can be made water soluble below certain temperatures making crystal recovery possible.[25] While it is a novel method for confined synthesis, this procedure does not give either a mesoporous or monodisperse yield of crystals. Moreover, the crystals are fairly large and of the order of 120 nm. This size range coupled with the lack of monodispersity makes the nanocrystals so obtained unsuitable for fabrication of thin membranes. No other literature on templating zeolites nanocrystals with a polymer matrix for confined synthesis was available.

At the beginning of the project, confined growth of zeolites had been demonstrated in porous three dimensionally oriented macroporous (3DOM) carbon materials and attempts were made by our groups to adapt these methods to grow zeolite in the confined spaces of porous plastics. The most suitable candidate was derived from PS-PDMA-PLA (Polystyrene-Poly(dimethylacrylate)-Poly(lactic acid)) block copolymers. Alignment of poreswas achieved with a channel die and subsequent etching of the PLA yielded porous polystyrene, where the pores were coated with PDMA. This coating made the pores hydrophilic, which was useful for taking up the aqueous solutions used to prepare zeolites. Porous PS monoliths, with and without PDMA lining the pores, are useful for templating nanomaterials largely because of the ease in altering the pore wall chemistry and the ability to remove the PS template by using an appropriate solvent. Once a general protocol was established for zeolite synthesis, variables like pore size, pore geometry and pore wall chemistry were investigated in terms of their effect on confined zeolite growth. Unfortunately, confined growth of zeolite in nanoporous polystyrene was not obtained and two hypotheses were proposed to explain this observation: 1) chemical incompatibility between the PS-PDMA monoliths and the synthesis conditions used for zeolite growth and 2) zeolite growth must occur at a temperature below the glass transition temperature (T_g) of PS to avoid pore collapse. It is possible that the kinetics of confined growth at the temperatures used in this study were too slow to observe growth in nanoscale pores. These hypotheses were significant because they implied that confined growth was possible using a different porous plastic with a higher T_g and different chemical composition. (For more details on work with the PS monoliths, refer to the post-doctoral report by Eric Todd.)

1.3 Thesis overview by chapter

Different research directions were explored in this project in terms of both choice of a suitable template and choice of a suitable synthesis method, until the correct conditions for confined synthesis of zeolite in nanoporous polymers were found. These efforts have been summarized in the following chapters.

Chapter 2

In this chapter, the motivation for using porous polymer thin films for confined synthesis of zeolites is discussed. The choice of an appropriate polymer and methods to make and characterize polymer thin films are discussed. Efforts towards making robust polymer thin films that are stable in zeolite synthesis conditions are summarized. These include changing the composition of zeolite synthesis solution, changing the temperature of zeolite synthesis, improving adhesion of polymer thin film by chemical modification of the substrate and changing the substrate. A difference in the adhesion of zeolite crystals to two different substrates – silicon and silicon nitride, is observed. This observation could be valuable because it can be applied to create sub-monolayers of zeolite seeds which can subsequently be grown into zeolite membranes. The difficulty in reproducibly creating stable polymer thin films is discussed and a rationale provided for the observed film delamination. Alternative methods to use thin films for confined synthesis are proposed.

Chapter 3

In this chapter, the motivation for switching to porous polymer monoliths is first explained. Pore geometry is an important consideration for confined synthesis which has

not been explored in detail in previous work. Polymer monoliths with highly interconnected, bicontinuous pores were tested for confined synthesis of zeolite, in contrast to most of the work done earlier, which focused on using cylindrical isolated pores in a polystyrene matrix for confined synthesis. Bicontinuous nanoporous polyethylene derived from a bicontinuous microemulsion was first tested. It was found that steaming led to the collapse of the nanopores. However, macropores were preserved and confined synthesis of zeolite was observed in them. Linear polyethylene (LPE), a more thermally stable material, was then used to test for confined synthesis of zeolite. The nanopores didn't collapse and successful confined synthesis of mesoporous zeolite in LPE was attained. The results of confined synthesis along with their implications have been discussed.

Chapter 4

In this chapter, alternate zeolite syntheses techniques that use non-aqueous media, called solvothermal synthesis methods are explored. These methods could be useful because they could facilitate confined synthesis of zeolites in hydrophobic templates due to improved wetting of the pores by choice of a solvent of appropriate hydrophobicity. A modified recipe for microwave assisted synthesis of MFI in ethanol solvent has been developed. Preliminary results for confined synthesis of MFI in LPE are discussed. Directions for future work have been proposed.

Chapter 5

In this chapter, conclusions and future prospects for confined synthesis of zeolites in polymers have been discussed. Future directions include selection of new templates,

use of different synthesis methods and alternate applications of confined synthesis for zeolites and zeotypes in the future.

2. Zeolite synthesis by polymer thin film route

2.1 Introduction and motivation

The observation (from previous work) that zeolites did not crystallize in the pores of the PS monolith led to consideration of alternative pathways for zeolite synthesis. It was hypothesized that reducing the diffusion path length and using a polymer with a high T_g would solve the problems suggested in the previous section, if indeed these were the reasons for failure of synthesis. The following thin film route was proposed (Refer to Figure 4):

1. Create a nano-patterned thin film of polymer on the surface of Si wafer.
2. Immerse the film in a solution containing the Structure Directing Agent (Tetrapropyl ammonium hydroxide or TPAOH) at a temperature high enough for zeolite synthesis but below the T_g of the polymer.
3. Synthesize zeolite in the confined patterns of the polymer film followed by recovery of the zeolite nanocrystals by dissolution of polymer in an organic solvent.

It was expected that the portions of the Si wafer that were exposed to the TPAOH solution would act as silica sources for the synthesis of Silicalite-1 and that areas that were shielded by the polymer thin film would be inert to the Structure Directing Agent

(SDA) solution. Thus, it was expected that MFI crystals would grow only in the exposed regions and that the crystal geometry would match the nanopattern in the polymer film.

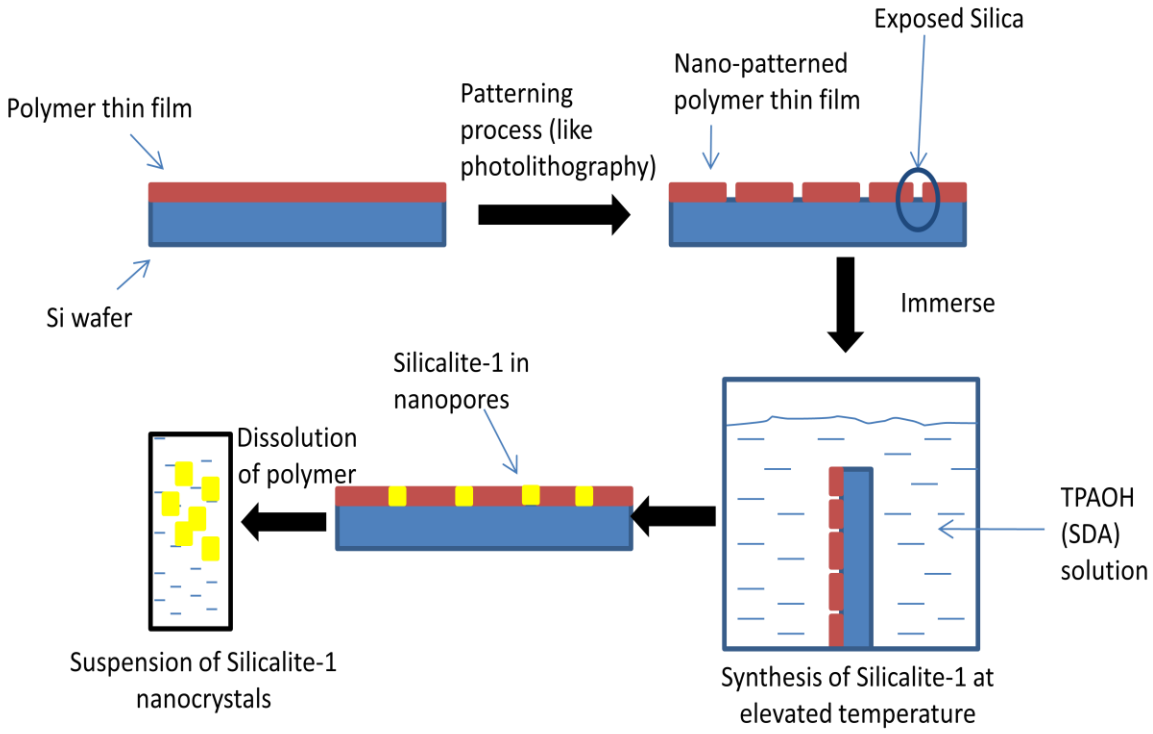

Figure 4: Suggested process to synthesize Silicalite-1 nanocrystals by confined synthesis within nano-patterned polymer thin film

2.2 Results and Discussion

This section discusses the selection of an appropriate polymer for the polymer thin film, experiments to test its stability in zeolite synthesis solution, and efforts to make the film robust under these conditions.

2.2.1 Making polymer thin films

The polymer used for coating silica wafer with a thin film should have certain properties that make it compatible with the relatively harsh conditions employed for zeolite synthesis. Some of these are – it should be inert to basic conditions (as zeolite synthesis occurs at high pH), should have a relatively high glass transition temperature (T_g) - preferably above 100 °C, as reaction kinetics slows down considerably at lower temperatures; and should preferably be soluble in a solvent at room temperature for easy recovery. Polycyclohexylethylene (PCHE) is a polymer formed by hydrogenation of polystyrene (PS) and meets all the requirements mentioned above. It has a high T_g of 145 °C, is inert to most chemicals and is resistant to oxidation. In addition, PCHE-PLA block copolymers can be spin-coated and PLA etched to give rise to nano-patterned thin films consisting of nano-sized cylindrical voids in a PCHE thin film. These material properties and the patternability of PCHE makes it a good choice for making a polymer thin film. For the preliminary experiments, PCHE thin films were spin coated onto a Si wafer (coated with a 250 nm thermally grown SiO_2 layer). This was done at 2000 rpm by a 'drop and spin' technique using a PCHE solution with a concentration of 15mg/mL.

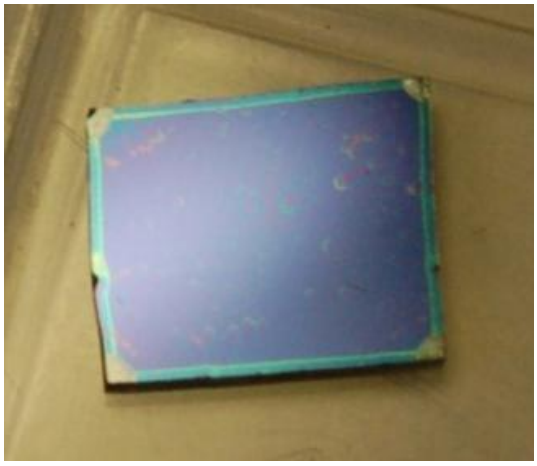

Figure 5: Photograph of a silicon wafer coated with a relatively uniform PCHE thin film

The polymer film thickness is dependent on concentration of the polymer solution and not on the amount of solution used in spin coating. This can be seen from the following data. As the number of drops of polymer solution put on a spinning wafer is increased, the thickness does not increase linearly. It increases to a small extent.

Table 5: Film thickness dependence on number of drops added

Run #	Thickness (1 drop)	Thickness (2 drops)	Thickness (3 drops)
1	67 ± 6 nm	68.1 ± 0.8 nm	74.8 ± 1.3 nm
2	59.9 ± 5.1 nm	55.1 ± 5.8 nm	76.5 ± 2.4 nm
3	62.9 ± 6.4 nm		

As a first step, the polymer film required to be characterized by several methods to determine its thickness before it was used in experiments. Some methods are listed below.

Contact Angle Measurements: The PCHE film gives a higher contact angle than the silica surface due to its hydrophobicity (Figure 6) and offers an easy way to detect presence of the PCHE layer.

(a)  **(b)** 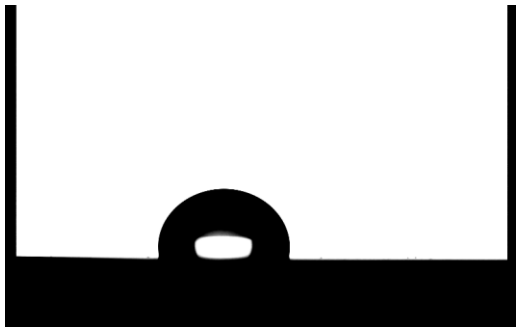

Figure 6: (a) Contact angle of water on Si wafer is about 60° (b) On coating a PCHE film, the contact angle increases to about 100°

Other methods described below give quantitative measurements of thickness.

1. *Ellipsometry:* The Cauchy Model, usually used for polymer thin films, was used for fitting the curves for the polarization angles. An isotropic polymer film atop a silica layer was assumed. A normal fit gave the film thickness as about 59.5 nm at 2000 rpm spin coating speed and 15mg/mL concentration of PCHE in chlorobenzene. (See data in Appendix A1.)
2. *Grazing Incidence X-Ray (GIXR) diffraction:* GIXR diffraction is a process by which an interference pattern can be generated by the interaction of X-rays with thin films. By analyzing the pattern, it is possible to calculate the film thickness. The PCHE film was found to have a thickness of 54.5 nm using this technique.

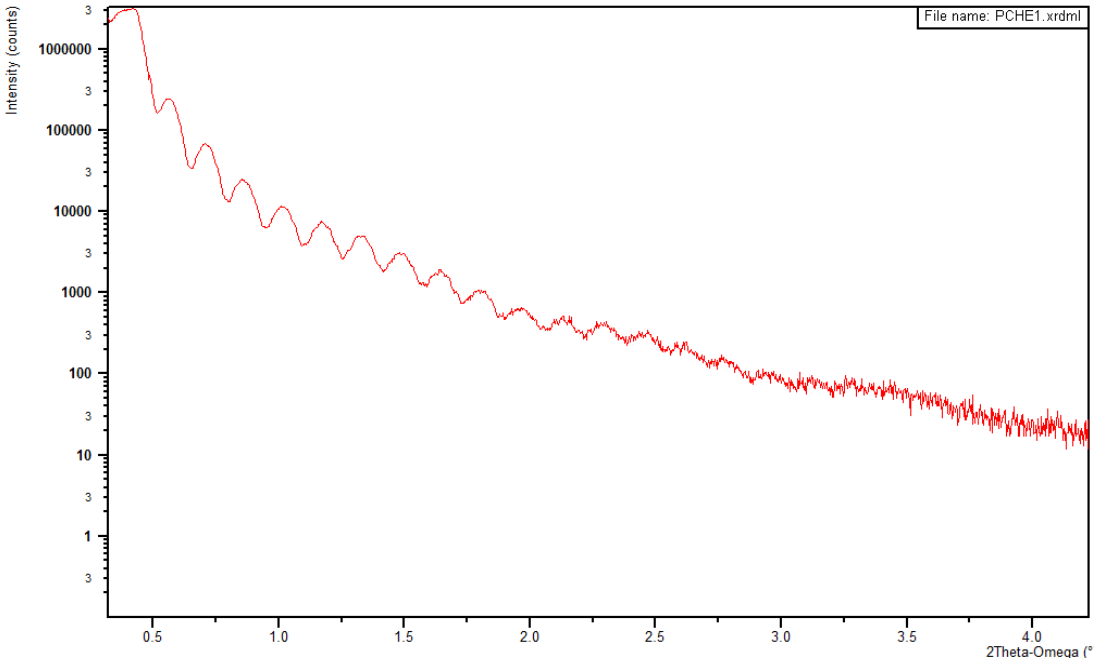

Figure 7: GIXR data for PCHE film

Atomic Force Microscopy (AFM): AFM was used to determine the depth of a scratch made on the PCHE film surface. The film thickness was thus determined to be 60.2 nm.

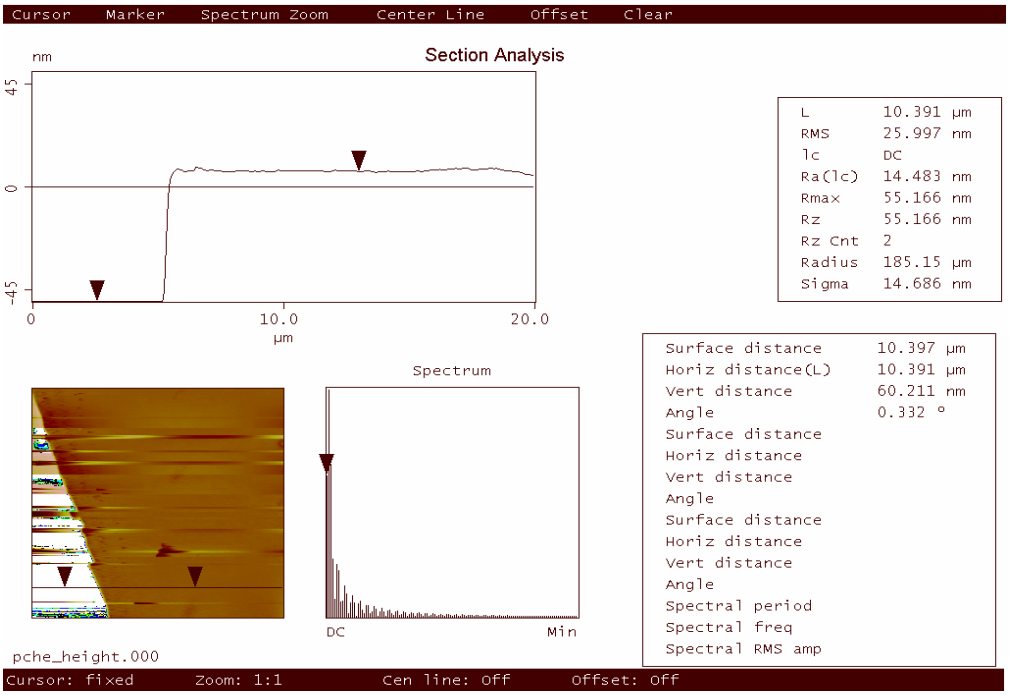

Figure 8: AFM image showing PCHE film thickness

3. *IR Reflectance:* The presence of multiple peaks in the IR spectrum indicates the presence of thin films, however, the silica layer present between the silicon wafer and the polymer film is also IR-transparent, which makes it a system of two thin films on top of each other, which is difficult to analytically analyze to calculate the polymer thin film thickness.

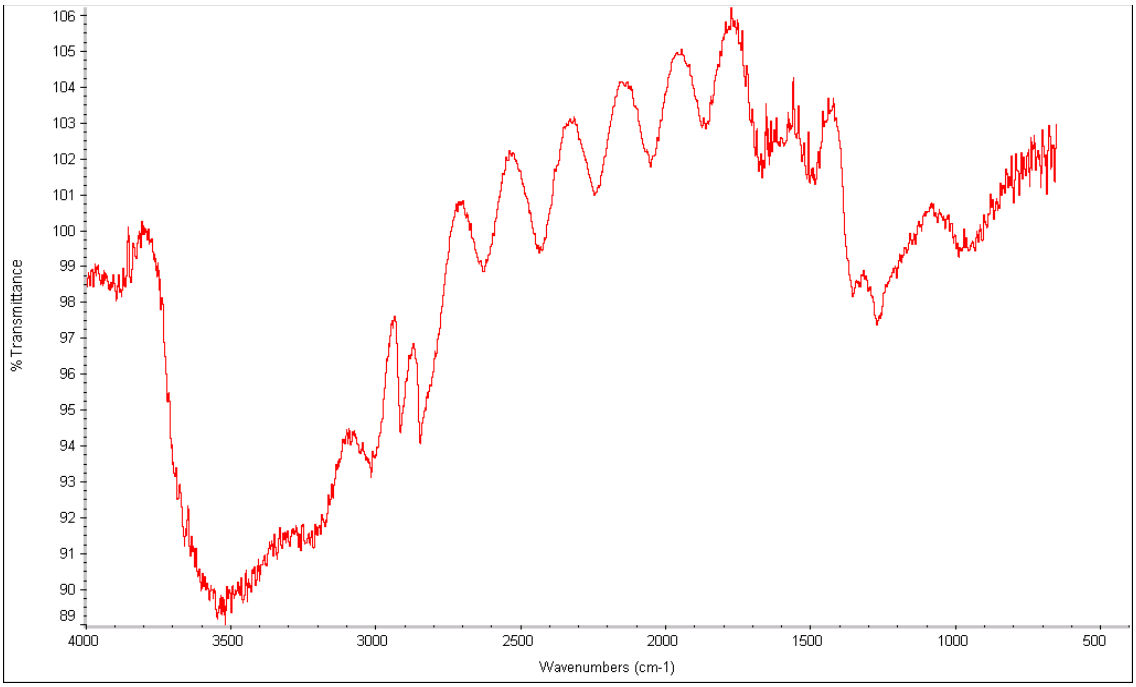

Figure 9: IR reflectance spectrum shows the presence of multiple thin films - silica and PCHE

Thus, different methods validated the thickness of the PCHE thin film to be approximately 60 nm.

2.2.2 Instability of polymer thin film in zeolite synthesis solution

Once the film thickness was established, the next step was to test the thin film for stability under the zeolite synthesis conditions. A wide range of conditions can be employed for zeolite synthesis. Jansen and Rosmalen provided conditions under which b-oriented MFI crystals (with the b-axis perpendicular to the substrate) could be grown on a

silicon substrate.[26] These were taken as the starting point for zeolite synthesis. The 'Jansen experiments' were used as a control and hydrothermal synthesis was done with a solution composition 139.6 SiO_2: 39.4 TPAOH: 558.3 EtOH: 16800 H_20 with a bare silicon wafer (1 cm x 1cm) placed vertically in the solution. The results are given below:

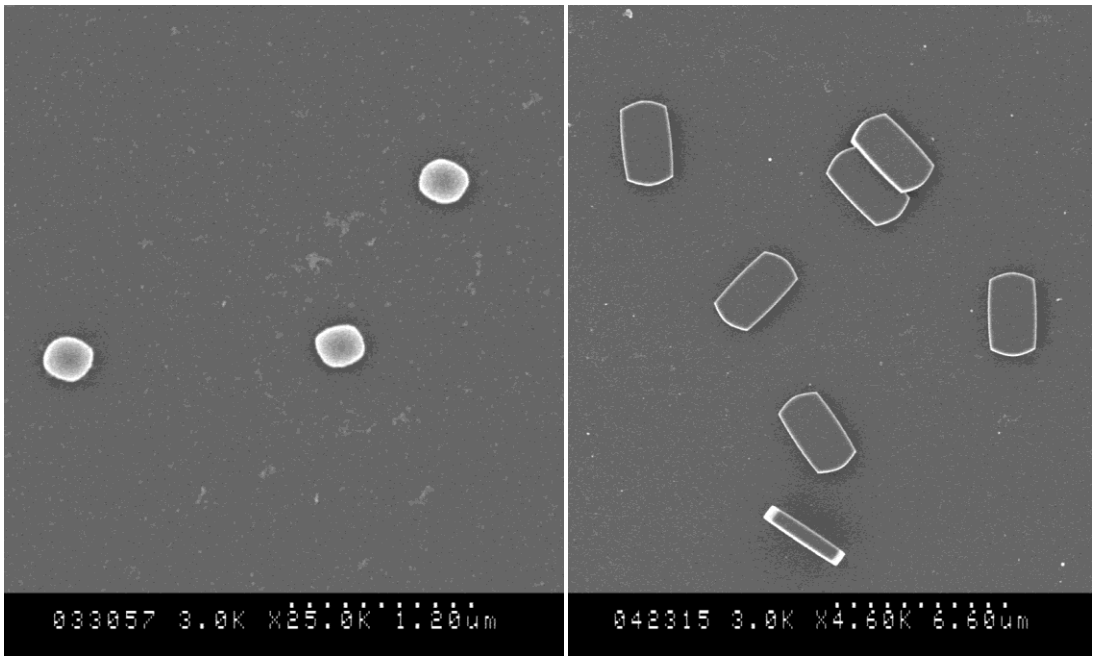

Figure 10: Silicon wafer surface after hydrothermal synthesis at 160 C for 1.5 and 3 hours

Next, the silicon wafer (now coated with PCHE thin film) was supported vertically in the synthesis solution (0.167M TPAOH), in a teflon liner, placed in an autoclave and subjected to hydrothermal synthesis at 125 °C. Multiple samples were prepared and monitored over different lengths of time ranging from 2 to 12 hours. However, film delamination was observed at times exceeding 2 hours (Figure 11). The temperature and concentrations were changed and it was observed that as temperature was decreased or pH was increased, the polymer film stayed on for longer.

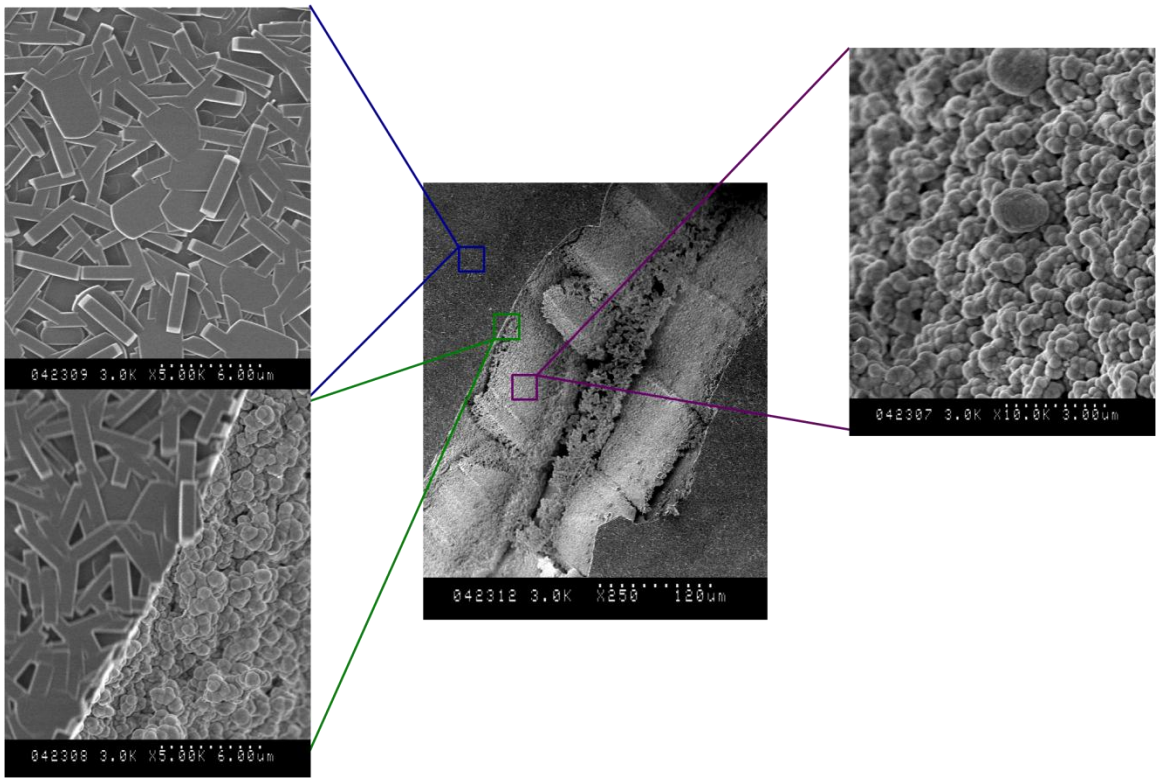

Figure 11: Hydrothermal synthesis done in the presence of a PCHE thin film on a silicon wafer. A scratch was made on the film prior to the synthesis to investigate the relative effects on silica and PCHE surfaces

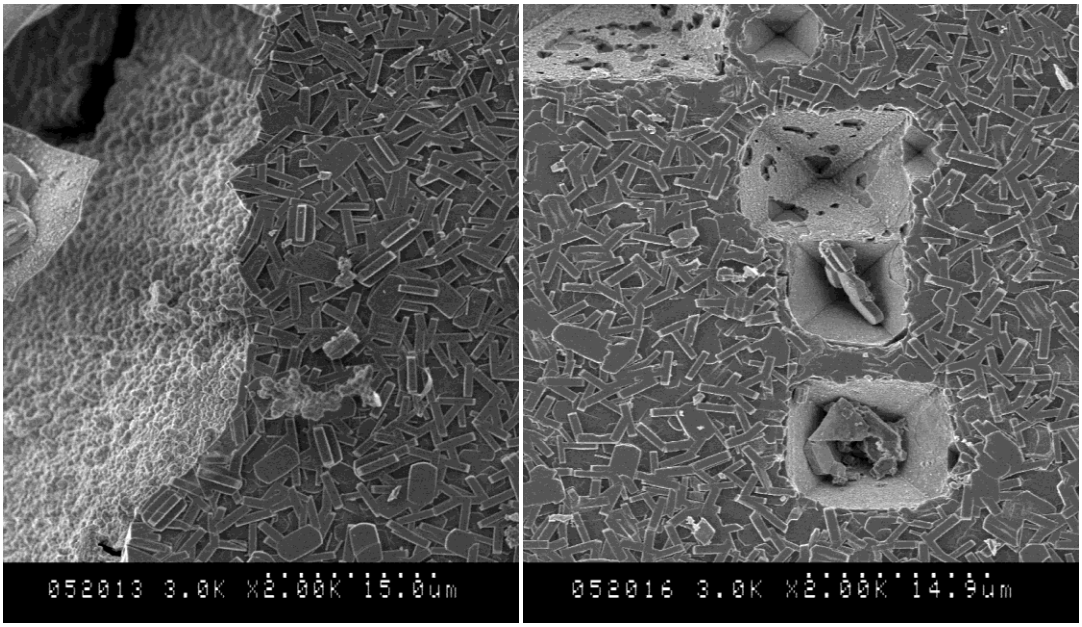

Figure 12: (A) After calcination to remove PCHE fim (C) Sonication of wafer in $CDCl_3$ reveals etched silicon wafer under the MFI crystals

(A) 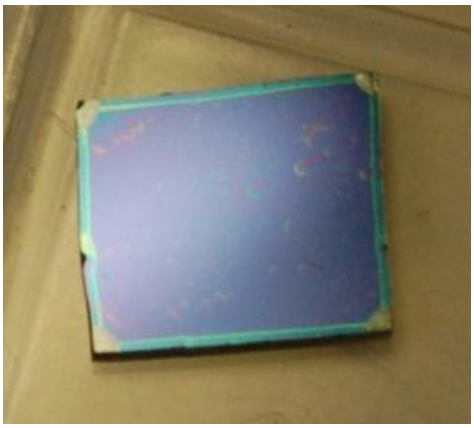 (B) 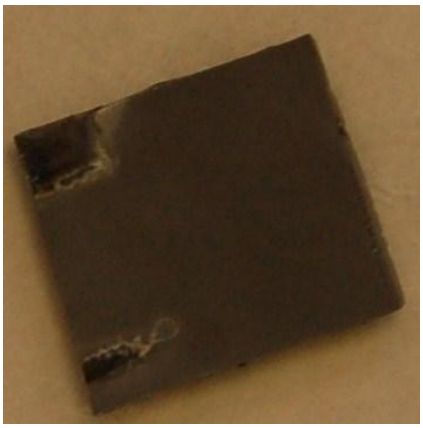

Figure 13: (A) Freshly prepared PCHE thin film on silica wafer (B) PCHE thin film delaminates after it is kept in a TPAOH (0.167M) solution for 2.5 hours

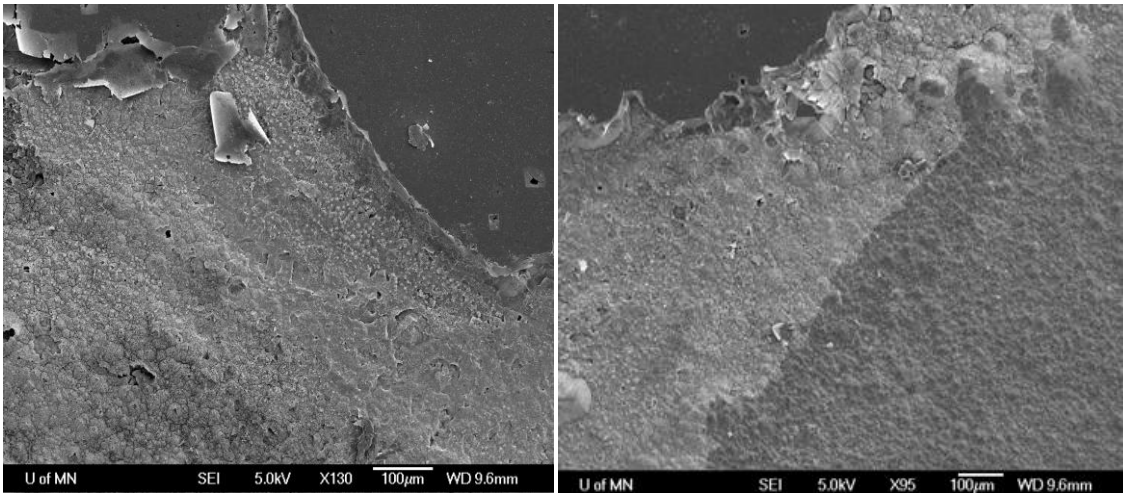

Figure 14: Delamination of PCHE thin film and etching of silicon wafer after exposure to zeolite synthesis solution for 2.5 hours

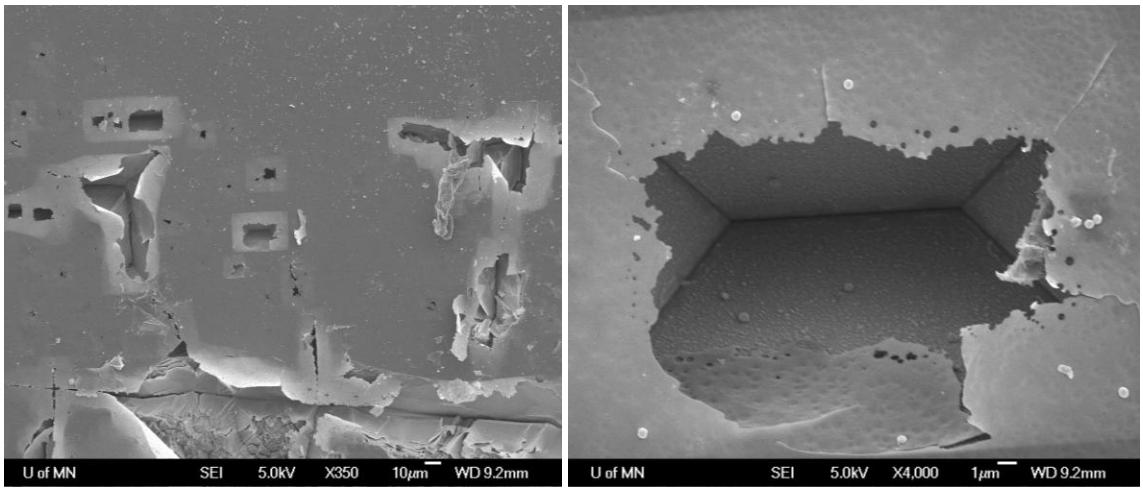

Figure 15: Coated wafers subjected to Jansen conditions at 125 C without silica source for 2.5 hours. Etched Si surface is clearly seen

The instability of the polymer thin films can be rationalized by considering the two processes running in parallel:

a. Delamination of the polymer thin film from the silica surface.
b. Growth of Silicalite-1 crystals in the synthesis solution by consumption of silica from the solution or from the silicon wafer.

The amount of time taken by each of the processes described above is independent of the other. For the proposed thin film technique (Figure 4) to succeed, we require to optimize the processes such that the timescale for the growth of crystals is smaller than the timescale for polymer film delamination. These timescales can be controlled by changing the zeolite synthesis conditions. However, while lower temperatures and pH increase the film's life, they also slow down the kinetics of crystal growth. Thus, it was observed that even under mild conditions, the time for which the film stayed on was not enough for crystals to grow in solution, due to slow growth kinetics under these conditions.

2.2.3 Efforts to prevent delamination

Some efforts made to increase the film life are listed below:

a. The film was annealed at 220 °C for 15 hours to improve its mechanical integrity prior to hydrothermal synthesis. This was done to heal nano-sized cracks present in freshly coated films. However, the cracks stayed and the resulting film also delaminated in a standard hydrothermal solution.

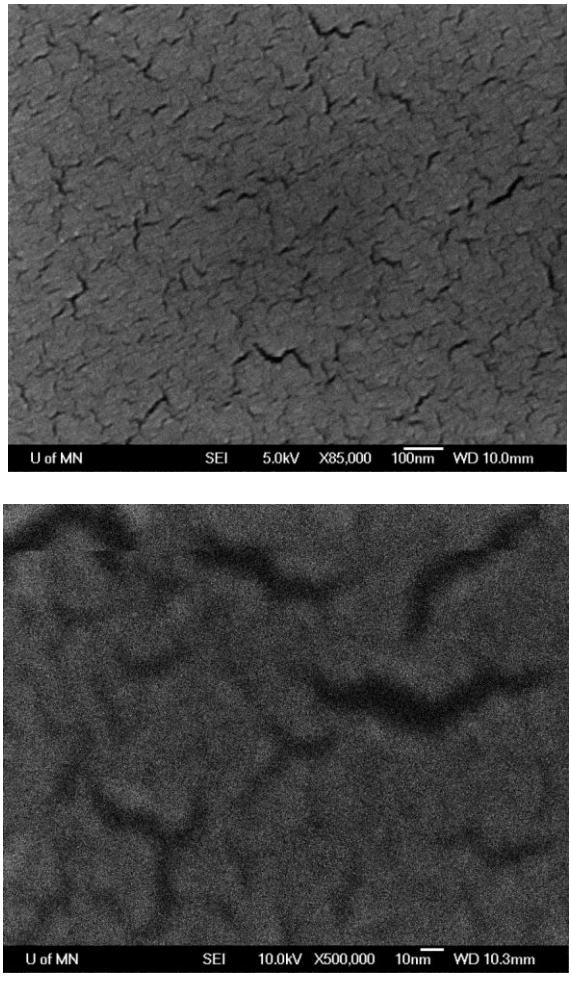

Figure 16: (a) Freshly coated PCHE film has cracks about 5-10 nm wide which could be causing its low adhesion to the silicon substrate (b) Cracks are present even after annealing

b. Film thickness was increased by about 50% by increasing the concentration of the polymer solution used for spin coating. It was observed that this did not in any way, affect the delamination time in a standard hydrothermal solution.

c. Si wafer surface was functionalized with HMDS (hexamethyldisilazane) prior to spin coating the PCHE film to modify the surface energy and make it hydrophobic to improve its adherence with the PCHE film (also hydrophobic). The process is outlined below:

    - Cleaning of Si wafers by sonication in EtOH for 30 minutes.
    - Hydroxylation of Si surface with piranha solution ~30mins.
    - Functionalization with HMDS (0.5% in dry toluene) for ~16 hours.
    - Thin films were spun on the functionalized wafers by 'drop and spin' method 12k PCHE in a solution of concentration 15mg/mL, spun at 2000 rpm.

    At the end of the functionalization, the wafer surface was hydrophobic. A drop of water when placed on the wafer did not spread out but formed beads instead. However, PCHE films coated on these surfaces still peeled off under hydrothermal conditions.

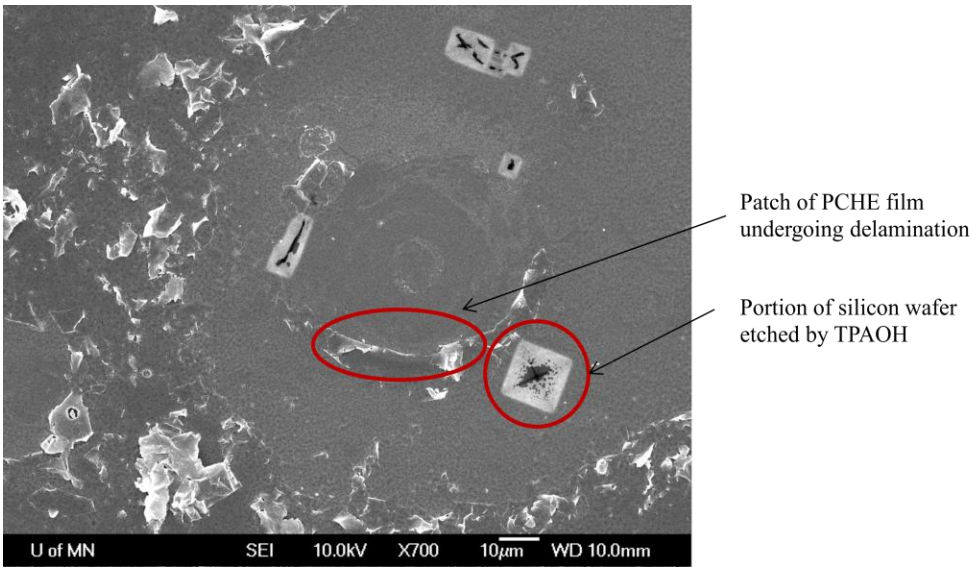

Figure 17: Different stages of delamination on the wafer treated with HMDS – PCHE film peels off and Si wafer gets etched in regions where the polymer has already come off.

d. Functionalization of Si surface with dichlorodimethylsilane was done in order to make the silica surface hydrophobic before coating it with PCHE. The aim was to bring the surface energies of the substrate and the polymer close to each other to get a better film. However, this had no effect on the film life under hydrothermal conditions. The maximum time for which the polymer film stayed on was about six hours for the case of functionalized silica surface. Table 2 shows the effect of functionalization and annealing on the stability of PCHE films on Si surfaces in standard and dilute hydrothermal solutions.

Table 6: Stability of PCHE thin film at 125 ^{o}C under different conditions

Type of PCHE film	In 0.167M TPAOH (Jansen conditions)	In 0.088M TPAOH (mild conditions)
Coated on bare Si wafer	Total delamination	Total delamination
Coated on Si wafer functionalized with HMDS	Partial delamination	Partial delamination
Annealed after coating on functionalized Si wafer	Total delamination	Total delamination

In all cases, the time for which a PCHE film was able to survive under hydrothermal conditions was not sufficient for zeolite growth. The longest time of survival was 6 hours for the PCHE film coated on HMDS functionalized silicon wafer. However, under the same conditions, i.e. at the same temperature and solution composition, zeolite growth was observed only at around 60 hours (Figure 18). Thus, the kinetics of zeolite growth is too slow to allow for zeolite synthesis on a stable polymer film.

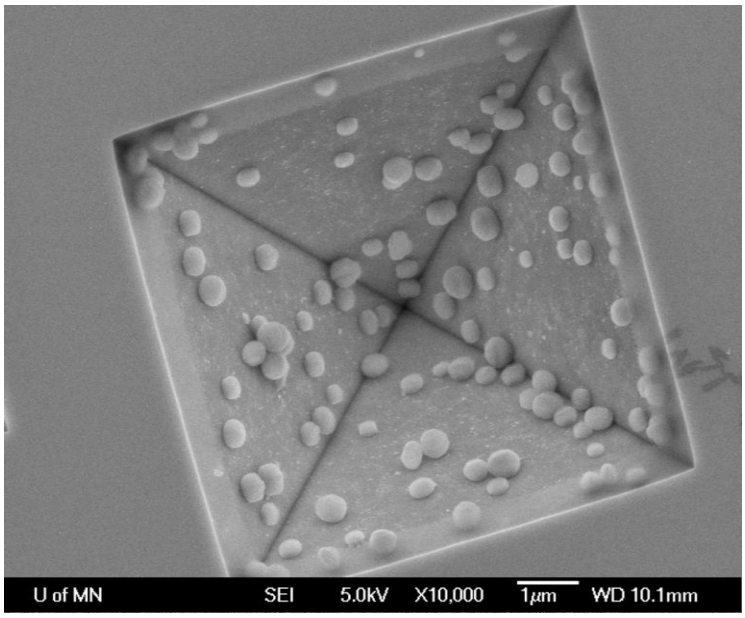

Figure 18: Zeolite growth observed in etched portions of the silicon wafer after 60 hours

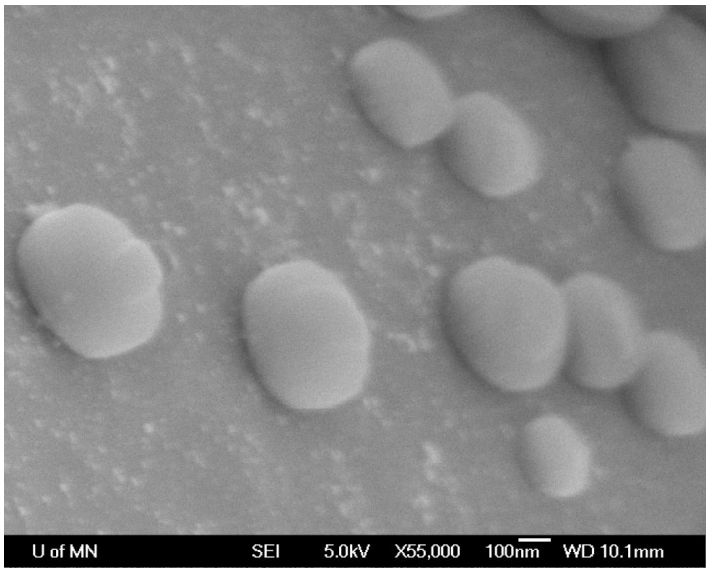

Figure 19: Characteristic coffin shape of zeolite crystals indicates MFI framework

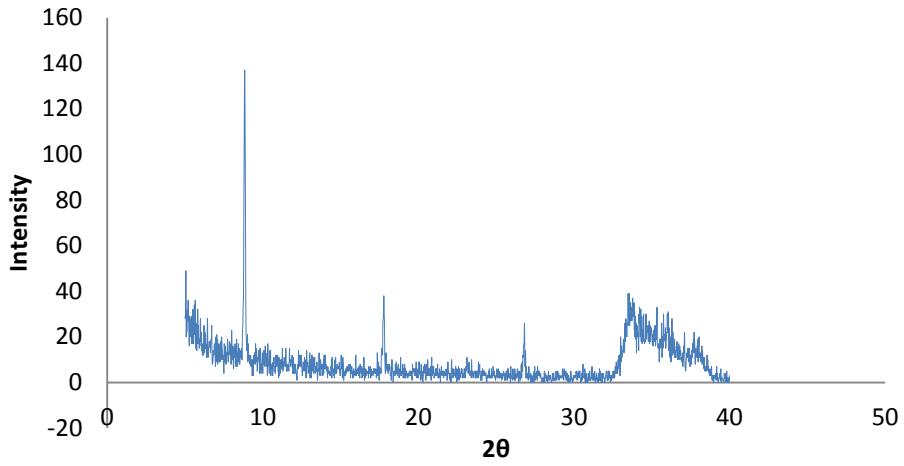

Figure 20: WAXS pattern of wafer surface corresponds to characteristic MFI framework

***<u>The rationale for delamination</u>*:**

Castro and coworkers have reported that salt ions and water molecules are capable of diffusing through defects in polymer films, after which they etch the silica layer underlying the polymer, thus causing the polymer film to peel off the substrate (Figure 21).[27] It is likely that a similar mechanism causes TPA^+ ions and water molecules to effect the delamination of the PCHE film. Since it is not possible to get a fully defect free thin polymer film, the only way to get around this problem would be to use an etch-resistant substrate to support the PCHE film. This substrate should also have a surface energy similar to PCHE to avoid spinodal dewetting so that spin coating is possible.

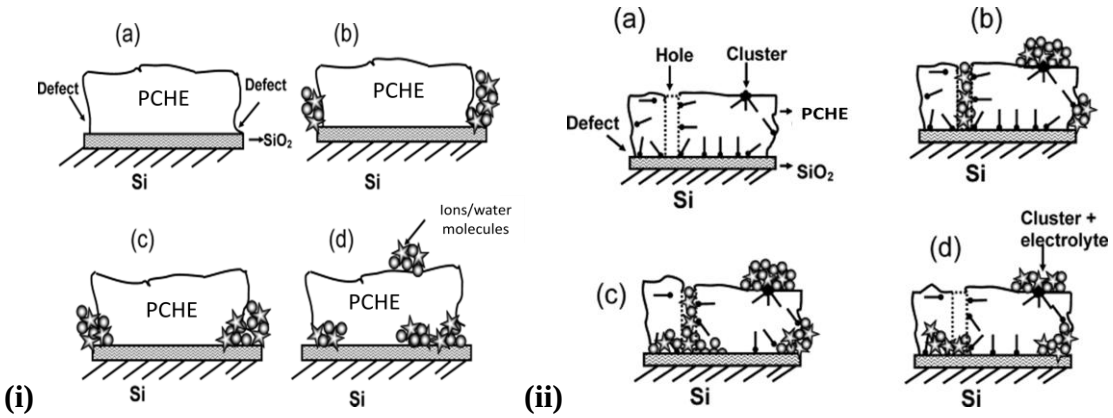

Figure 21: The etching of the silica layer under the polymer film through edge defects and holes on the polymer leads to its delamination

After trying a few inert substrates, silicon nitride was identified as a material that would fulfill both criteria. Additionally, it is easy to create a silicon nitride layer by a Chemical Vapour Deposition (CVD) process. A Silicon Nitride film (about 800 nm thick) was deposited on the Si wafer prior to spin coating the PCHE film using PECVD (Plasma Emission Chemical Vapor Deposition). First, a Si wafer coated with silicon nitride (no polymer film present) was kept under hydrothermal conditions for a day. SEM images revealed that the wafer did not get etched, proving that the nitride was indeed protecting the Si surface from etching (Figure 22). The nitride was coated with a PCHE film and the experiments were repeated with no silica source in solution. This time too, the nitride layer did help prevent delamination of the polymer film.

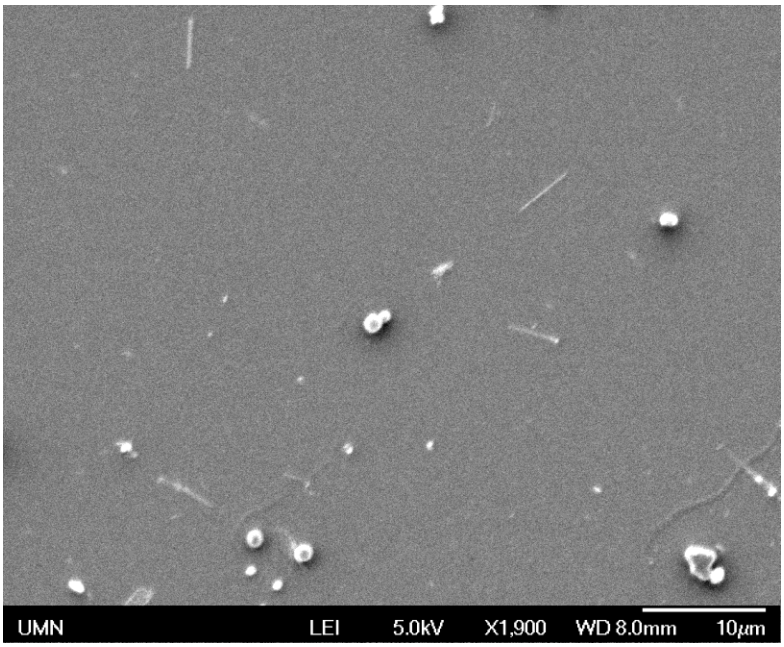

Figure 22: Silicon nitride coated Si wafer shows no signs of etching after being in a TPAOH solution for 24 hours Small particles seen are from etching of the unprotected back of the wafer.

Figure 23 shows SEM images of zeolite crystals on the polymer surface. It was observed that nucleation of crystals preferentially occurred on the PCHE film compared to the nitride, as can be seen form Figure 23(b). Furthermore, the crystals that were observed on the PCHE surface were a- b- oriented as was verified from both the SEM and X-ray diffraction patterns. Oriented MFI monolayers such as these have great potential use in membrane fabrications. In order to further study the growth of zeolite monolayers on PCHE surfaces, controlled experiments were performed by varying the amount of silica in the hydrothermal synthesis solution. To prevent the silicon wafer itself from getting etched and becoming a silica source, wafers with silicon nitride coated on both sides were used as substrates to coat PCHE thin films. Hydrothermal synthesis solutions with different silica concentrations (known in literature as C1, C2,C3,C4 conditions) were prepared and zeolite growth was carried out on these films at 120^{o}C.

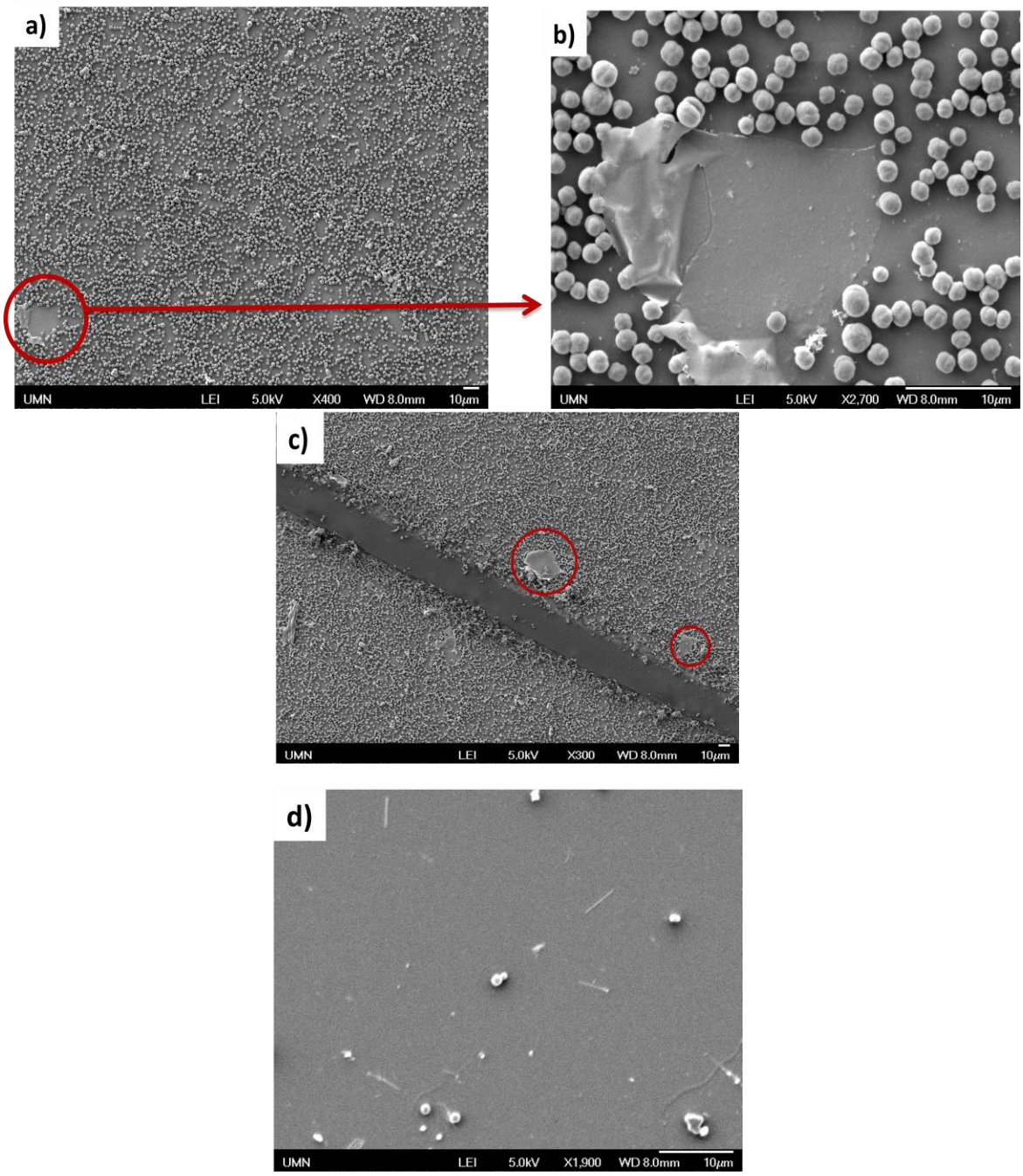

Figure 23: (a) SEM of surface of polymer film after the wafer was subjected to Jansen's hydrothermal synthesis conditions at 120 ^{o}C for 20 hours. (b) A magnified image of the PCHE film locally peeling off. (c) A scratch made on the film after zeolite synthesis to test for presence of polymer. Patches of polymer which have come loose from the scratch have been marked. (d) Nucleation on a bare silicon nitride film under the same conditions as in (b). Compare high density of nucleation on PCHE film in (b) with sparse nucleation on silicon nitride in (d).

However, obtaining reproducible etch resistant silicon nitride coatings was challenging. Often, delamination of silicon nitride film was also observed under hydrothermal conditions as can be seen in Figure 24. Inspite of efforts to improve adhesion of silicon nitride to the silicon wafer (by modifying surface properties with a HF (to make hydrophobic) and piranha solution (to make hydrophilic)), the nitride layer peeled off the silicon wafer under zeolite synthesis conditions unpredictably.

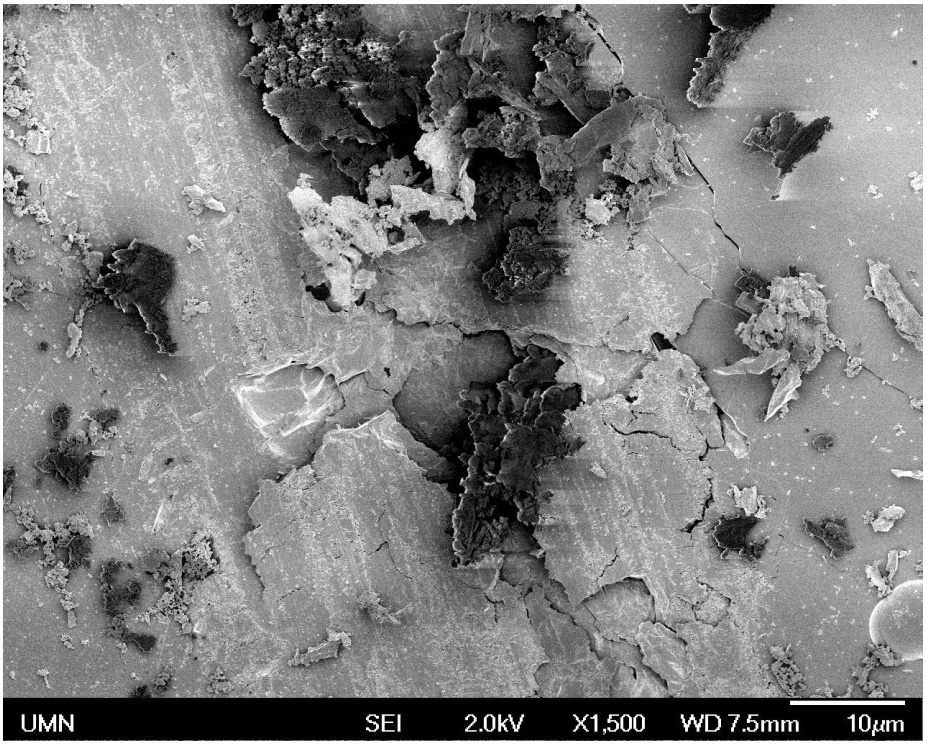

Figure 24: Representative image of silicon nitride coating peeling off

2.3 Conclusions

The results of the previous sections indicate that PCHE has a preference for Silicalite-1 nucleation compared to silicon nitride and that experiments can be controlled to nucleate a dense monolayer of zeolite on its surface. Keeping this in mind, attempts were also made to create the right nucleation conditions by controlling the amount of silica in solution. Unfortunately, the results presented above could not be reproduced every time the experiment was conducted. The silicon nitride layer peeled off unpredictably in some cases and stayed on in some. A probable reason for this observation is the presence of defects in the PECVD deposited layer. A few pin-hole defects are enough to act as pathways for diffusion of molecules or ions, causing the film to come off. While some parts of the wafer are defect free, some are not. Hence, wafer pieces from the same Si wafer can still have silicon nitride films with different mechanical integrities. This problem could not be solved by increasing the thickness of deposited layer or by pre-treating the wafer to make it hydrophilic or hydrophobic and improve the adherence of silicon nitride. Hence, these attempts were abandoned in favor of a system which offered better control.

3. Confined synthesis of zeolites in nanoporous bicontinuous monoliths

3.1 Introduction and Motivation

Since attempts to use thin films to synthesize MFI did not work as expected, we decided to revert to the confined synthesis approach in monolithic nanoporous plastics. We hypothesize that the reason for failure of confined synthesis attempts in the PS monoliths (see Section 1.3) was the lack of connectivity between the pores, which hindered the transport of the zeolite precursor solution required for growing crystals. This argument is supported by the fact that 3DOm (Three Dimensionally Ordered mesoporous carbon) carbon, a bicontinuous template, has successfully been used in the past to grow monodisperse nanocrystals of zeolite. 3DOm carbon (inverse opal carbon) has a bi-continuous structure and has been used as a template for growing nano sized MFI crystals by both the SAC method and hydrothermal synthesis (Figure 25).[13, 14] The carbon is synthesized by infiltrating closed packed arrays of monodisperse silica spheres (prepared by the Stöber method[28]). Zeolite nanocrystals as small as 10 nm have been prepared using this template. Scanning Electron Microscopy, Small Angle X-ray Scattering, Wide Angle X-ray Scattering, Transmission Electron Microscopy are some of the methods used to characterize the carbon template and the zeolite nanocrystals. Most of the 3DOm pores were filled with a single, faceted MFI nanocrystals, as can be seen from the SEM image in Figure 26. The size of the chambers can be controlled by varying the size of the colloidal crystals used as templates for the 3DOm carbon. For example, PMMA spheres

have sizes of the order of a few hundred nanometers, while silica nanoparticles can be tuned to 5 nm.

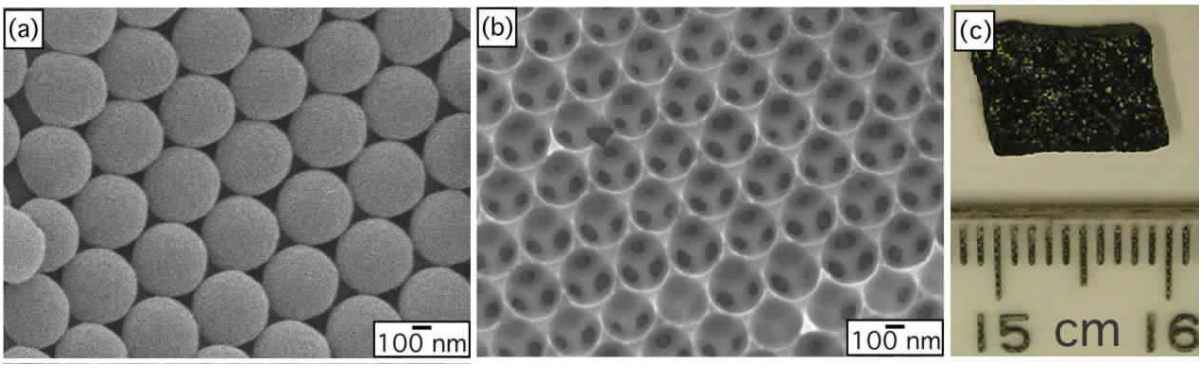

Figure 25: (a) PMMA colloidal crystals used as template for 3DOM Carbon (b) The 3DOM Carbon template (c) A 3DOM carbon monolith14

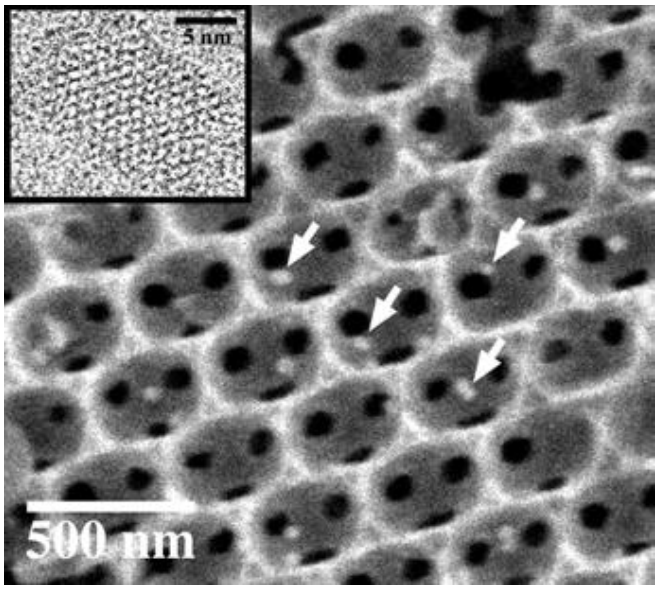

Figure 26: Nanozeolite synthesized in 3DOM carbon. Inset is an HRTEM image of the crystal[13]

Monolithic nanoporous plastics which also have a 3-dimensionally connected structure could offer advantages over 3DOm C. For instance, the pore window size in 3DOm C is about 30% of the size of the chamber, which can present challenges for transport of synthesis solution between chambers at very small chamber sizes below 10 nm. So these templates may not be optimal for filling with zeolite crystals to create

mesoporous zeolite that can be used for catalysis. On the other hand, bicontinuous polymers are known to form by self assembly or in the emulsion form, as will be described later. These could be good candidates for growing mesoporous zeolites due to the extremely high degree of connectivity they offer in the nanoporous network. All the pores are of similar size and there are no constrictions in pores, which is a significant advantage compared to 3DOm Carbon.[29] However, absence of isolated 'chambers' means that growing monodisperse zeolite in these polymers (like the crystals grown in 3DOm Carbon) could be a challenge. Instead, bicontinuous porous polymers would be good templates for growing mesoporous zeolites. Nevertheless, showing that confined synthesis in nanoporous plastics can be done, either in an engineered or a self assembled polymer would be a significant achievement.

Preliminary results suggest that pore connectivity strongly affects the mass transport of zeolite precursor solution between the pores. The absence of a co-continuous pore network (as in the case of the parallel cylindrical pores in PS) restricts confined synthesis by limiting the transport of the species that eventually crystallize into zeolite. Hence, for confined synthesis, it is crucial to select a polymer template that has interconnected pores. The following section builds up on the preliminary work and presents a plan to utilize polymeric materials for confined synthesis of zeolite crystals, primarily for growing mesoporous zeolite for catalysis applications.

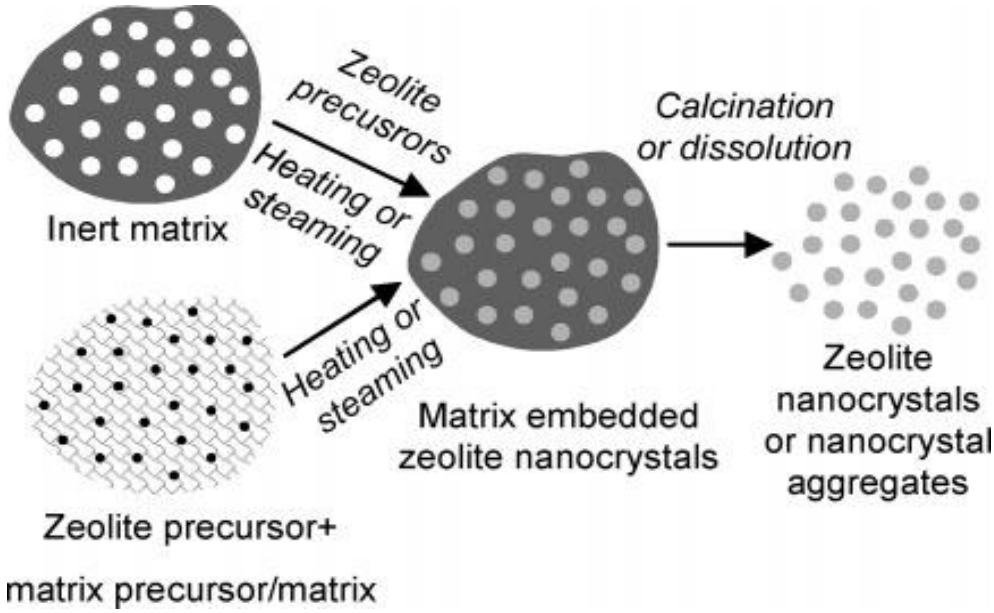

Figure 27: Schematic of confined synthesis in porous templates to grow zeolites by two routes[12]

The process of zeolite crystallization from silica precursors involves aggregative steps in the initial stages. It is possible to constrain the extent of aggregation by ensuring that these steps occur in a restricted amount of space. By doing so, one can limit the maximum attainable size of zeolite crystals. Keeping these factors in mind, the 'confined synthesis' method has been chosen as the most suitable pathway to grow zeolite nanocrystals/mesoporous zeolite. A general schematic of the method is shown in Figure 27. This method uses a mesoporous inert matrix as a template for the growing zeolite crystals. The confined synthesis technique has been used to grow crystals of well defined and precisely controllable shapes and sizes ranging from spheres to needles, which is a crucial requirement for hierarchical nanomanufacturing of membranes from these crystals.[14] In the past, mesoporous carbon has been a popular choice as a template due to its inertness and ease of crystal recovery - the matrix can be burnt off after the completion of synthesis.[30] For successful synthesis of zeolite crystals, the template should be inert so

that it does not interfere with the zeolite synthesis chemistry. It should be bicontinuous to allow the transport of synthesis precursors through it and at the same time have pores small enough to constrain the growing crystal and prevent its movement.

The potential of the confined synthesis technique has been discussed. Now, we specifically aim to design appropriate templates for this process. We wish to explore the possibility of using polymeric materials as templates to grow zeolite nanocrystals due to the following reasons: 1) Bicontinuous morphologies with highly interpenetrating pores and channels to allow for zeolite precursor transport exist in polymeric systems, 2) Zeolite crystals can be recovered by simple dissolution of the polymer matrix in an organic solvent, 3) Very narrow pore size distributions are attainable in nanoporous polymeric structures prepared by self assembly, microstructure alignment and selective etching of structures prepared by self assembly of block copolymers.[31, 32] 4) High tunability of pore sizes, for instance, by changing the composition ratio of a block copolymer derived matrix and 5) Feasibility of functionalization of pore walls to improve the penetration of the zeolite precursor solution.

Nanoporous polymers are especially versatile for templating zeolites because of the combination of high surface area and monodisperse confined spaces they can provide. In addition to engineering the geometry of the nanopores, we can change their surface chemistry to control properties like nature of surface charge, charge density, surface energy and functional

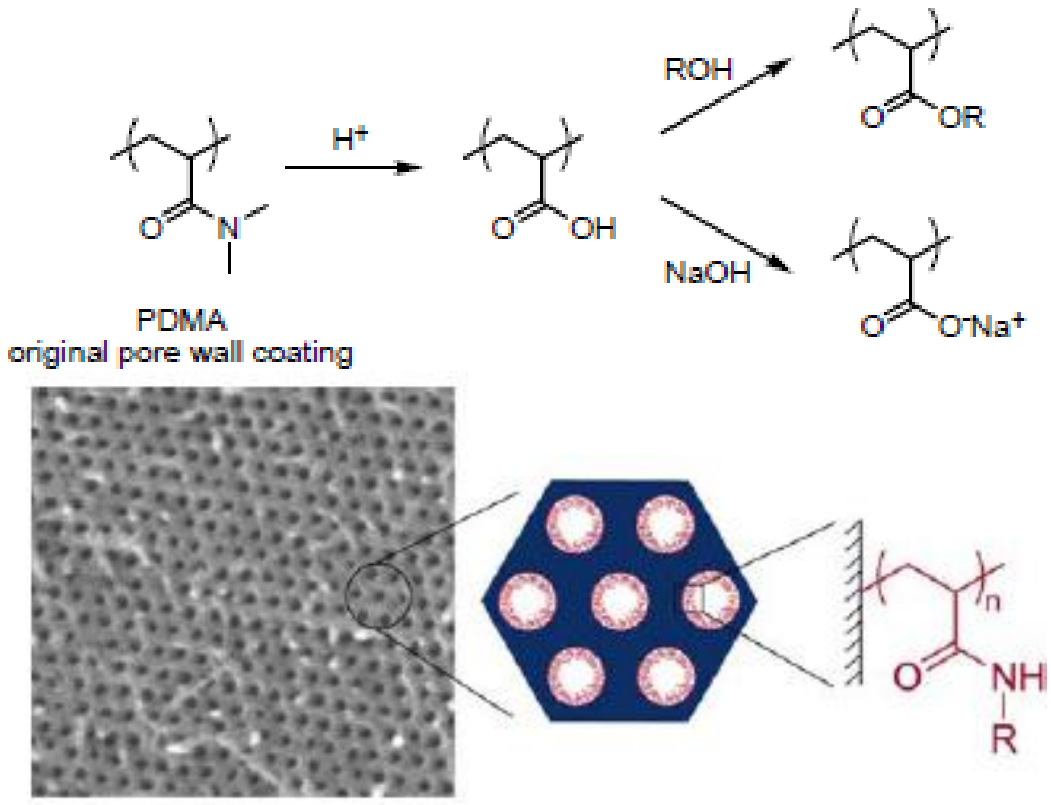

Figure 28: Nanoporous PS made from PLA-PDMA-PS triblock copolymer by etching PLA. Here the hexagonally packed nanopores are coated with PDMA (hydrophilic) [33]

group composition.[34] Pore wall chemistries can be tuned by appropriate chemical treatment to increase the hydrophilicity of the pores to improve permeability of the hydrothermal synthesis solution into the polymer template. For the purpose of confined growth, we propose to synthesize a range of nanoporous plastics which have bicontinuous mesostructures. They will have different combinations of pore sizes and pore wall chemistries. Figure 28 shows nanoporous PS which has been synthesized in such a way that it has hydrophilic nanopores because of the polyamide coating. The polyamide can be subsequently converted to other functional groups like carboxylic acid or esters, thus making the pores hydrophilic. The other important factor to be considered

is the inertness of these polymer templates to zeolite synthesis conditions, namely, high alkalinity and elevated temperatures. The structural integrity of the pores will be preserved at temperatures below the glass transition temperature (T_g) of the chosen polymer, so we should choose a polymer with a relatively high T_g (at least 80-100 °C) The hydrolysis step in the synthesis of nanoporous PS mentioned earlier was carried out at 80 °C at 1M NaOH alkalinity. Zeolites can be synthesized under similar conditions. Hence, we expect these nanoporous plastics to be compatible with the strong conditions for zeolite synthesis.

Block copolymers form a number of nanostructures due to microphase separation (depending on the degree of incompatibility between the polymer blocks). Of the four equilibrium morphologies formed by diblock copolymers, only the double gyroid structure is three dimensionally bicontinuous. However, it is stable over a pretty narrow window which could be difficult to control from the synthesis point of view. Pore sizes in the structure can also be tuned only in the range of 5-30 nm.[35, 36] Polymeric bicontinuous microemulsions (BμE) are an alternate pathway to bicontinuous structures. They can readily be formed by adding copolymer to a roughly half-and-half mixture of two immiscible homopolymers and the phase morphology and pore size can be controlled in the range of 10-100 nm by changing the amount of copolymer added. Although composition windows are somewhat narrow (they can vary only about 3 % while preserving the BμE phase), they are very achievable.

Polymeric Bicontinuous Microemulsions as favourable templates for nanomaterials:

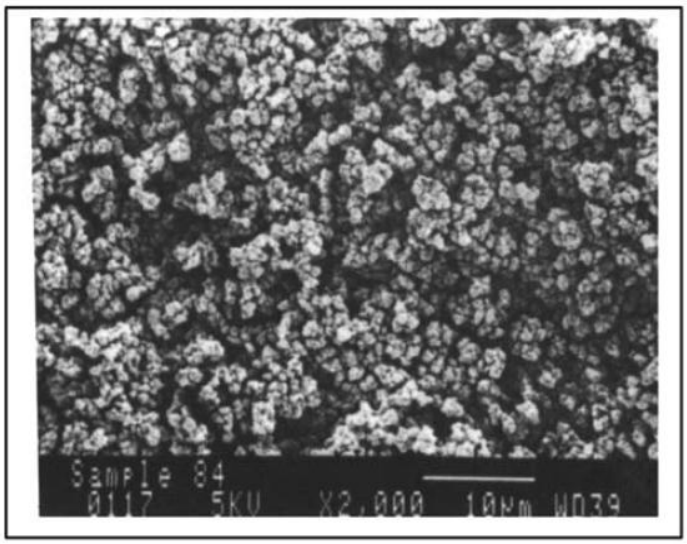

Figure 29: Early microporous material made by polymerization of styrene in a bicontinuous microemulsion.which acted as a 'soft template'. The main purpose was to produce materials with high surface area to volume ratios.

In the past, several groups have used polymeric BμE's as templates for growing nanomaterials. Cussler and co-workers first used a crosslinked BμE formed from an oil/ surfactant/water system (Figure 29) by polymerization of the oil.[37, 38] Though porous materials were produced successfully, there were unavoidable large scale heterogeneities, which illustrates that 'soft' material templates made by self assembly are difficult to handle, especially when it is required to freeze one micro-domain and remove the other. Polymeric BμE's have an advantage in this respect because they have much better mechanical and dimensional robustness as they are thermodynamically stable.[39] Polymeric BμE's with their three-dimensionally continuous nanoporous structure have a tunable lengthscale of the order of 10-100 nm (controlled by the amount of copolymer added) which spans both the mesoporous and macroporous ranges.

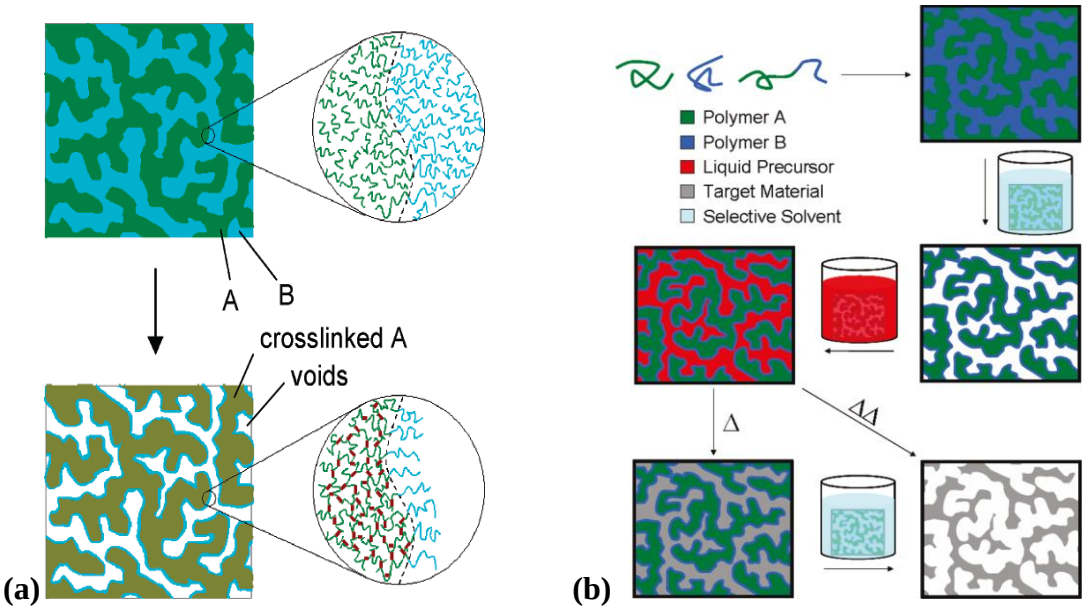

Figure 30: (a) Schematic for making Nanoporous PS (b) Schematic for making an inverse BμE template[39]

Zhou and co-workers, in 2006, made an isotropic nanoporous polymer from polystyrene (PS)/ polyisoprene (PI)/ PS-b-PI polymeric BμE precursor.[39] The protocol for generating the nanopores was selective crosslinking in the PI domain with subsequent removal of the PS homopolymers by simple solvent dissolution, as shown in Figure 30. Such a crosslinked nanoporous PI template could be an ideal template for high temperature synthesis of zeolite. In 2010, Jones and Lodge followed up on this work and synthesized the inverse structure of the nanoporous material by a method of nanocasting.[40]

3.2 Results and Discussion

3.2.1 Confined synthesis of zeolite in a polymeric bicontinuous microemulsion derived template

Mesopores occur in the range of about 2-50 nm. This range corresponds to two polymeric nanostructures discussed earlier– the gyroid and the bicontinuous microemulsion. Bicontinuous microemulsions have less sensitivity to composition than gyroids and are expected to be easier to synthesize. Hence, they are good templates to use for synthesis of mesoporous zeolite. A specific system of polymers has been proposed for use as a zeolite template. Their synthesis method will also be discussed in detail. In order to carry out confined synthesis in monoliths, the steam assisted crystallization technique, previously employed by Fan et al. [13] for 3DOm Carbon, was used. First, confined synthesis was reproduced in the 3DOm Carbon template to establish expertise in the technique. The results are summarized in the appendix (Section A2). A polymeric bicontinuous microemulsion made of Polyethylene (PE) and Poly(ethylene-propylene) (PEP) was made by mixing PE/PEP/PE-PEP in a specific ratio (42.5% PE, 42.5% PEP, and 15% PE-PEP by volume) and the PEP was removed by dissolution in a selective solvent as described by Jones and Lodge[40]. The nanoporous PE template left behind (Figure 31) was used to synthesize Silicalite-1 by the steam assisted crystallization technique described earlier. Differential scanning calorimetry (DSC) data showed that the PE template had a melting temperature of ~100 ^{o}C (Figure 32). Hence the temperature for synthesis of Silicalite-1 was chosen as 90^{o}C in order to prevent the collapse of the nanopores during zeolite synthesis.

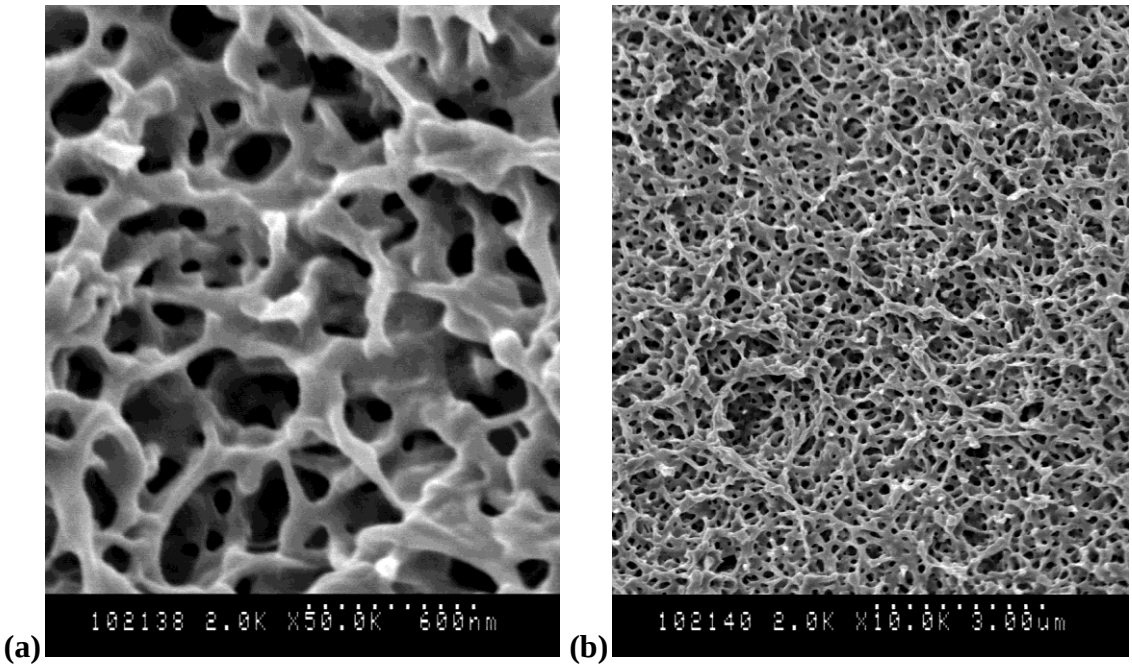

Figure 31: (a) High resolution and (b) Low resolution images of nanoporous PE. Imaging by Brad Jones (Lodge group)

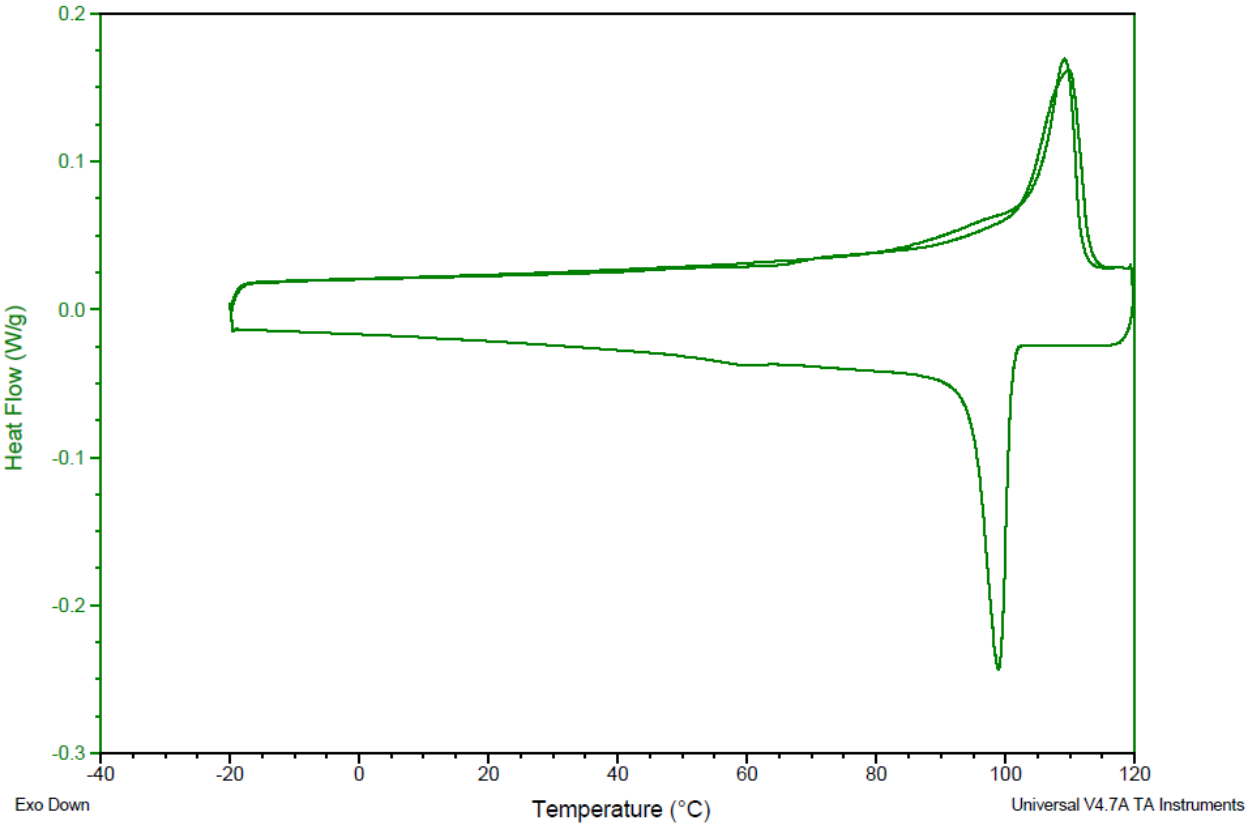

Figure 32: DSC data shows that the melting temperature of porous PE is ~100 ^{0}C

Zeolite synthesis was then done using the steam assisted crystallization protocol summarized in the appendix (Section A.2). The synthesis temperature was 90 ^{o}C and synthesis time was 5 days. The synthesis setup is shown in Figure 33. Incompatibility of surface energies of the solution and the PE pores prevented wetting at normal pressure. So, infiltration of the synthesis solution into the PE monoliths was done under vacuum as shown.

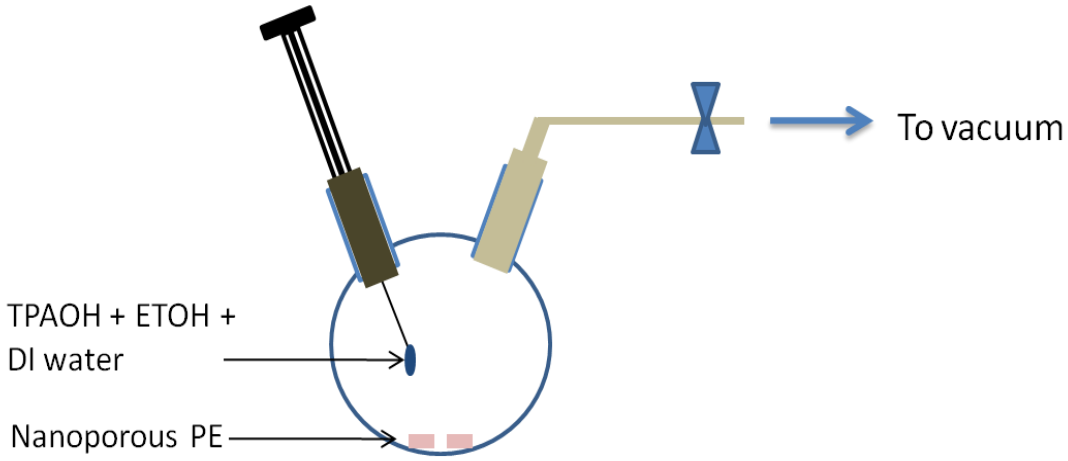

Figure 33: Setup for synthesis of Silicalite-1 in PE

After the precursors were infiltrated, a zeolite gel was allowed to form inside the pores. The PE monoliths along with the gel were sealed in hydrothermal vessels and were steamed under pressure under the synthesis conditions mentioned earlier. After synthesis, the monoliths were recovered, carefully washed and dried. A cross section of the monolith which was now a PE/zeolite composite was examined by SEM. It revealed white inorganic domains present in the pores of the PE template. Not all pores were filled and the percentage of filling was estimated as roughly 30-50% by eye. Figure 34 shows a representative cross section of the PE/zeolite composite.

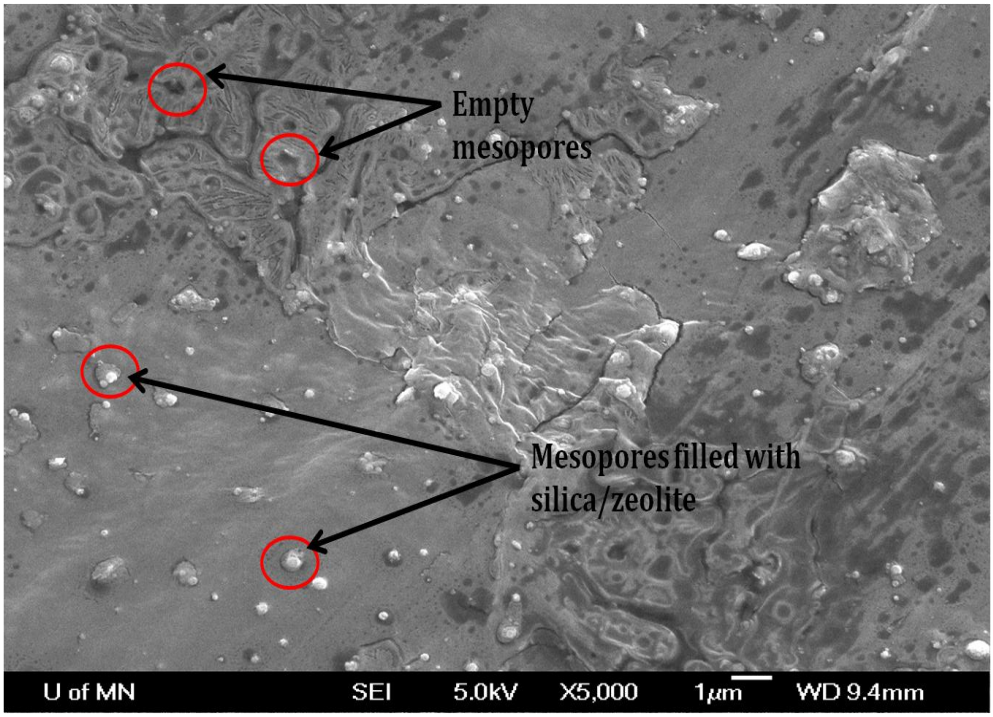

Figure 34: Representative cross section of PE/zeolite composite after zeolite synthesis in pores

A part of the PE/zeolite composite was washed, crushed and characterized by WAXS. The resulting diffraction pattern was compared to patterns of pure zeolite and pure PE. It can be seen clearly that the composite has peaks both from the zeolite and from the polymer (Figure 35). The peaks from the polymer appear dominant because most of the composite is PE and a low volume fraction of the pores is filled with zeolite.

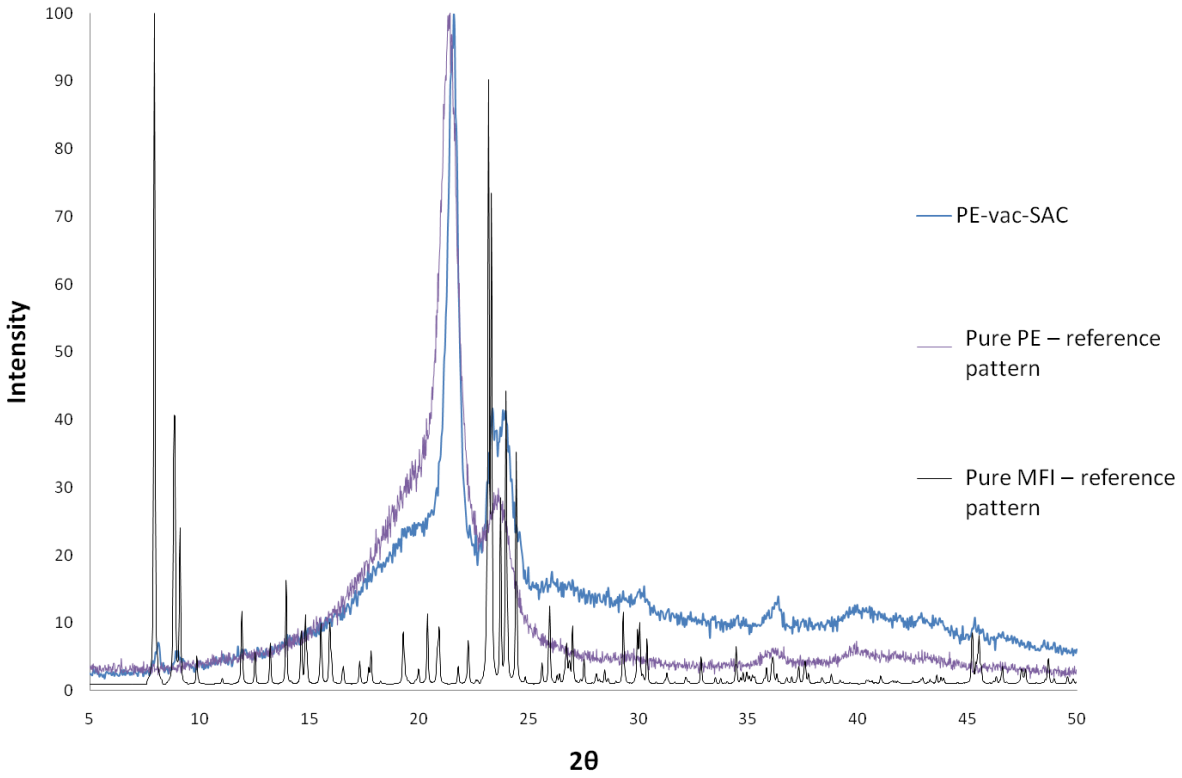

Figure 35: WAXS patterns of PE/MFI composite (blue), pure PE (purple) and pure MFI (black)

Next, the composite was calcined in a furnace at 550 ^{o}C for 12 hours under airflow to completely remove the PE. The inorganic material obtained after calcination was characterized by WAXS and TEM to determine if it was zeolite or silica. Figure 36 compares the WAXS pattern of the calcined material to MFI powder pattern and PE pattern. The polymer peak is absent from the calcined material, confirming that it has been removed by calcination. Additionally, the peaks in the sample diffraction pattern correspond to MFI framework, confirming that the material recovered after calcination is indeed zeolite.

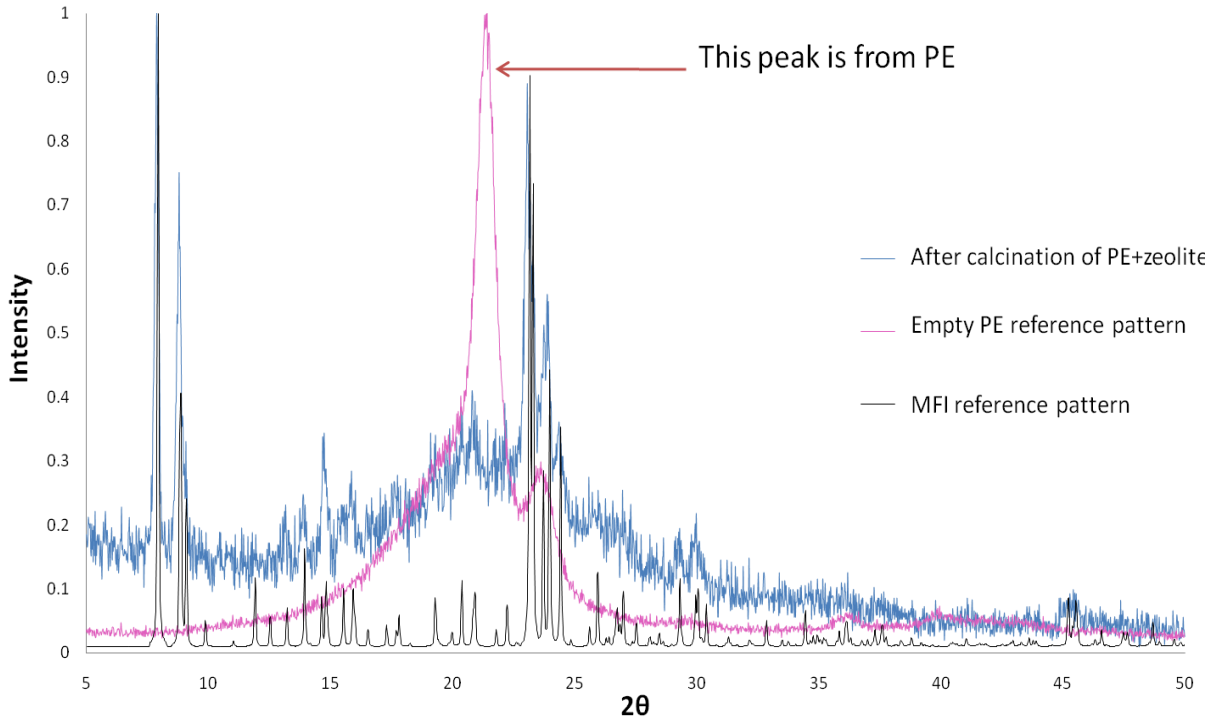

Figure 36: WAXS patterns of zeolite (blue), pure PE (purple) and pure MFI (black)

SEM imaging was done to see product morphology. Inorganic material, part of which looked amorphous and part of which looked crystalline, was seen (Figure 37).

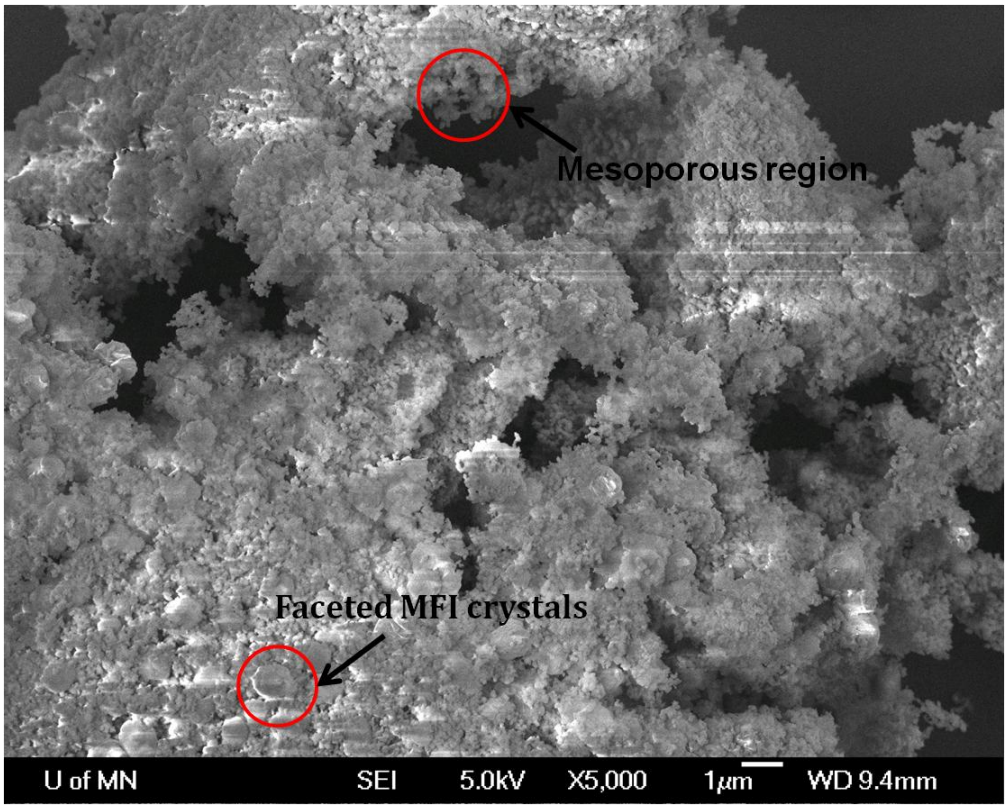

Figure 37: Material recovered after calcination

Most of the sample looked like Figure 38. Small spherical particles could be seen throughout most parts of the sample. These spheres were irregular and seemed to comprise of smaller domains. The details of the particle morphology could not be elucidated by SEM alone, so TEM imaging was done next in order to get a higher resolution picture of the particle morphology.

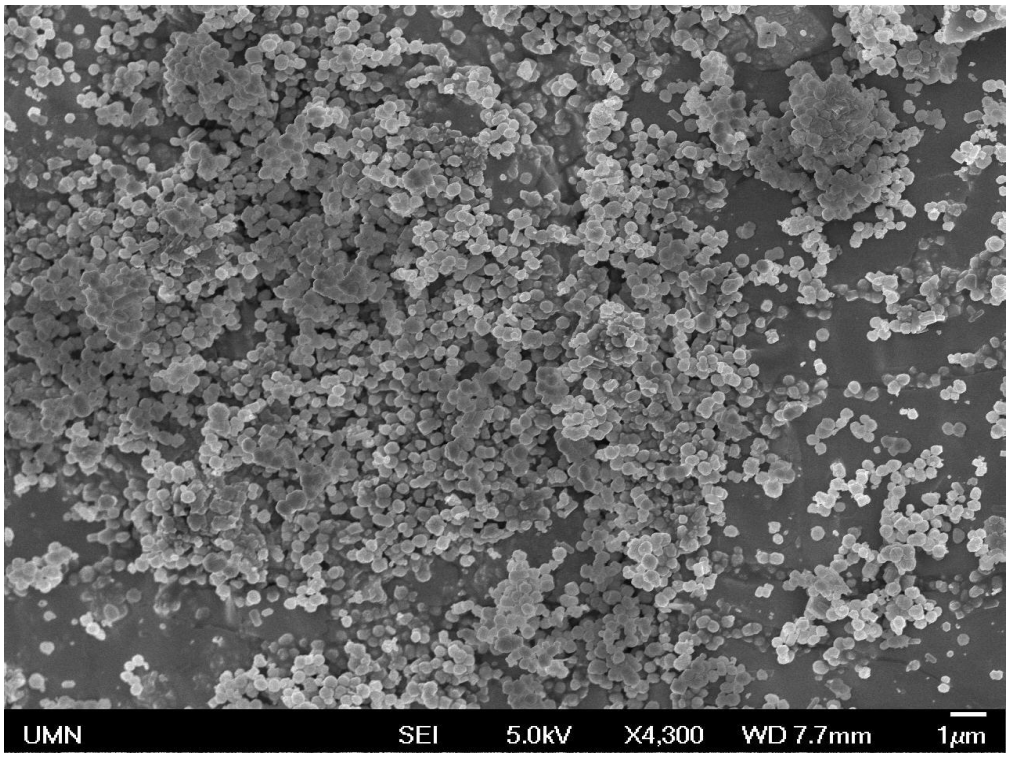

Figure 38: Material recovered after calcination

Figures 39 and 40 show higher resolution images of the spherical particles. The SEM images are not conclusive in the sense that it is difficult to determine if these are single crystals that are mesoporous or agglomerates of smaller crystals that stuck together due to the calcination process.

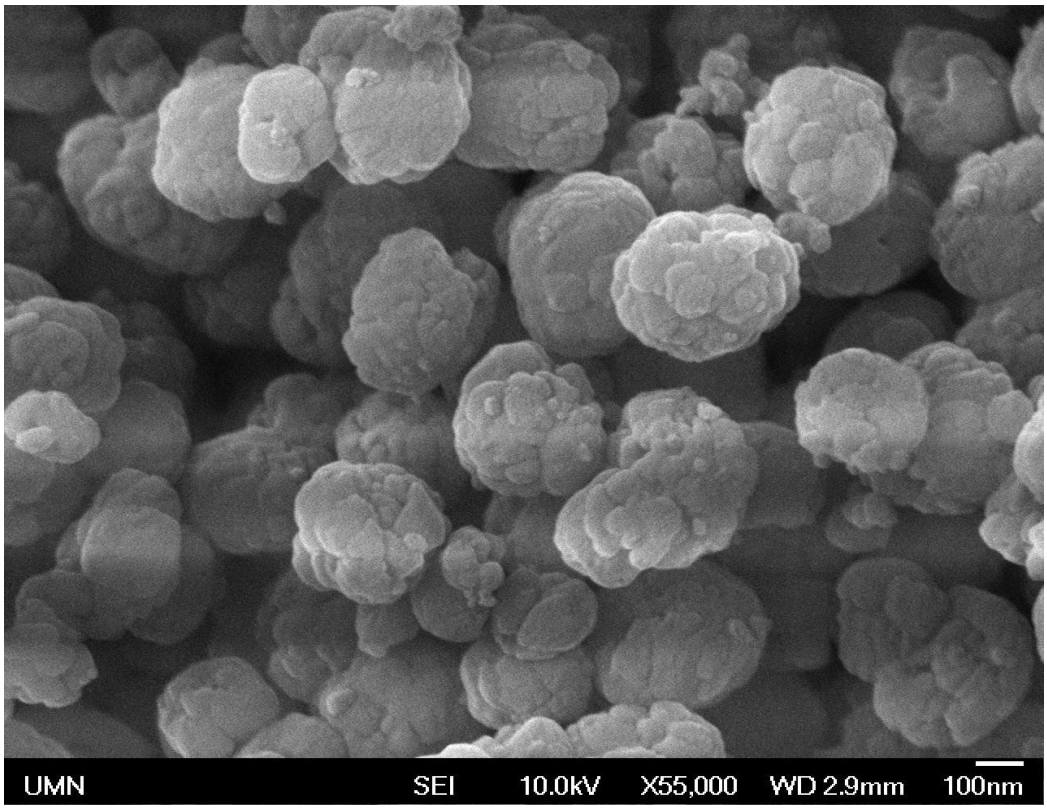

Figure 39: Low resolution SEM image of spherical agglomerates in calcined material

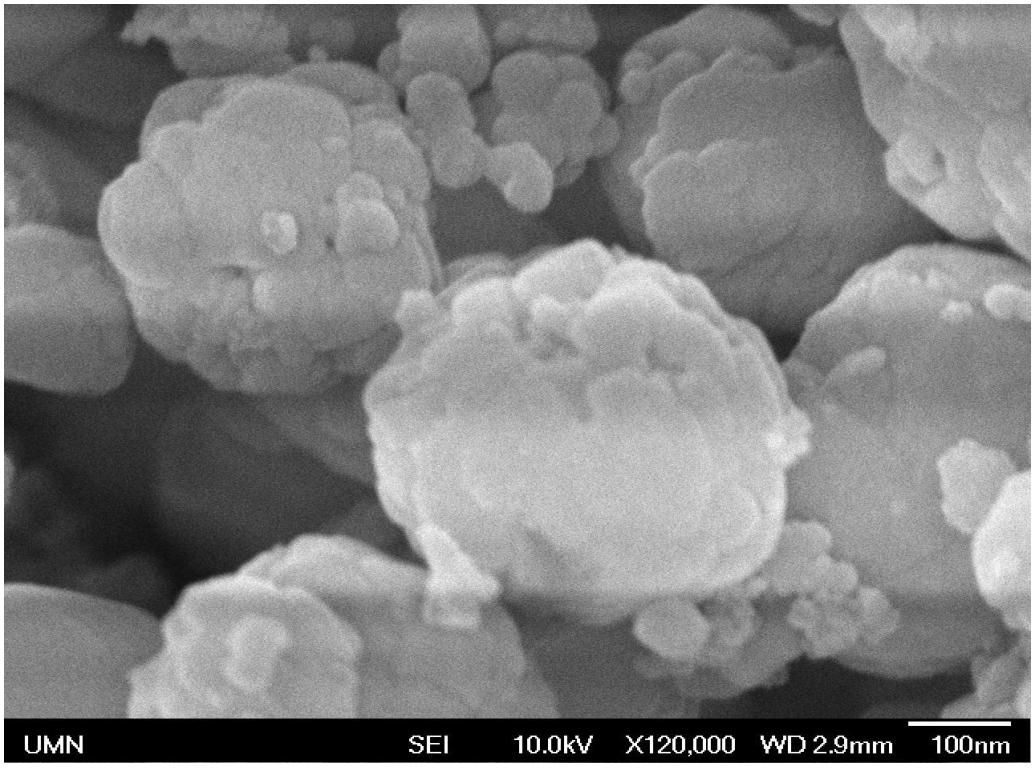

Figure 40: High resolution SEM image of a spherical agglomerate in calcined material

The calcined product was then sprinkled on a TEM grid and TEM imaging was carried out. The techniques that were employed were low and high resolution imaging, visualization of lattice fringes, bright and dark field imaging and electron diffraction to get information on crystallinity and microstructure. As can be seen, Figure 41 shows that the spherical agglomerates are indeed zeolites because high resolution imaging enables the visualization of the lattice fringes corresponding to the MFI framework of Silicalite-1.

(a)

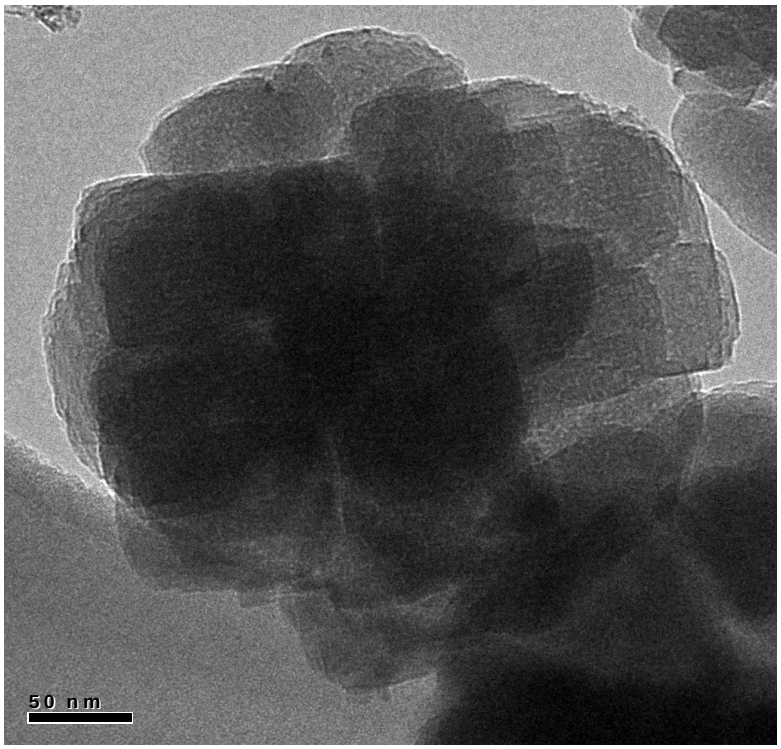

(b)

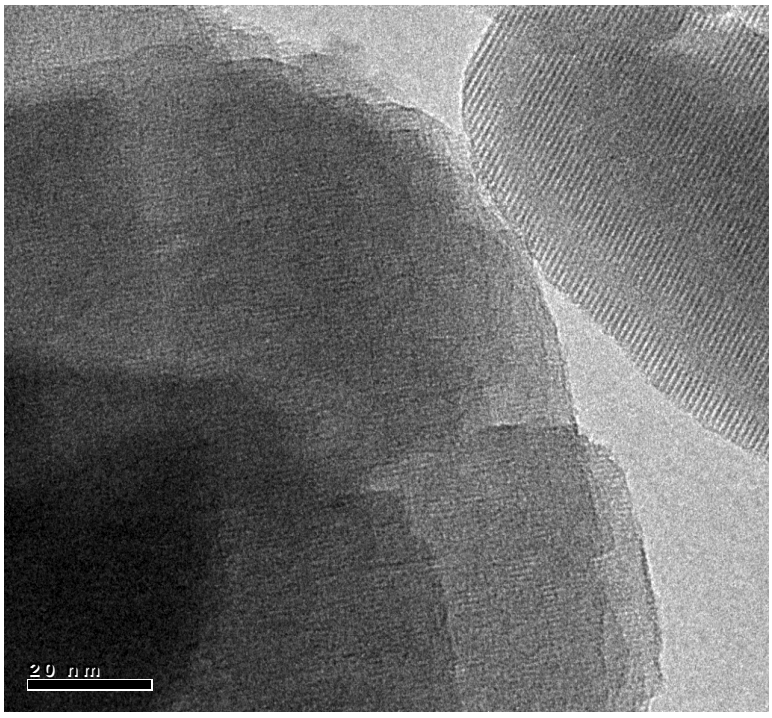

Figure 41: (a) TEM image of a spherical agglomerate (b) High resolution image of the same particle revealing lattice fringes of MFI

Figure 42 shows the electron diffraction pattern from selected area diffraction which shows characteristic spots from the MFI crystal framework. However, mesopores cannot be seen in the spheres which probably means that they have been formed by agglomeration due to calcination. Small nanoparticles close to the size of the mesopores (around 80 nm) could not be seen.

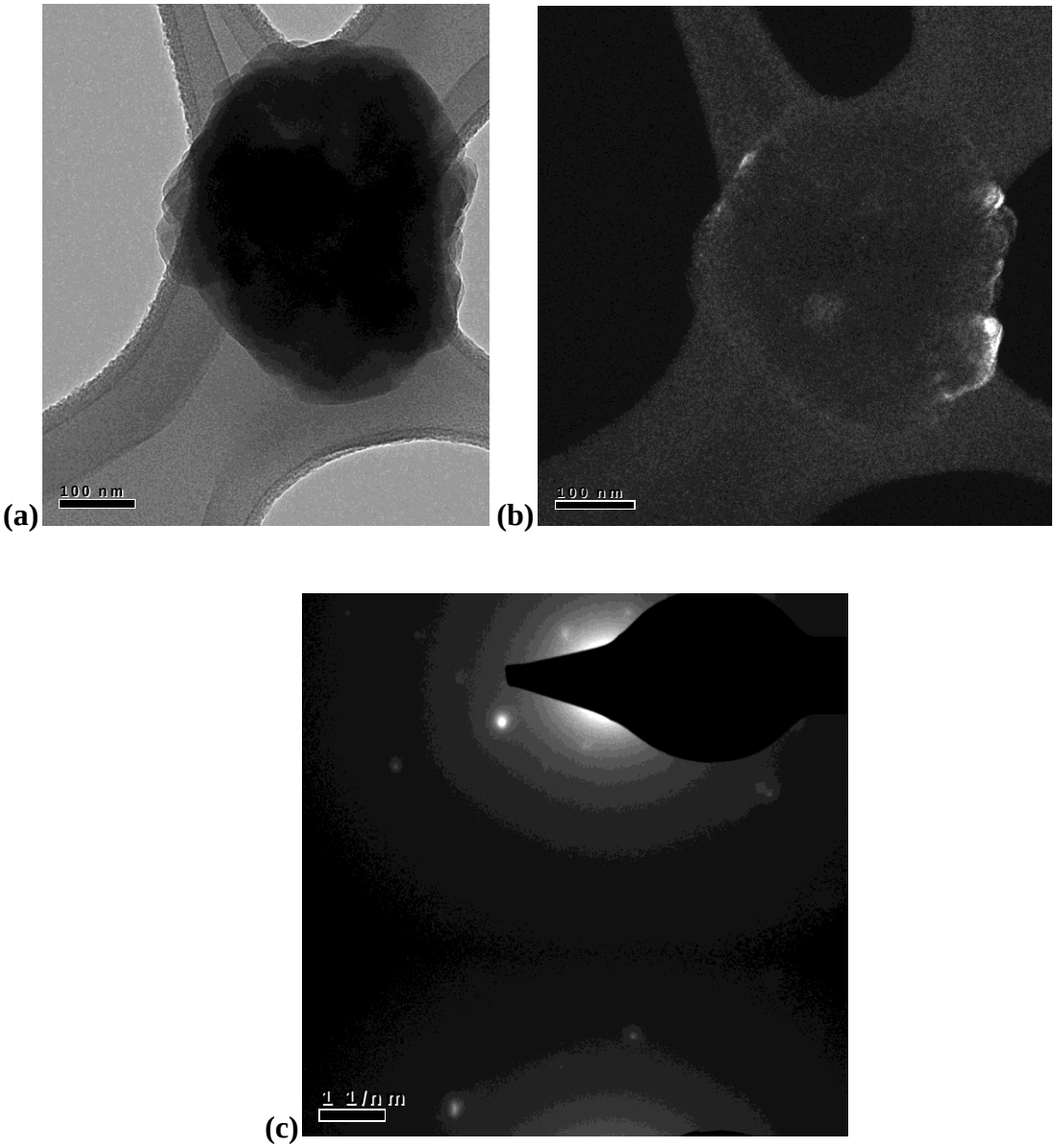

Figure 42: (a) A spherical agglomerate (b) Corresponding dark field image (c) Electron diffraction pattern showing diffraction spots from the MFI crystal

To summarize the experiment - WAXS data (Figures 35 and 36) shows that after synthesis of Silicalite-1 has been carried out in the PE template, tiny peaks of MFI framework can be seen in the XRD pattern. After calcination, these peaks become significantly more intense and sharper clearly indicating the presence of Silicalite-1 in the calcined product. However, it is not clear whether these peaks come from zeolite crystals that have been templated in the nanopores of the PE or from crystals that have grown outside the pores, on the surface of the PE monolith. SEM images (Figures 37, 38, 39, 40) revealed the presence of a few large, well faceted zeolite crystals that were clearly not templated and had grown outside the monolith. There were also some inorganics that looked mesoporous and a lot of spherical agglomerates of what looked like zeolite/other inorganics. The spheres were uniformly sized at around 200-300 nm. These could have potentially grown as single crystals in the mesoporous template or could be nanoparticles that agglomerated during calcination. To investigate the nature of the spherical particles in more detail, TEM imaging was carried out (with the help of Xueyi Zhang, Tsapatsis group). Zeolite has clearly been templated in the mesoporous PE, albeit of a bigger size than expected. One explanation for this is that pore collapse could have happened due to prolonged heating of the PE template, causing the smaller nanopores to collapse and leaving behind large (micron-sized) pores. Confined synthesis of zeolite could have taken place in these larger pores. In order to investigate pore stability under the conditions for steam assisted crystallization, an empty PE template was steamed at the same temperature, for the same duration of time as the original experiment. The PE was

visualized by SEM both before and after the steaming to compare the two pore structures. As can be seen in Figure 43, the nanopores collapsed after steaming.

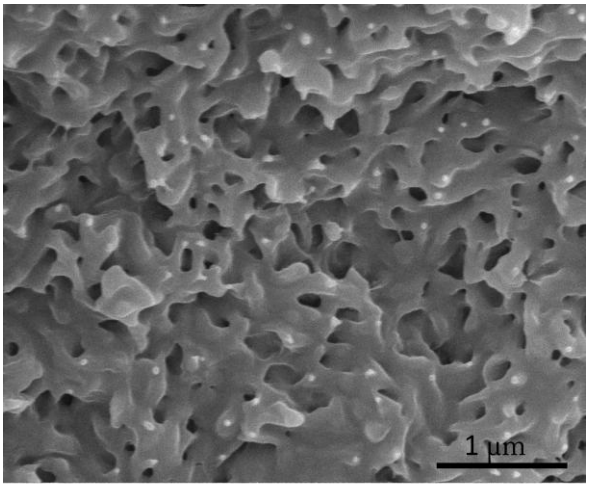

(a)

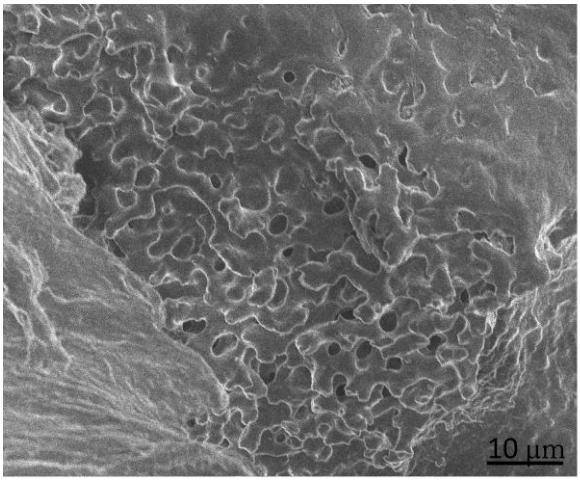

(b)

Figure 43: (a) PE before steaming (b) PE after steaming at synthesis conditions

The bicontinuous microemulsion derived PE monoliths are not suitable for zeolite synthesis because their pores are not stable under zeolite synthesis conditions. Lower temperatures cannot be used for zeolite synthesis because the kinetics of crystallization

slows down too much. However, larger zeolite crystals did successfully get crystallized in the bigger pores that didn't collapse, which shows that the bicontinuous pore structure is suitable for confined synthesis of zeolites. So an appropriate template would be one that has similar pore geometry but higher thermal stability.

3.2.2 Confined synthesis of zeolite in linear polyethylene template

In order to select an appropriate porous polymer for confined synthesis of zeolite, one has to go through a trial-and-error testing of different potential polymer templates to check for stability under zeolite synthesis conditions. The porous polymers to be tested were narrowed down by looking for certain criteria (derived from analysis of previous unsuccessful choices of polymer templates). The criteria that were taken into consideration were:

(i) The polymer should have sufficiently high melting point/glass transition temperature such that it retains its porous structure even upon exposure to zeolite synthesis temperatures (about 90-100 ^{o}C)

(ii) The polymer should be inert to the chemicals used for zeolite synthesis, which create a highly alkaline environment.

(iii) The polymer should have bicontinuous pores, because from previous research experience, isolated pore networks have difficulty in templating crystals of zeolite. This has been attributed to insufficient transport to/within isolated pores which prevents crystallization of zeolite precursors.

(iv) Pore size and tunability is also an important aspect. It is preferable not to cross the mesoporous range: 2-50nm, because mesoporous zeolites have useful applications. At the same time, the polymer should preferentially not have

high polydispersity in pore sizes. A polydisperse system would not be ideal for a controlled study of confined synthesis. Mesoporous material could find interesting applications for catalysis, while nanocrystals could find applications for membranes.

Eventually, after testing for stability under prolonged steaming, nanoporous linear polyethylene (synthesized in the Hillmyer Lab)[41] was selected as a good template. It did not show pore collapse on prolonged steam treatment at 95°C for four days (Figure 44 shows SEM images. Later on, it will be quantitatively shown by nitrogen adsorption that pore structure does not change.)

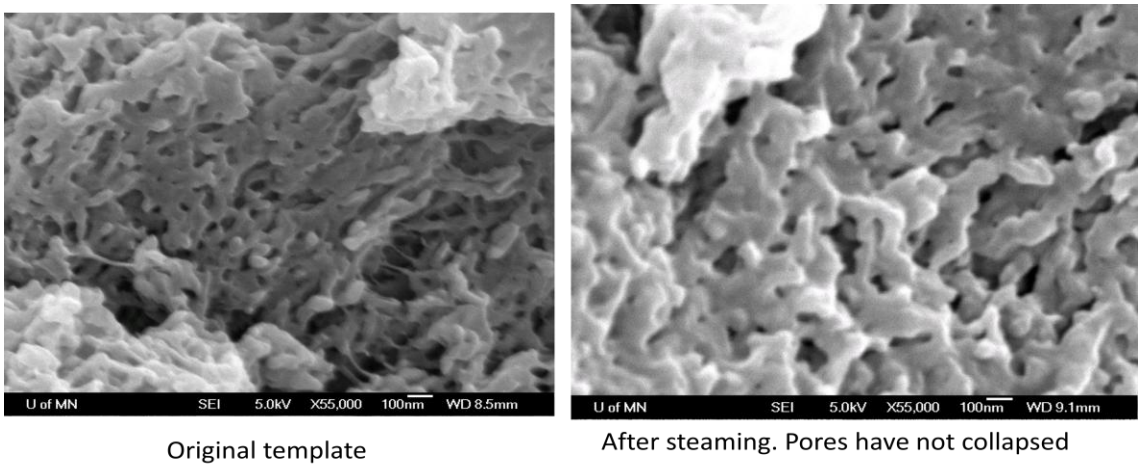

Figure 44: LPE pores do not collapse on steaming at zeolite synthesis conditions

So, steam assisted crystallization was carried out in the LPE template. This has been dealt with in detail in a following section. For the purpose of this target (i.e. synthesis of appropriate porous polymers), the synthesis protocols for LPE which were executed are presented along with supporting data.

Synthesis protocol for linear polyethylene[41]

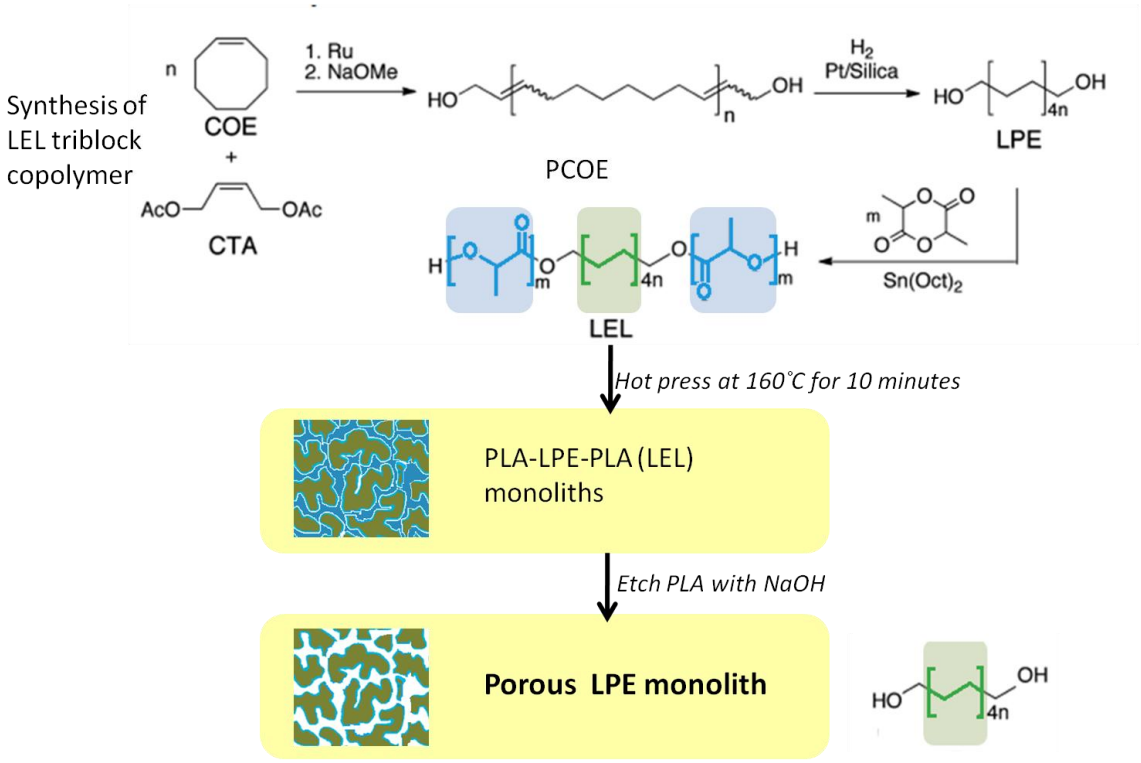

Figure 45: Synthesis route to make LEL triblock

The LEL triblock shown above consists of two PLA (polylactide) blocks at either end of a highly linear polyethylene (LPE) block. The LPE block is prepared by a Ring Opening Metathesis Polymerization (ROMP) of cyclooctene (COE) into PCOE, followed by hydrogenation of the PCOE. The lactide blocks are then attached by lactide polymerization to get the LEL block, which self-arranges into bicontinuous morphology. The LEL product is hot-pressed into pellets or disks of desired shapes. Finally, the lactide component is etched off using a 40% wt. solution of NaOH in methanol for two days to yield porous polymer. The entire process takes about three weeks starting from the monomer. Two batches of polymers were made – each with different molecular weights,

to demonstrate pore tunability by varying the molecular weights of each component. NMR, SEM and BET were carried out to characterize the product.

A batch with molecular weights of PLA-LPE-PLA as 37k-28k-37k was prepared. Volume fraction of PLA was about 0.6. The starting polymer was 28kmol/g OH-LPE-OH supplied by Louis Pitet (Hillmyer group). Lactide polymerization was carried out to attach the 37k blocks on either side of the LPE block. After hotpressing the triblock into a pellet (about 20mm diameter, 5mm thickness), it was immersed in the alkaline etching solution for two days at 333K. After the pellet was etched, it was washed with dilute HCl and DI water and dried at ~333K for a day.

The polymer synthesis experiments were then repeated for LPE of molecular weights 50kg/mol with volume fraction of LPE 70%. We shall refer to each of these LPE materials as LPE40 and LPE50, as explained in the following sections. In the sections that follow, characterization of polymer, confined synthesis and characterization of mesoporous zeolite are discussed in detail for both batches of polymers one after the other. First, the data for confined synthesis of Silicalite-1 in LPE40 is presented. Then, data for confined synthesis using LPE50 template is presented.

Characterization of polymer (Porous LPE40):

Characterization of the LPE derived from the 28kg/mol OH-LPE-OH precursor was done to probe the pore size, check the melting temperature of the porous polymer and image the pores to visualize the porous structure. Nitrogen adsorption (BET) was done to

probe the polymer and obtain values for pore volumes, surface areas and average pore sizes (BJH method).

Ideally, small angle x-ray scattering should provide us with a broad peak corresponding to the average domain size, but in this case, it is too large (>50 nm) to be detected by the instrument available. Typically, the SAXS characterization for such samples is done in Argonne National Labs with a much smaller wavelength of x-rays (0.084 nm). So, SAXS data is not available for this report.

The SEM data has been given below. (Figure 46). The sample was prepared by cryofracturing the porous polymer after freezing it in liquid nitrogen. This is necessary to prevent deformation of the ductile LPE and correctly visualize pore structure. The LPE is clearly highly porous and bicontinuous.

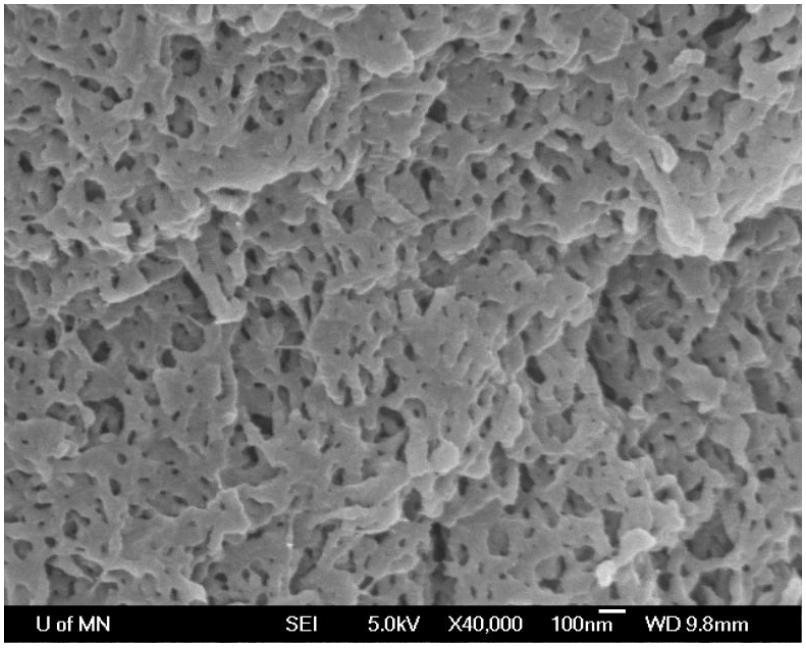

Figure 46: Representative SEM image of a cross section of the porous LPE40 monolith

Next, nitrogen adsorption was carried out to characterize the mesoporosity and pore structure of the porous LPE (Figure 47). A clear hysteresis loop between adsorption and desorption isotherms is present at higher pressures, indicating mesoporosity. Analysis of the adsorption data was done by the standard BET method and the BJH method was used to calculate pore size distributions. The BJH analysis for the average pore diameter is calculated from the incremental pore volume change, from the desorption isotherm. The average is taken as the peak. Average pore size is ~40 nm as can be seen from Figure 48. This polymer sample has been called 'LPE40' based on its pore size.

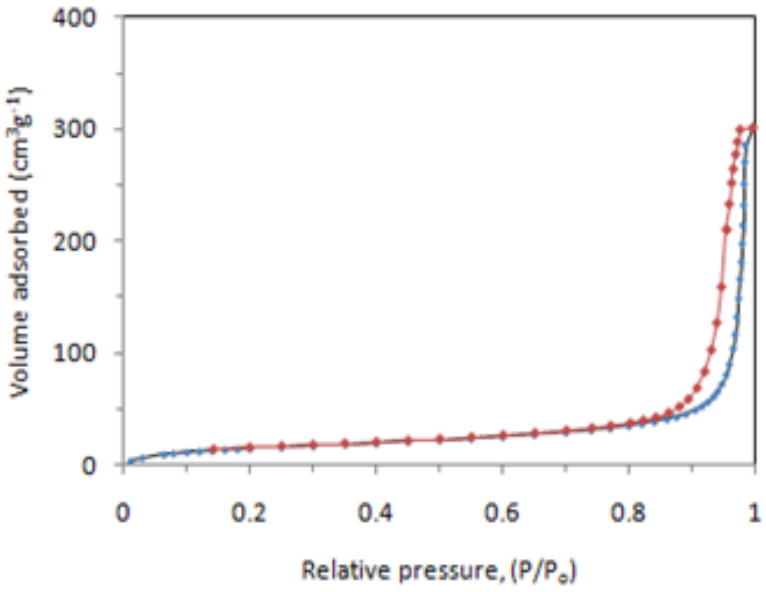

Figure 47: Nitrogen adsorption and desorption isotherms for LPE40

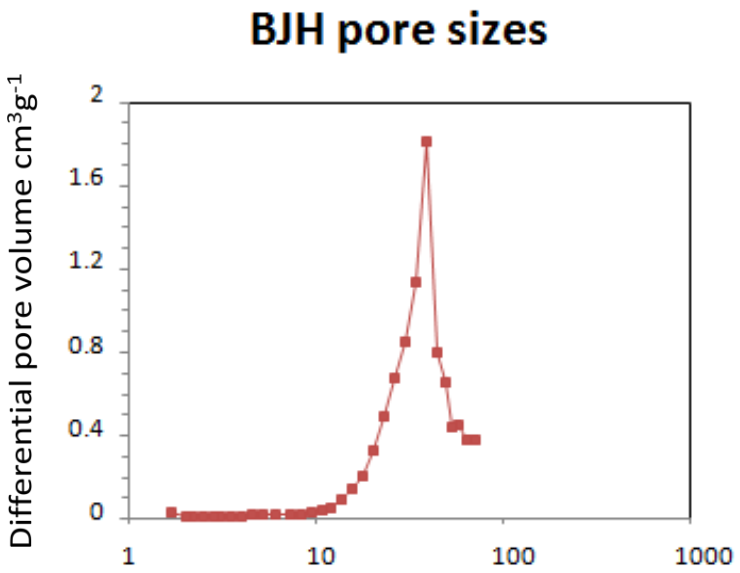

Figure 48: BJH pore sizes for LPE40 calculated by the software give average pore size ~40 nm

NMR data for the polymer has also been provided to show end group functionality for OH-PE-OH (Figure 49).

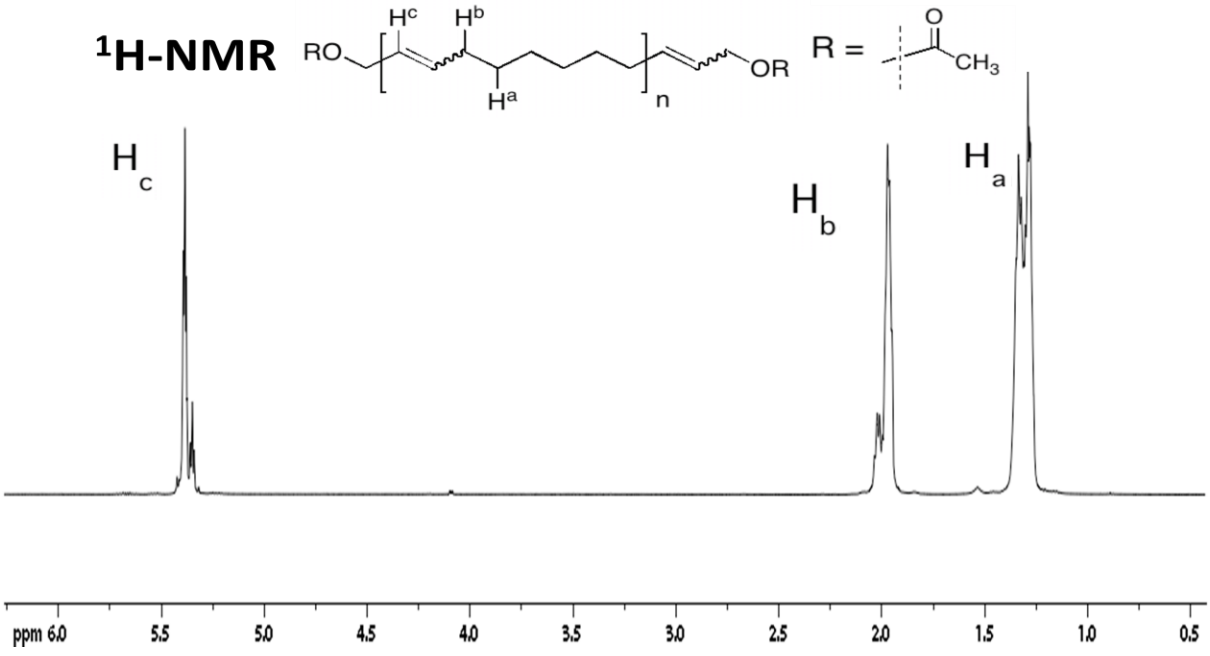

Figure 49: NMR data for LPE40 sample precursor (PCOE) elucidating its structure.

Confined synthesis of zeolite in LPE40:

The steam assisted crystallization protocol outlined for 3DOm Carbon was followed for the LPE monoliths provided by the Hillmyer group for 4.5 days at 90 ^{o}C. Non-templated crystals which would have grown on the surface of the monolith were removed by slicing away a thin outer layer from the monoliths. A cross section of the polymer-zeolite composite was viewed under SEM and TEM. The LPE template was then calcined away to recover pure mesoporous Silicalite-1 crystals, which have been characterized by TEM, SEM and WAXS. Evidence of confined synthesis of mesoporous zeolite is presented below.

LPE40 has been characterized in detail in the previous section. The same LPE40 sample was used to carry out confined synthesis of Silicalite-1 by the SAC protocol described earlier and in more detail in the appendix. After synthesis, the LPE40 monoliths were washed and dried.

The outer surface of the monolith was viewed by SEM. Large, faceted crystals were seen. These have clearly not been templated in the pores and have just grown by the reaction of zeolite precursors on the outer surface of the monolith. Growth of large untemplated crystals is an indicator that zeolite synthesis conditions succeeded in causing crystal growth (Figure 50).

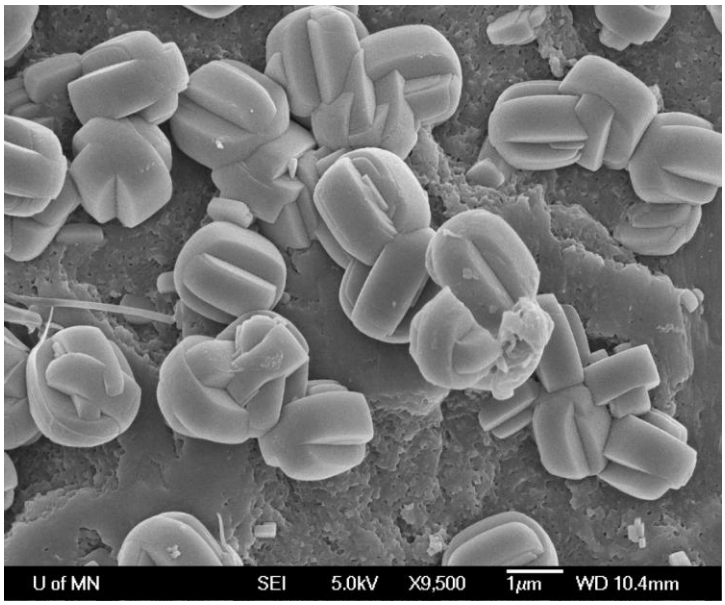

Figure 50: Crystals grown on the outer surface of the monolith (outside the LPE40 pores)

The outer surface of the monolith was then removed by slicing thin layers away from all surfaces. This was done to remove all untemplated crystals. The monolith was cross sectioned and viewed by SEM. The images showed that inorganics were seen growing in the LPE40 pores (Figure 51).

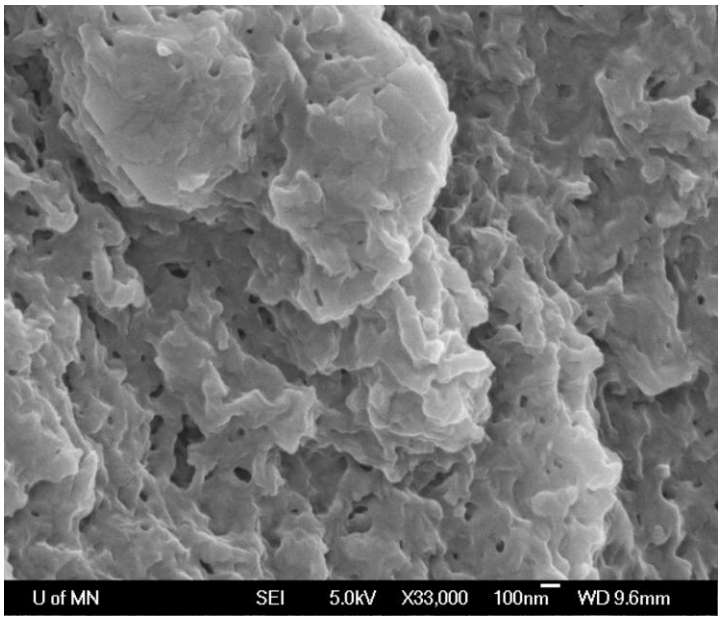

Figure 51: Cross-section of the LPE40 after confined synthesis of zeolite by SAC

The monolith was also microtomed using a diamond knife to prepare ultrathin slices (<100 nm thick) for TEM imaging. The slices were mounted on a TEM grid and high resolution images and electron diffraction patterns were obtained.

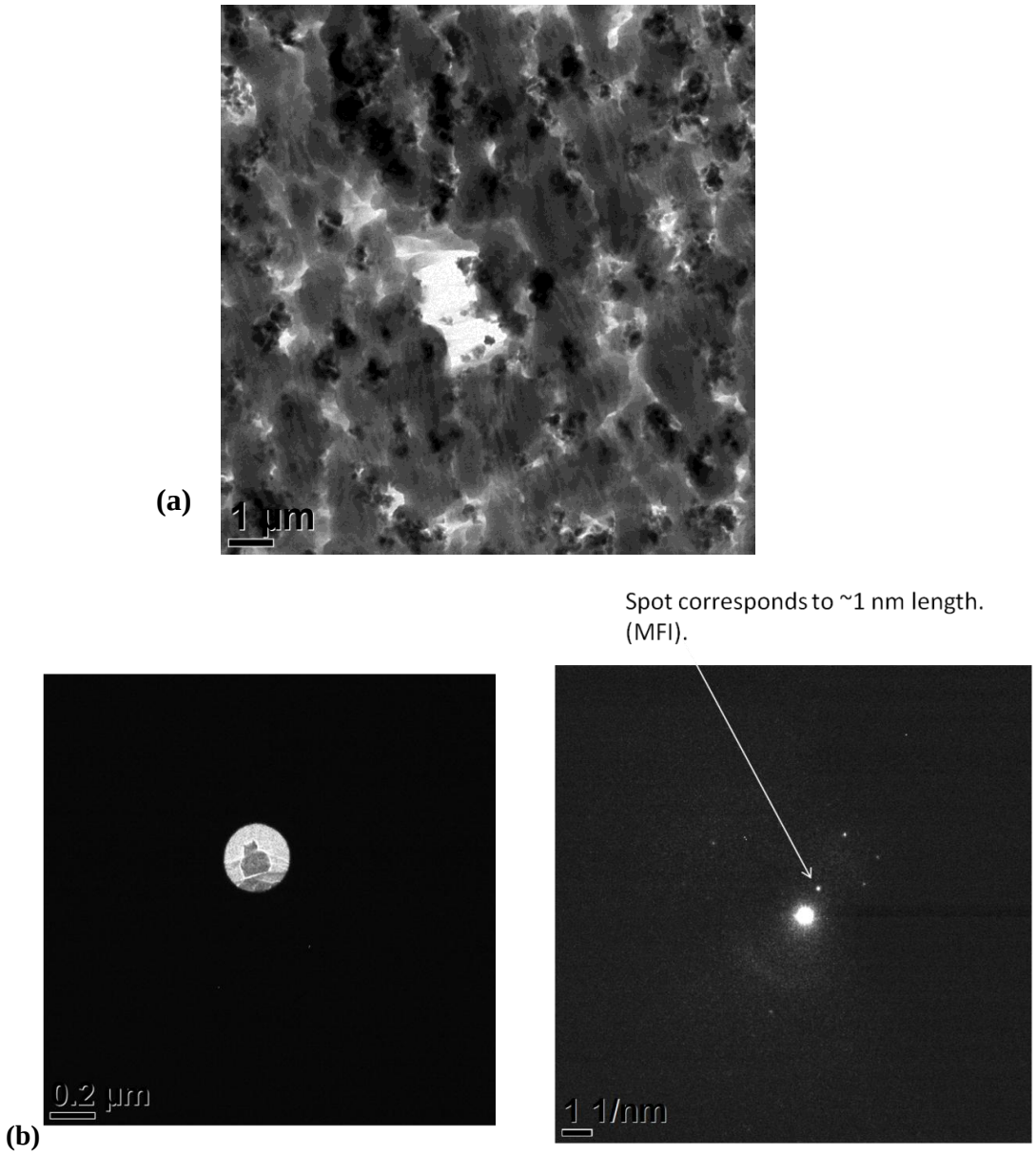

Figure 52: (a) TEM image of microtomed cross section of LPE40 sample. Dense crystalline domains can be seen dispersed in the LPE40 cross section. (b) A small area of crystals was selected and the corresponding electron diffraction spots are from the MFI framework, indicating that zeolite has grown in the LPE40 template.

Figure 52 shows that zeolite has grown throughout the cross section of the LPE40 monolith. Electron diffraction spots from the crystalline zeolite are also seen. Figure 53 shows a high resolution image of a templated zeolite crystal which has a highly unusual crystal morphology due to confined synthesis. The lattice fringes from the crystal upon analyzing by fast fourier transform (inset) gives spots from the MFI framework.

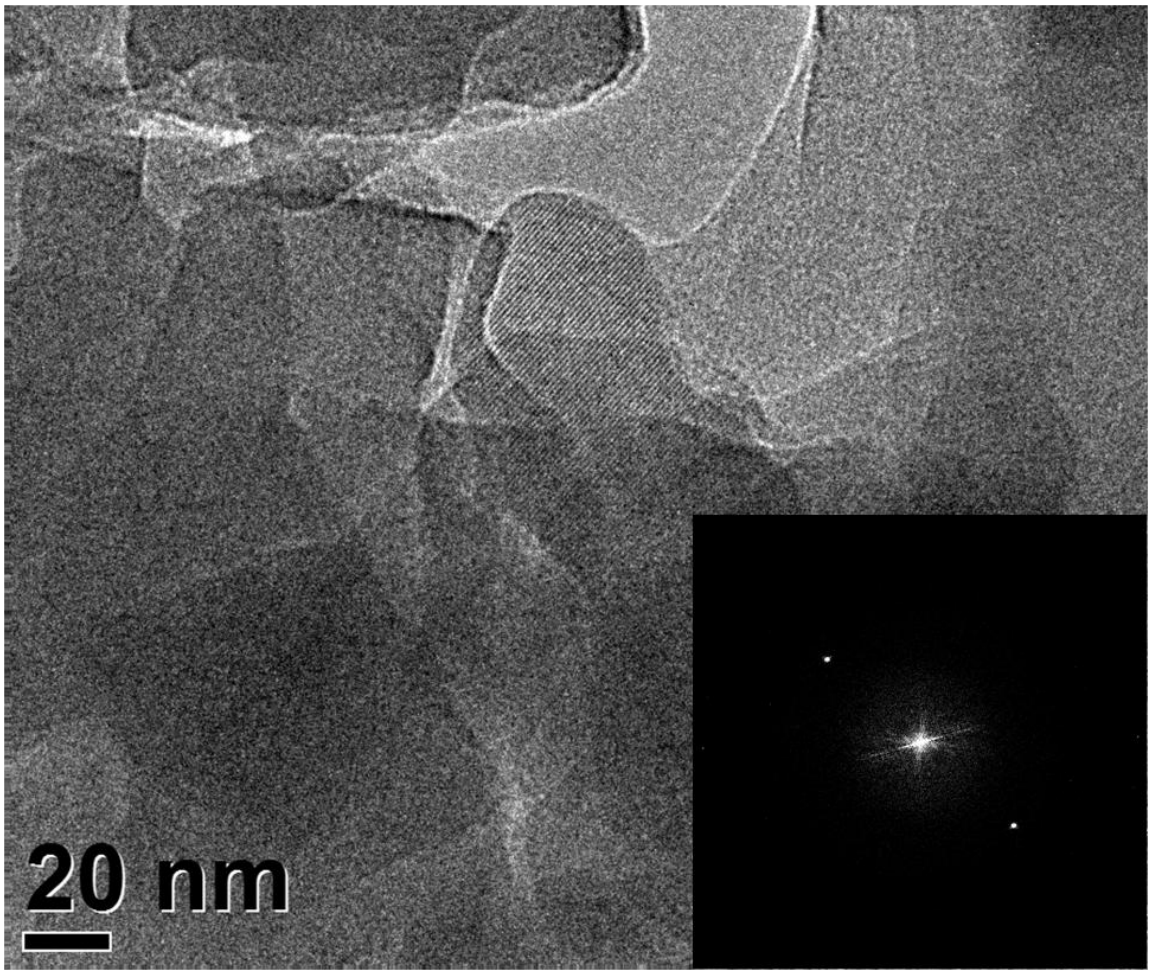

Figure 53: Worm like morphology of templated MFI crystal from LPE40 with width approximately equal to pore diameter. Inset is an FFT of the image showing spots from the zeolite crystal

Next, the polymer was removed from the composite LPE40/Silicalite-1 by calcination in air in a furnace at 550 ^{o}C for 12 hours. The templated zeolite was recovered in the form of a white powder. It was characterized by SEM, TEM and WAXS.

For SEM imaging, the powder sample was directly sprinkled onto a carbon tape mounted on an SEM stub. The sample was coated with Pt to lessen the effect of charging during imaging. Figure 54 shows representative high and low resolution images of crystals synthesized within LPE40. They look mesoporous and each crystal is comprised of smaller domains. At this point, SEM is not sufficient to determine if these have grown as single crystals or if they are simply agglomerates of tinier crystals.

(a)

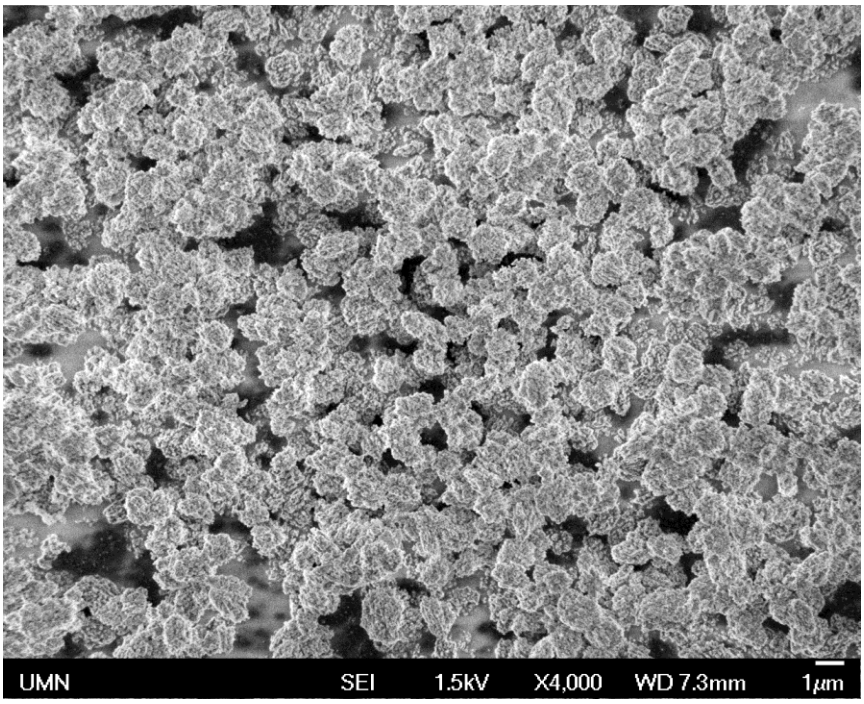

(b)

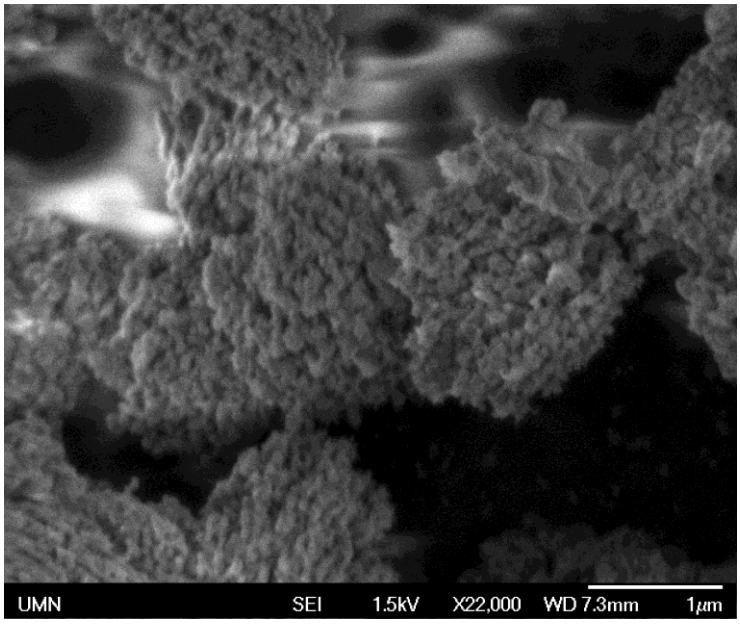

Figure 54: (a) Low resolution SEM image and (b) High resolution SEM image calcined product of confined synthesis large crystals comprised of small domains

In order to elucidate the microstructure of the crystals, WAXS was carried out on the calcined powder (Figure 55). The diffraction pattern obtained from the powder had characteristic peaks corresponding to the microstructure of Silicalite-1.

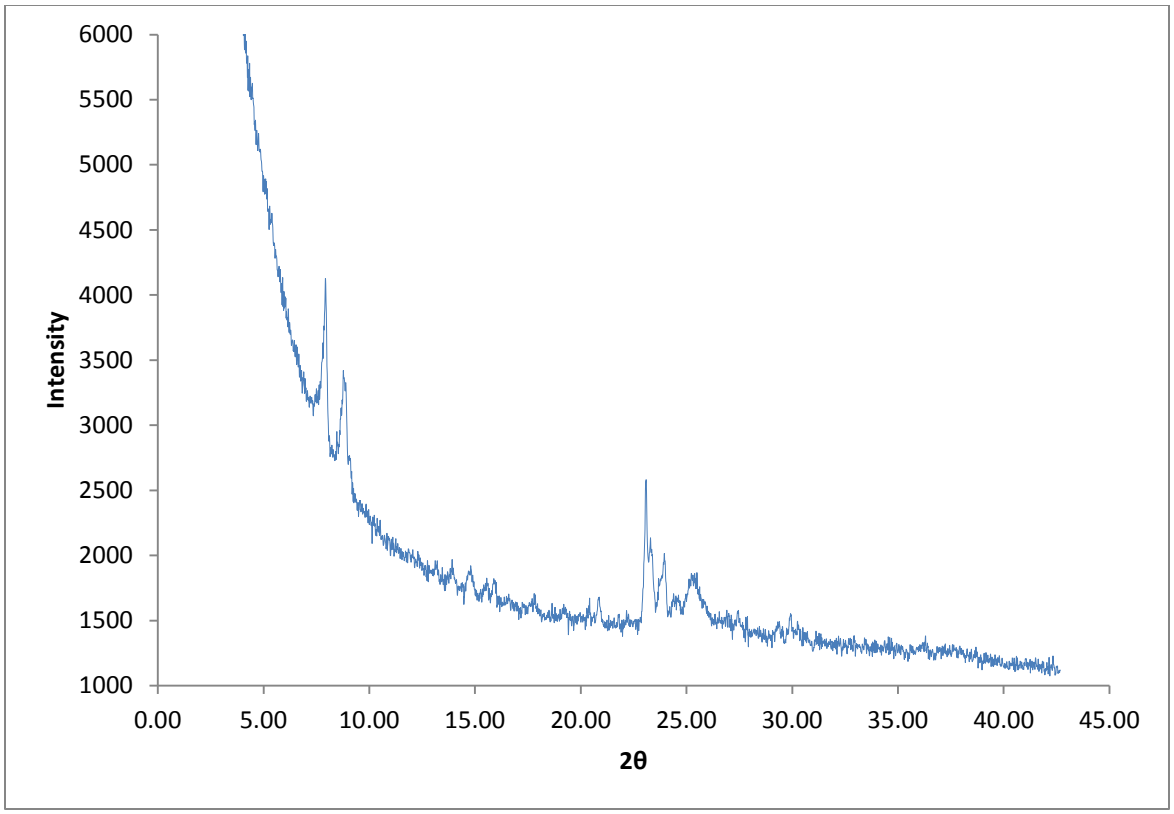

Figure 55: WAXS pattern of calcined zeolite from LPE40. The microstructure corresponds to the MFI framework

To gain a better understanding of the morphology and mesoporosity of the product, TEM imaging was carried out on the calcined zeolite powder. The sample was prepared by making a solution of zeolite powder (~1mg/mL) in isopropanol and depositing a drop of the solution onto a TEM grid. This method reduces agglomeration caused due to drying while ensuring that a sufficient number of particles are deposited on the grid. Low and high resolution imaging allowed visualization of the smaller domains and the mesoporous structure of the crystals. Selected area electron diffraction was also done and yielded an electron diffraction pattern corresponding to b-oriented MFI crystal (Figure 56).

(a)

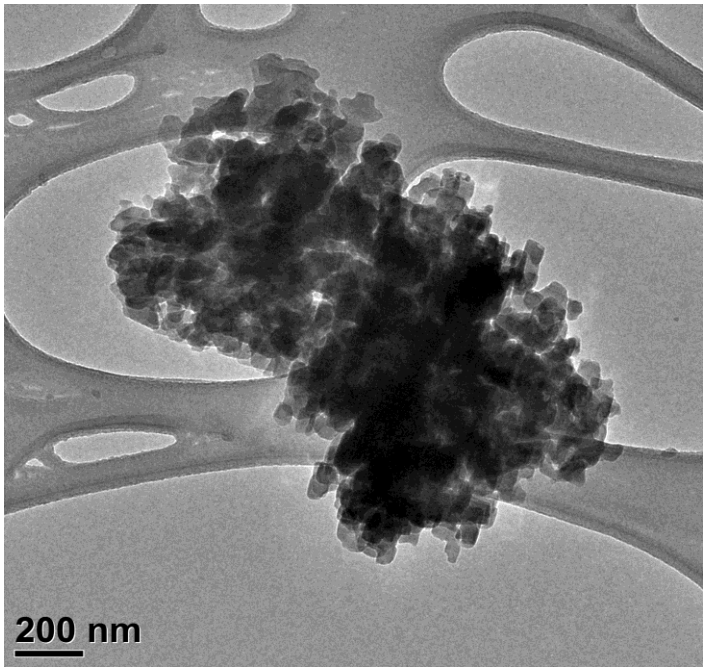

(a)

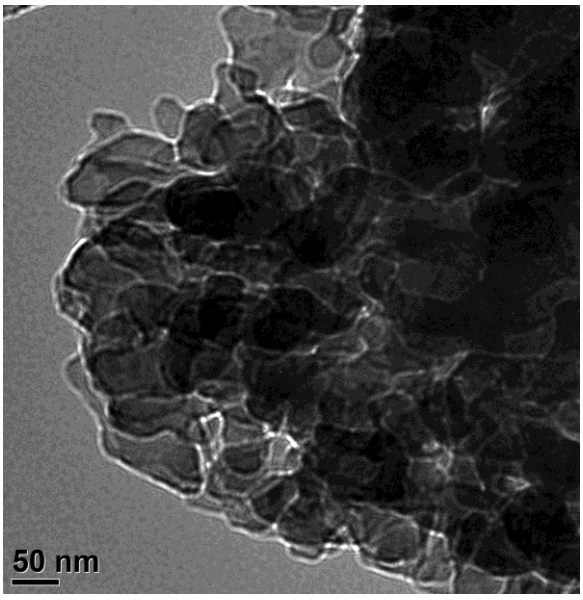

(b)

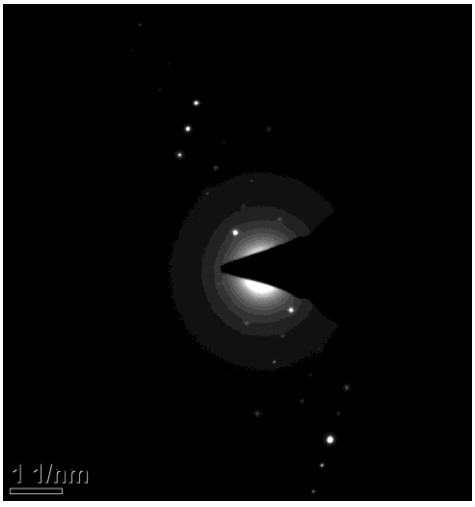

Figure 56: (a) TEM images of a mesoporous MFI crystal grown in LPE40. (b) Selected area of crystal for SAD (c) Electron diffraction pattern corresponding to selected area

The crystal is too thick to see the smaller domains clearly, so the edges of the crystal were visualized at high resolution (Figure 57). At the edges, the crystal is thinner and small crystalline domains that are templated in the LPE40 pores can be clearly seen. Lattice fringes corresponding to the MFI crystal are also visible.

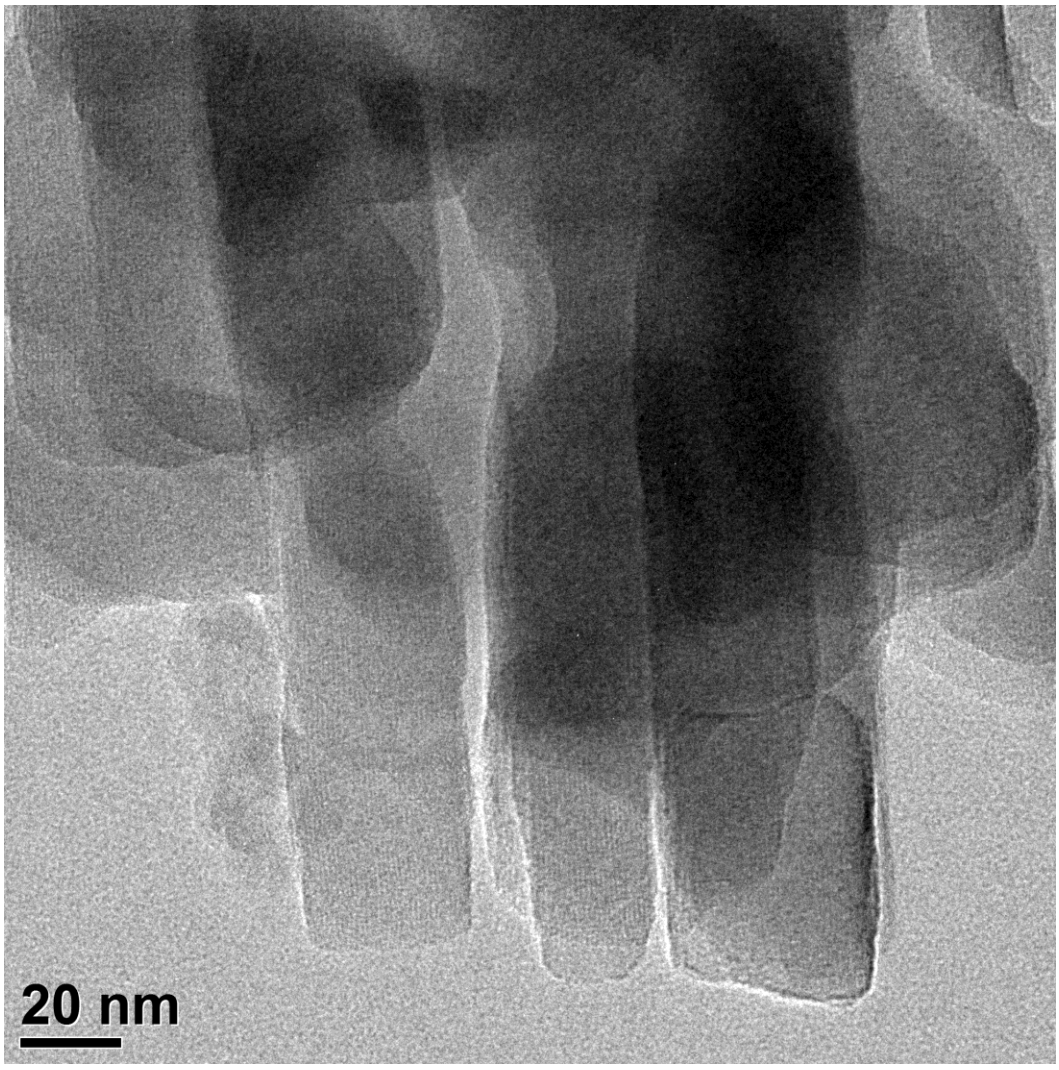

Figure 57: TEM image of the domains of a mesoporous zeolite crystal. The width of the projecting domains corresponds to the mesopore size of the LPE40 polymer

A few other experiments were carried out with other LPE samples with different pore sizes. Figure 58 shows an example of zeolite templated in 28nm pore size LPE. The details of this experiment are not presented here because of insufficient characterization

due to limited amount of sample synthesized. However, it shows that there is scope for synthesizing a variety of crystal sizes and shapes in different porous LPE templates.

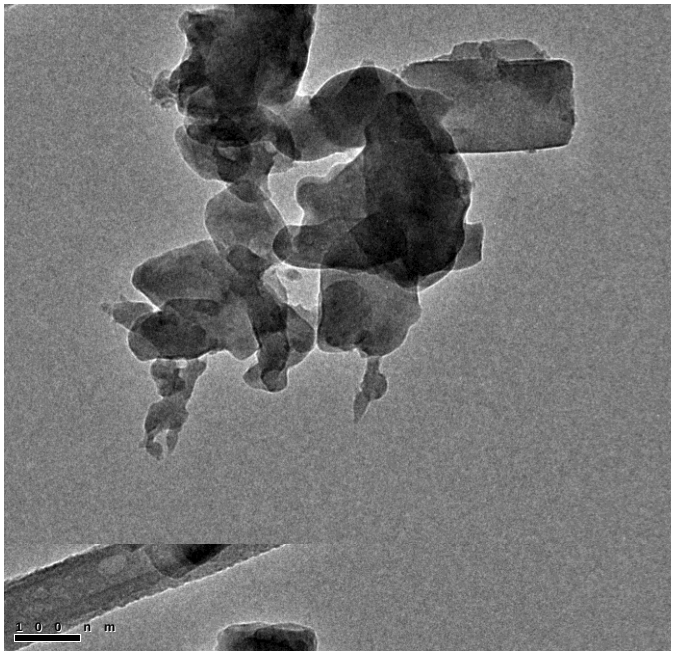

(a)

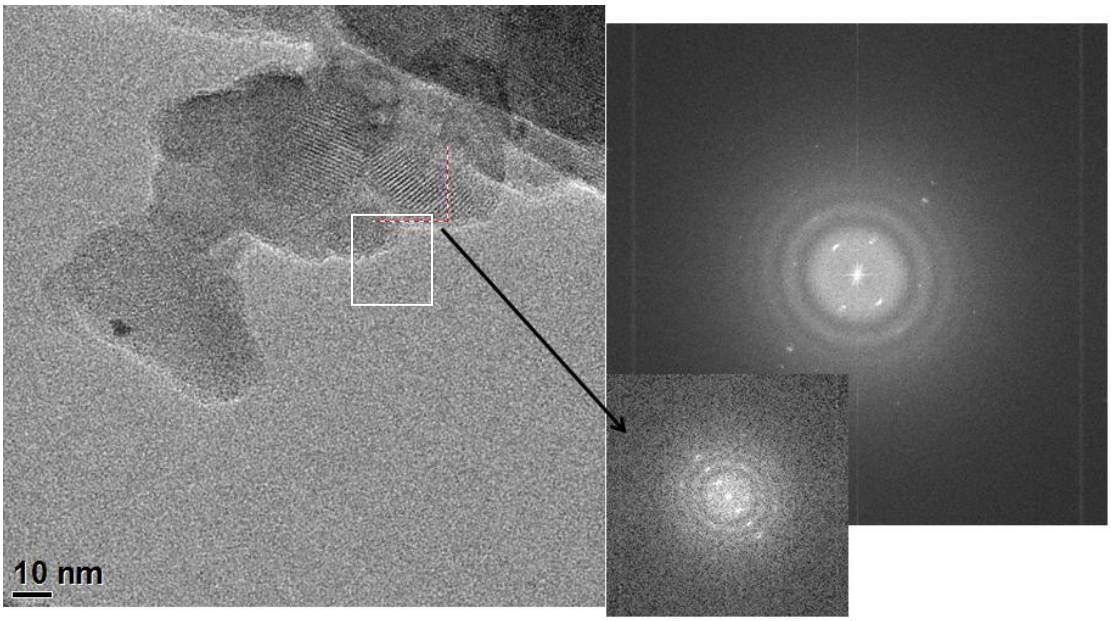

(b)

Figure 58: (a) Another example of a crystal grown in a different experiment in LPE (experiment not discussed in the text) with a small average pore size (~28 nm) (b) Diffraction patterns show presence of spots corresponding to MFI framework

The results presented in this section show that the steam assisted crystallization technique described for the confined synthesis in 3DOm carbon has been successfully reproduced for nanoporous polymer (LPE) template LPE40. A similar set of experiments were conducted for confined synthesis in LPE50 (mean pore size 50 nm). The characterization of polymer and experiments for confined synthesis of zeolites in LPE50 have been discussed in the next two sections.

Characterization of porous polymer (LPE50):

Porous LPE50 was made by the protocol outlined earlier. It was characterized by SEM and nitrogen adsorption.

SEM imaging was done on a cryo-fractured cross section of the LPE50 monolith, done after freezing the monolith in liquid nitrogen. Cryo-fracturing is necessary for correct pore visualization because room temperature sectioning causes pores to distort due to the ductile nature of LPE50. Figures 59 and 60 show low and high resolution images of the pores structure, which is clearly highly bicontinuous. The high porosity (70%) of this polymer is also evident from the images.

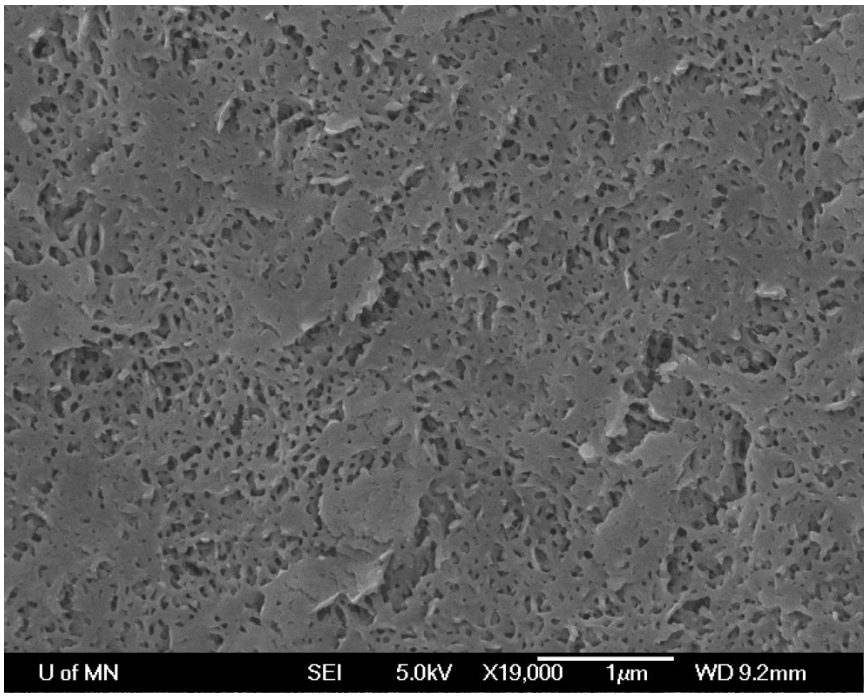

Figure 59: Low resolution SEM image of LPE50

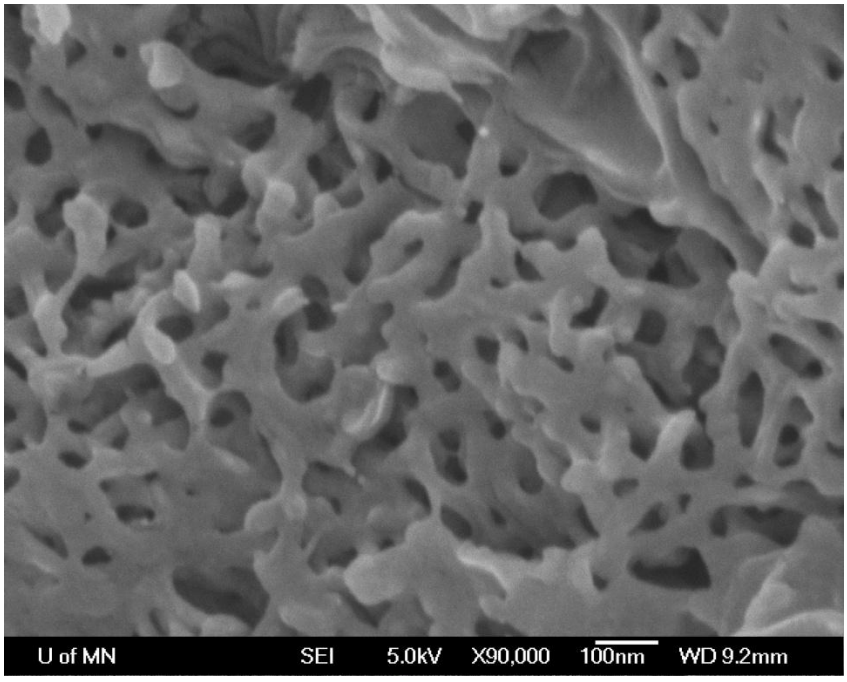

Figure 60: High resolution SEM image of LPE50

Nitrogen adsorption was carried out on the LPE50 sample. The adsorption and desorption isotherms are presented in Figure 61. The presence of a clear hysteresis loop between them points to the mesoporosity of the LPE50 sample. The nitrogen adsorption data was analyzed by the standard BET method and pore size distributions were calculated using the BJH method.

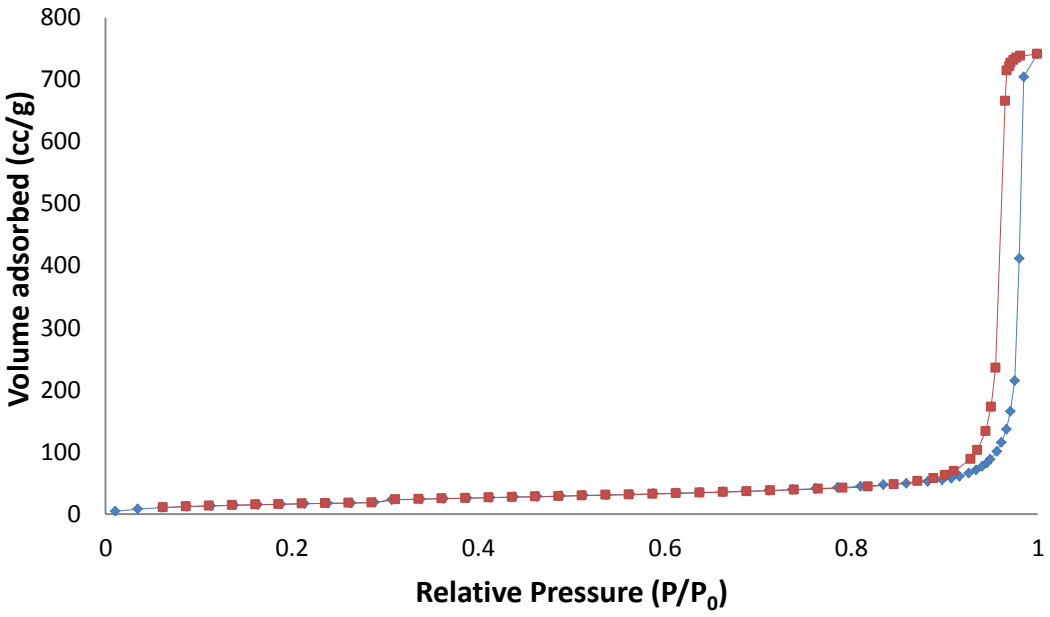

Figure 61: Nitrogen adsorption data for LPE50 shows that it is mesoporous

The BJH analysis for the average pore diameter is calculated from the incremental pore volume change, from the desorption isotherm. The average is taken as the peak. Average pore size is ~50 nm as can be seen from Figure 62. This polymer sample has been called 'LPE50' based on its pore size. However, there is a fair amount of polydispersity in the sample.

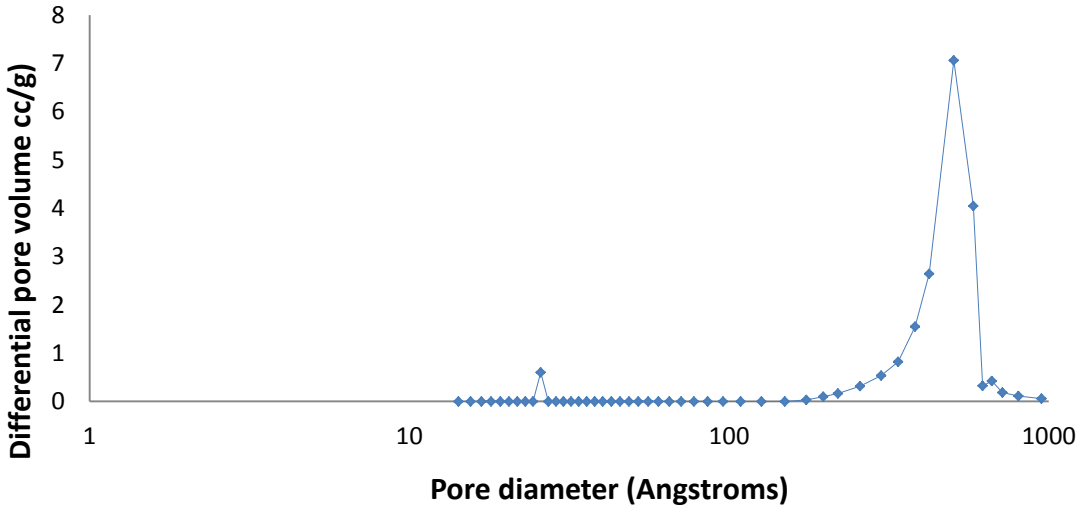

Figure 62: BJH pore size distribution of LPE50 shows that mean pore size is about 50 nm

Next, the porous LPE50 template was steamed at zeolite synthesis conditions to check for pore integrity. This was done to quantify pore structures before and after steaming under zeolite synthesis conditions. It was found that he BJH pore distribution does not change significantly (Figure 63), indicating that there is no pore collapse or deformation during the steaming process and the pore structure stays intact.

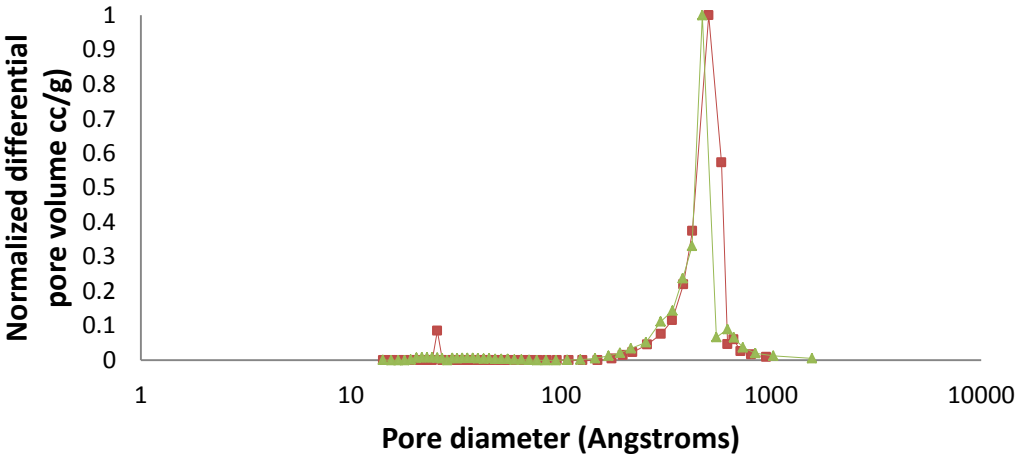

Figure 63: BJH pore sizes of steamed LPE50 (squares) is almost the same as original LPE50(triangles)

Confined synthesis of zeolite in LPE40:

Confined synthesis was carried out by steam assisted crystallization at 90^{o}C for 5 days. After synthesis was completed, the monoliths were recovered and washed and dried.

The surface of the monoliths were examined under SEM after coating with Pt to reduce charging during microscopy. Large, well faceted zeolite crystals could be seen (Figures 64 and 65). These crystals are clearly not templated and have grown on the monolith surface, outside the pores. They are an indication that the synthesis experiment succeeded in crystallizing the zeolite precursors into zeolite.

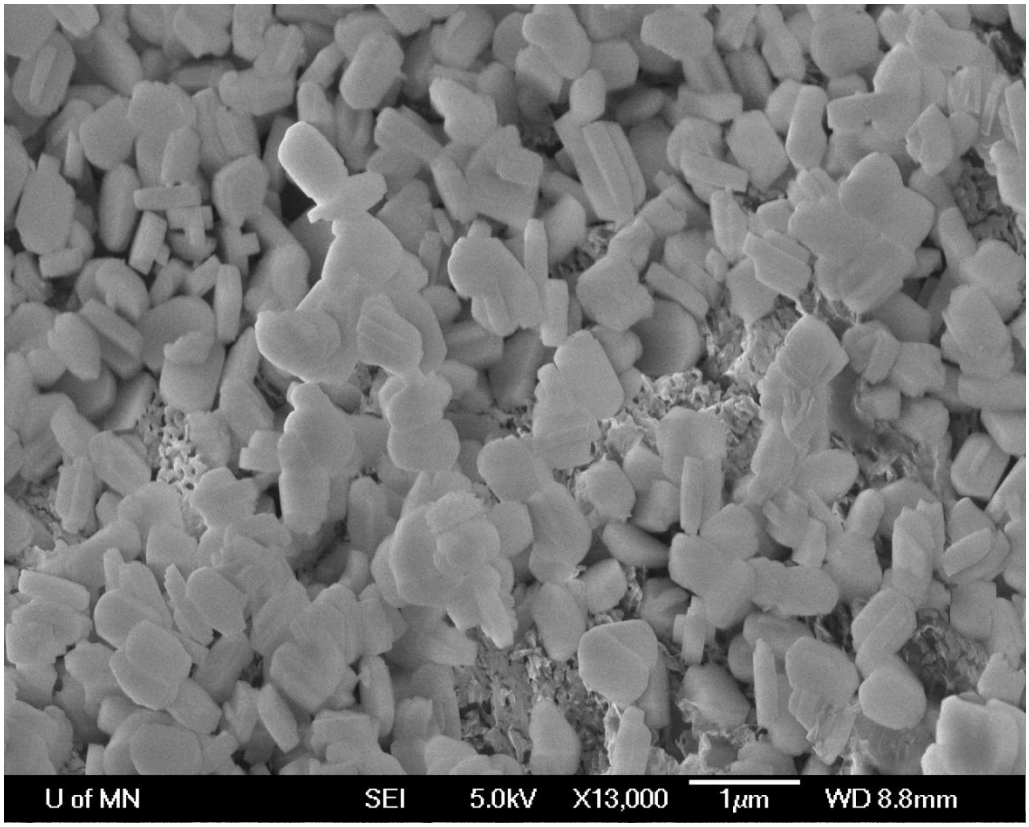

Figure 64: Non-templated Silicalite-1 crystals grown outside the pores of LPE50

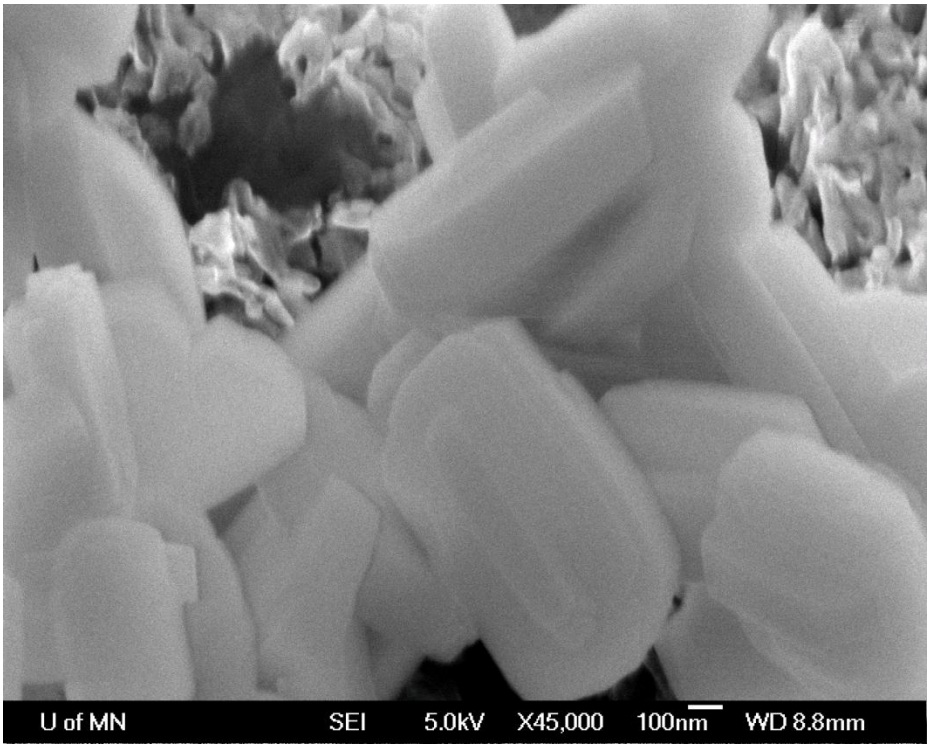

Figure 65: High resolution SEM image shows that the crystals growing outside the pores have smooth facets

Thin slices of the outer surface of the monolith were then cut off and discarded in order to remove the large untemplated crystals. The resulting zeolite/LPE50 composite was sectioned with a blade at room temperature and the and cross section was coated with Pt to prevent charging and then visualized by SEM. Zeolite crystals can be seen growing in the cross section. They are penetrated by the pore walls of LPE50. The templating can clearly be seen in Figures 66 and 67.

(a)

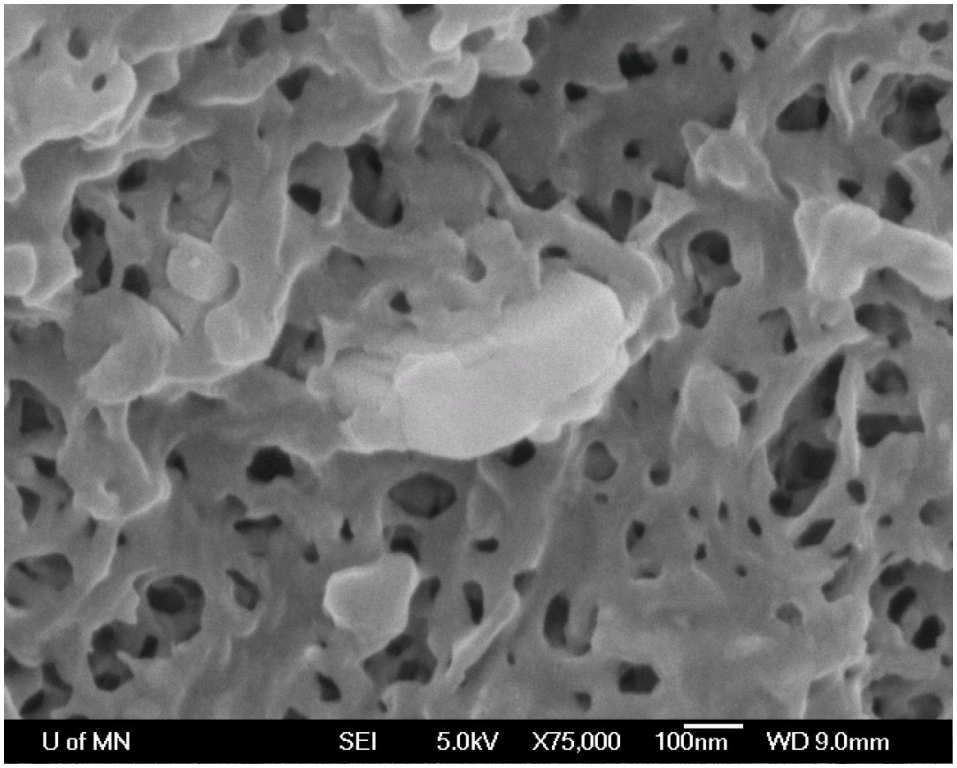

(b)

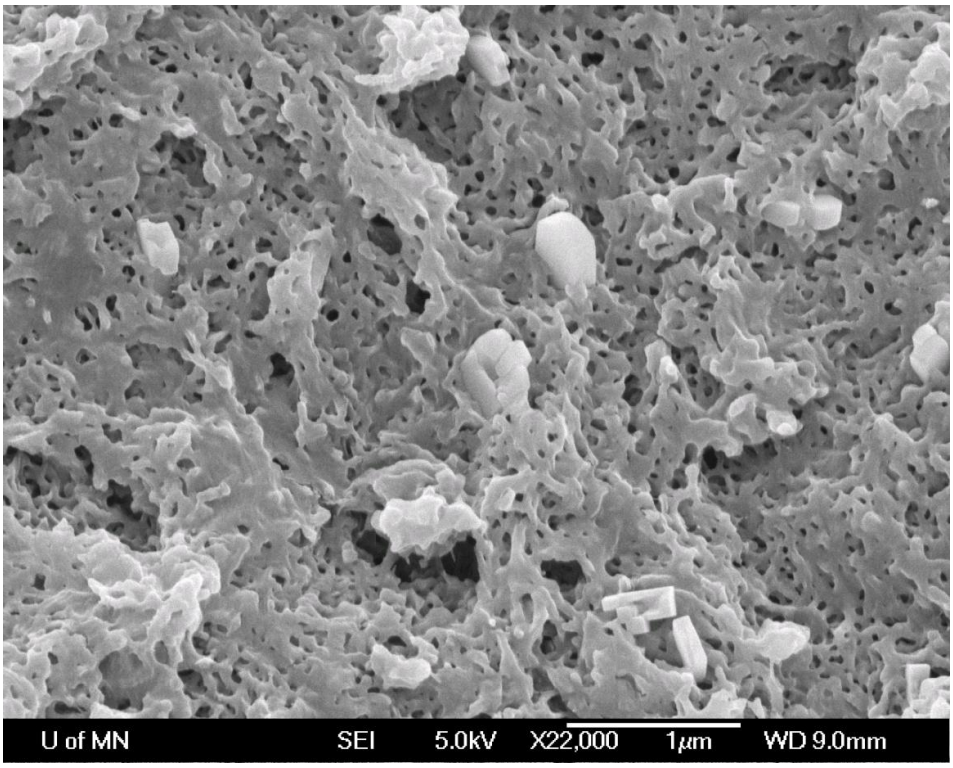

Figure 66 (a), (b): Cross sections of LPE50 template showing templating of Silicalite-1 crystal in the LPE pores

The LPE50 was then burnt from the composite by calcination at 550^{o}C for 12 hours, leaving behind a white zeolite powder. The calcined zeolite was characterized by SEM, Nitrogen adsorption, WAXS and TEM.

SEM samples were prepared by sprinking the calcined zeolite powder on a carbon tape mounted on an SEM stub. The sample was coated with Pt to prevent charging during imaging. Figures 67, 68 and 69 show representative images of the sample. These crystals look considerably thicker than the ones synthesized in the LPE40 template. One of the reasons could be that the synthesis time was 12 hours longer in this case. It would be interesting to see the growth of these mesoporous crystals with time in further studies. The crystals tend to the characteristic hexagonal shape of MFI crystals but are irregular and smaller domains can be seen, specially towards the edges and on the cross section of the crystal. SEM offers limited visualization of mesoporosity and morphology of the smaller domains. It also does not tell us about single crystallinity of these crystals. For detailed characterization, WAXS, TEM and nitrogen adsorption were carried out on this sample.

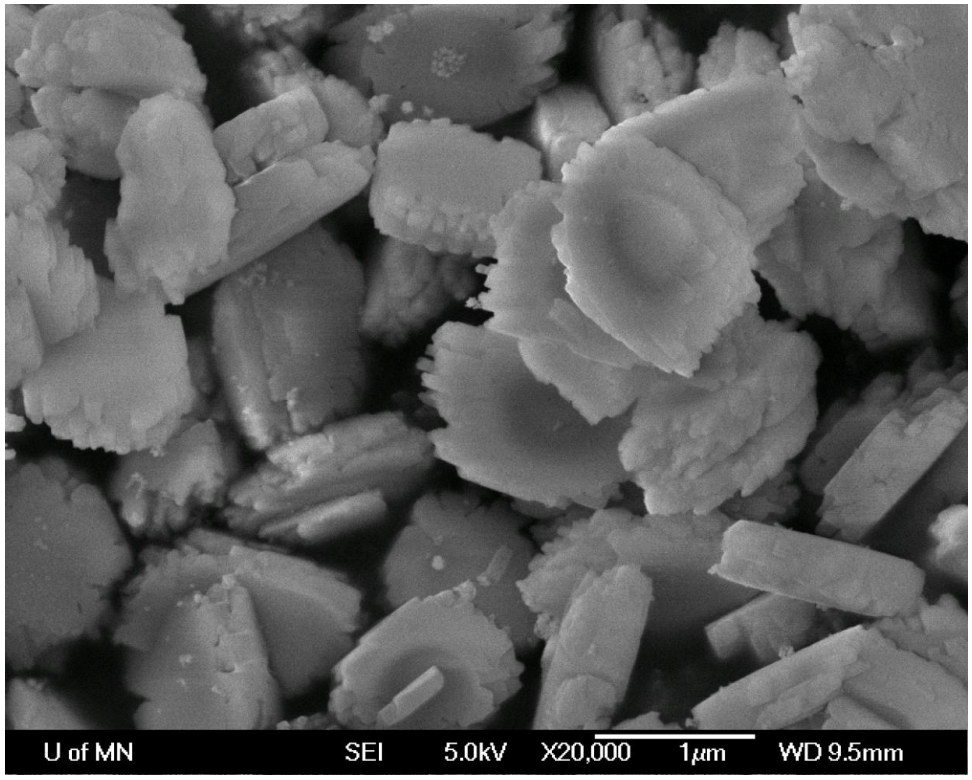

(a)

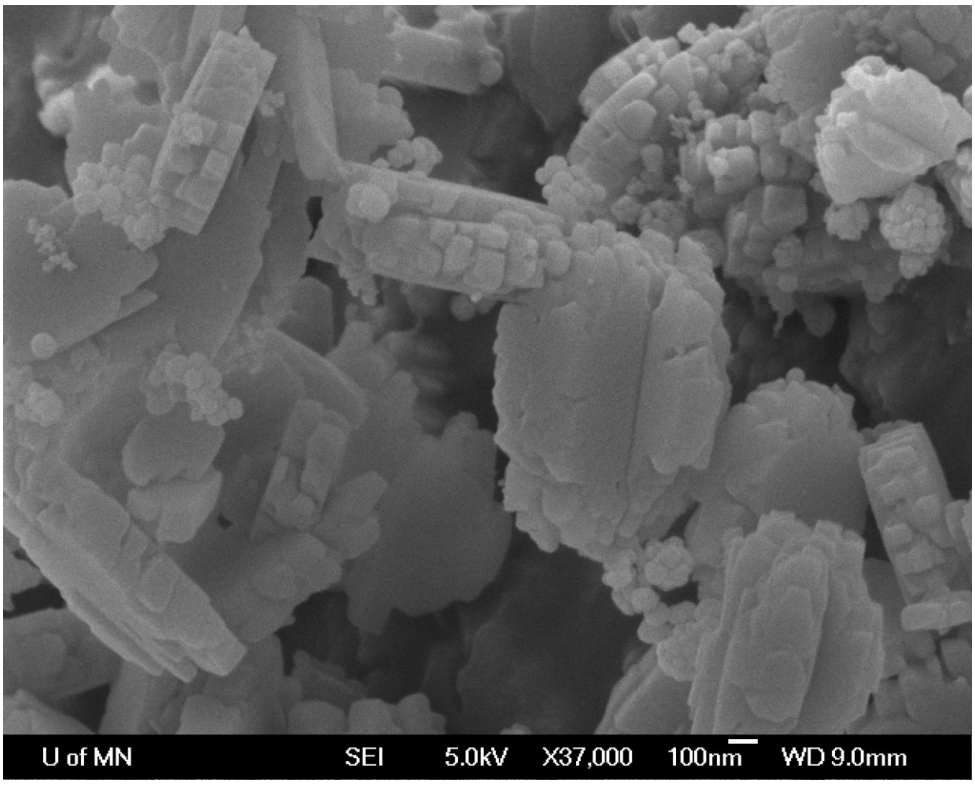

(b)

Figure 67: (a), (b) are representative images of templated Silicalite-1 crystals recovered after removing the LPE50 template by calcination

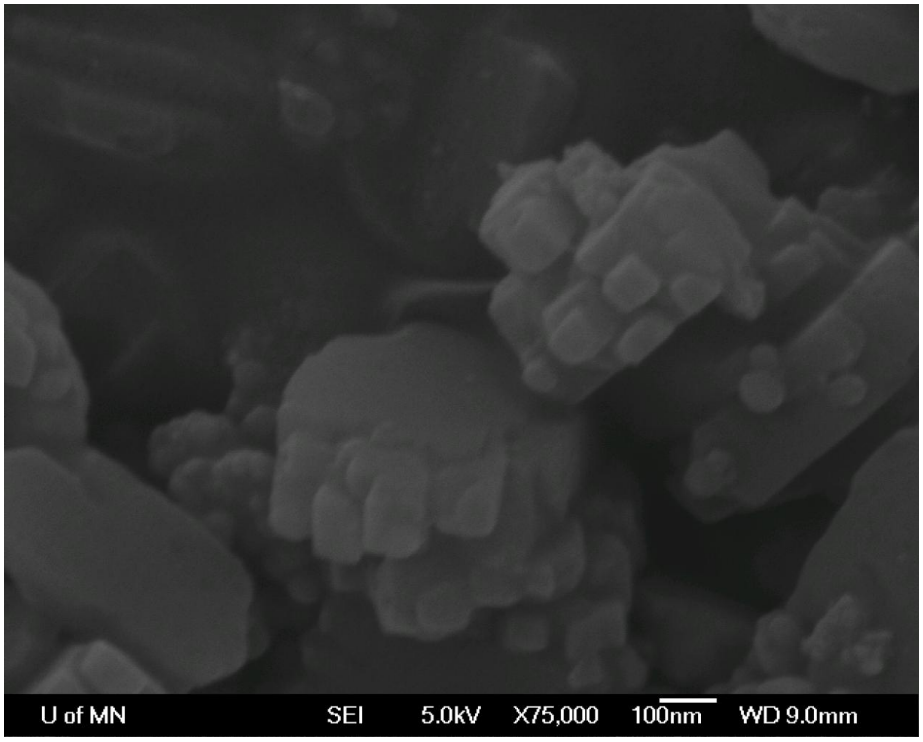

Figure 68: High resolution SEM image showing smaller domains which comprise a mesoporous Silicalite-1 crystal grown in LPE50

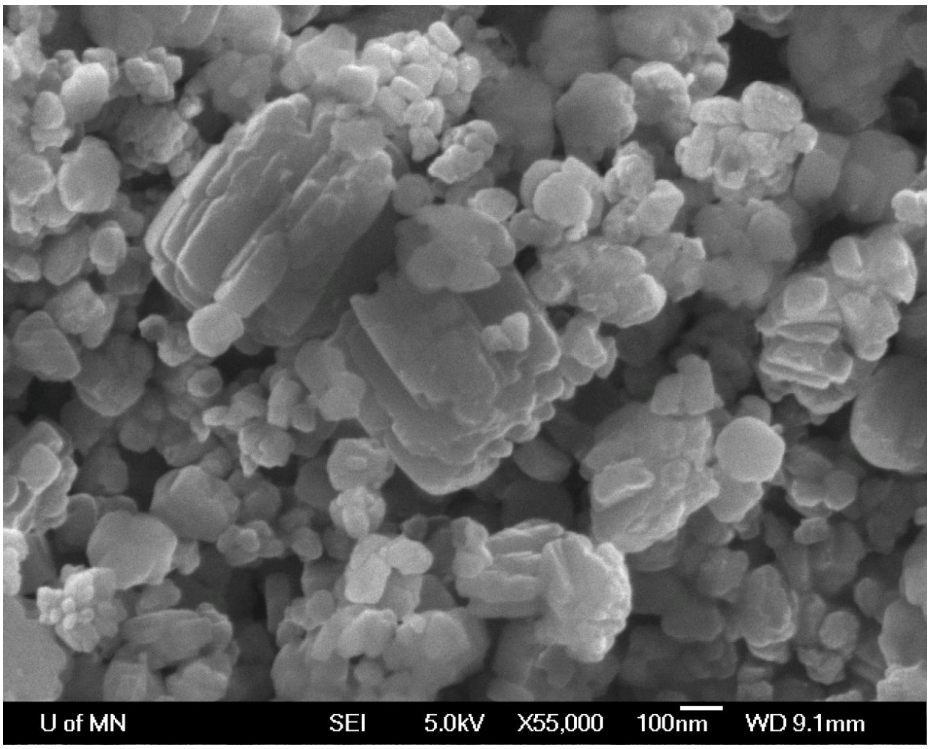

Figure 69: Few nanocrystals are also observed in addition to mesoporous Silicalite-1 grown in LPE50

Sufficient zeolite (~30 mg) was synthesized for characterization by nitrogen adsorption. There is a hysteresis loops between the adsorption and desorption isotherms over a large range of pressure, which indicates a large, dispersion of mesopores (Figure 70). The standard BET analysis was done to calculate pore volumes and surface areas and the BJH method was applied to calculate pore size distribution in the sample. The BJH analysis for the average pore diameter is calculated from the incremental pore volume change, from the desorption isotherm. The average is taken as the peak.

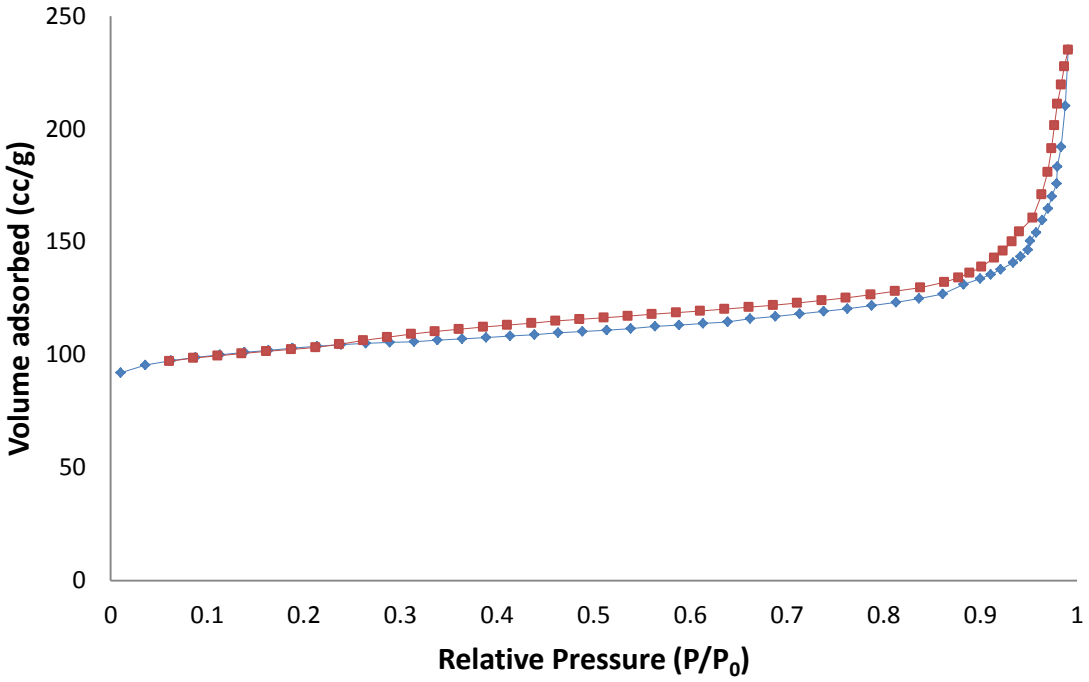

Figure 70: Nitrogen adsorption data – adsorption and desorption isotherms for mesoporous Silicalite-1 grown in LPE50

The BJH pore sizes have been plotted in figure 71. The pore size distribution is wide as predicted. The mesopores seem to be bimodal with one set of pores clustered around 23 nm and the other clustered around 80 nm. For comparision, the BJH pore size distributions of empty and steamed LPE50 have also been plotted. It is difficult to interpret the pore sizes of obtained in the Silicalite-1 product. The peaks in the distribution point to the domain sizes of the LPE in the LPE50 template, which we do not know quantitatively. SAXS can be potentially done to determine domain sizes of LPE and make a quantitative comparision. However, it is certain that the zeolite templated in the LPE50 is mesoporous – a useful property that could lend it importance in applications like catalysis.

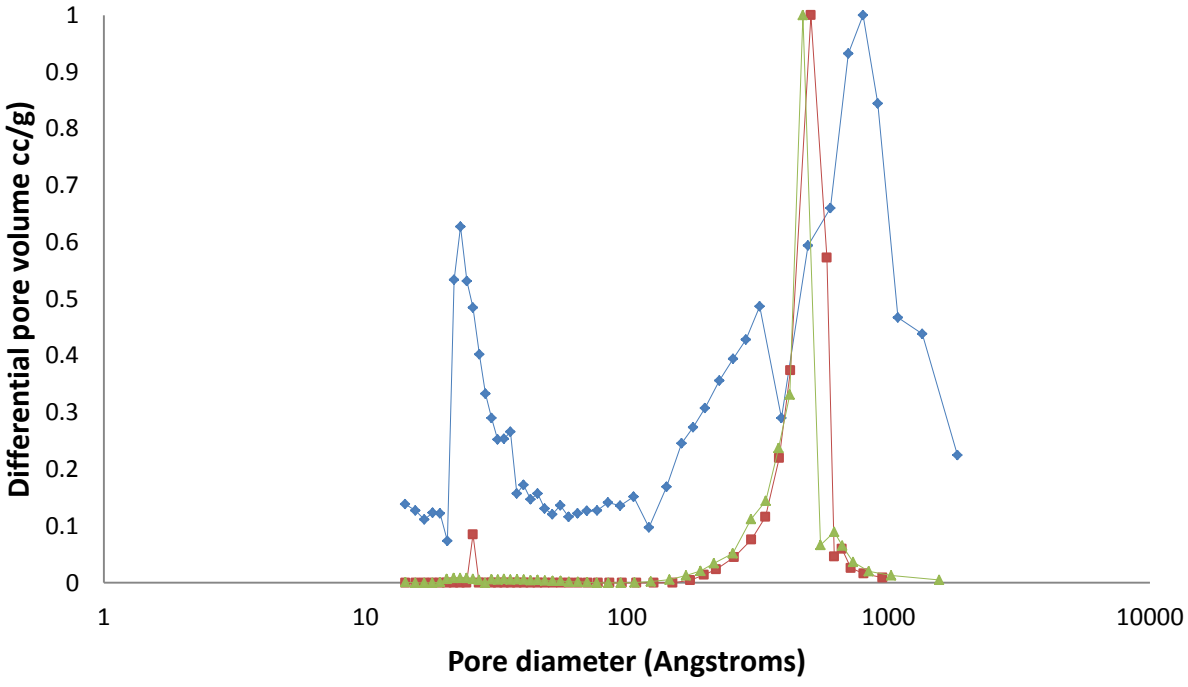

Figure 71: BJH pore sizes for LPE50 (squares), steamed LPE50 (triangles) and Silicalite-1 grown in LPE50 (diamonds)

WAXS was performed on the sample in order to elucidate its microstructure. The diffraction pattern obtained was compared to a simulated powder diffraction pattern and

it was determined that the pattern was indeed from the MFI framework of Silicalite-1 (Figure 72).

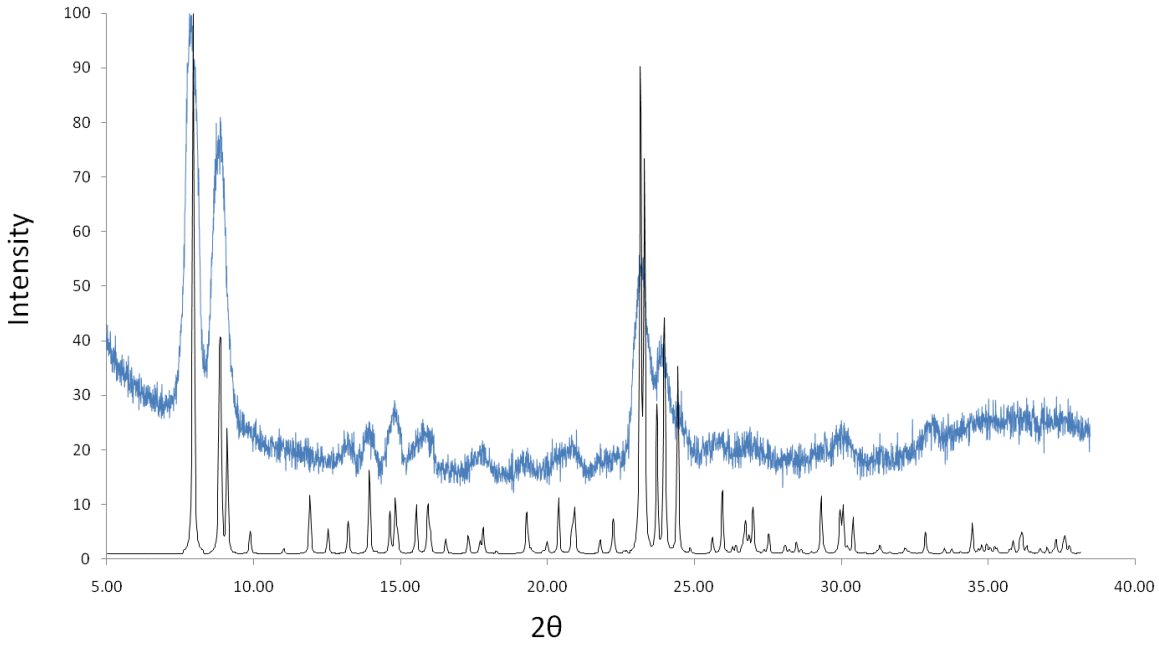

Figure 72: WAXS pattern of calcined product (blue) grown in LPE50. The microstructure corresponds to the MFI framework (black).

In order to characterize the morphology and mesoporosity of the final product in detail, TEM imaging was done. Techniques employed were low and high resolution imaging, dark field imaging and electron diffraction. Figure 73 shows a typical low resolution image of a single crystal. The crystal appears very thick and for high resolution imaging, the edges of the crystals were used in order to obtain good visualization of the smaller domains (Figure 74).

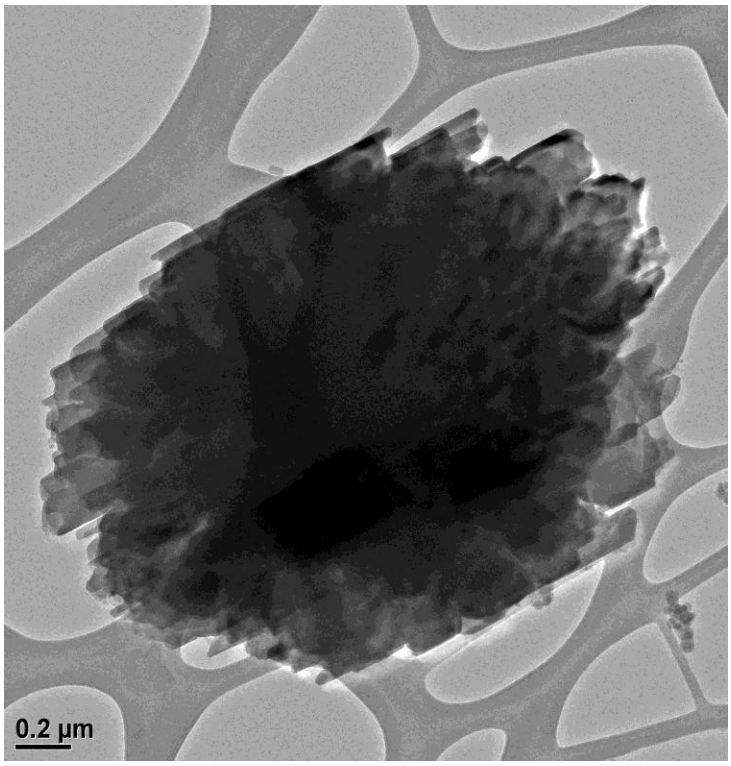

Figure 73: Low resolution TEM image of a single mesoporous crystal grown in LPE50

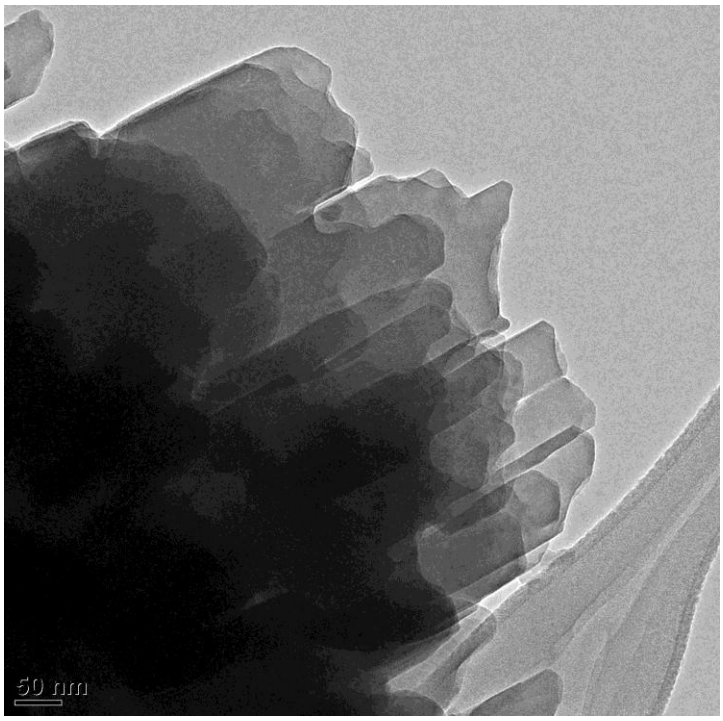

Figure 74: High resolution TEM image clearly shows small domains which are part of a mesoporous single crystal templated by LPE50

High resolution images of the crystal's edge show lattice fringes from MFI crystal (Figure 75). Upon taking a fast fourier transform of the image, diffraction spots from the MFI framework can be seen (inset in Figure 75). The features seen here projecting outward have diameters in the range of pore sizes of the original template, which is further proof of templating within LPE50 pores.

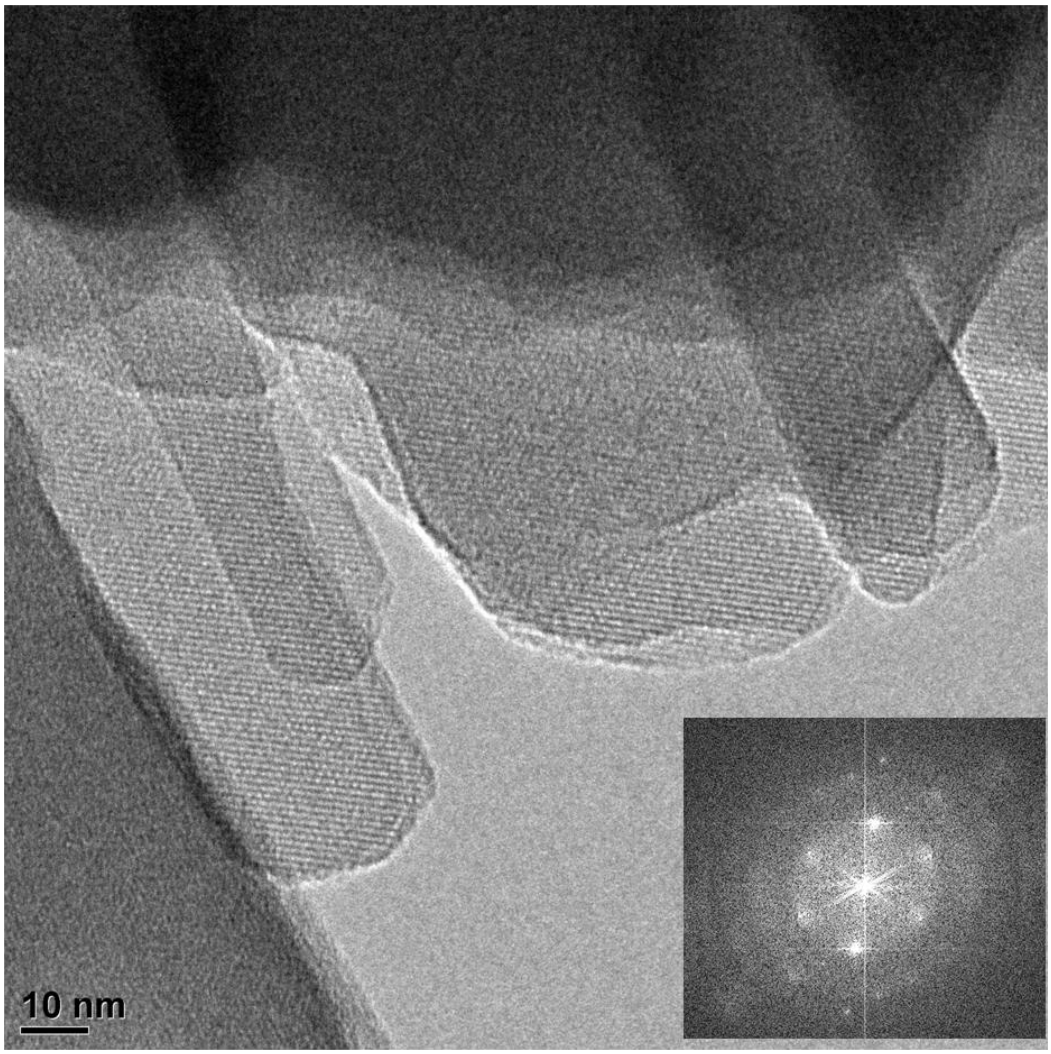

Figure 75: Lattice fringes corresponding to the MFI framework can be seen clearly in the mesoporous crystal templated in LPE50. Inset is an FFT of the image showing spots which are at a distance corresponding to the unit cell of Silicalite-1

Electron diffraction patterns from the crystals comfirmed that the crystals are single crystalline and not agglomerates of smaller nanocrystals (Figure 76). 76(a) and (b) show the aperture being positioned around the entire crystal and 76(c) shows the corresponding electron diffraction pattern.

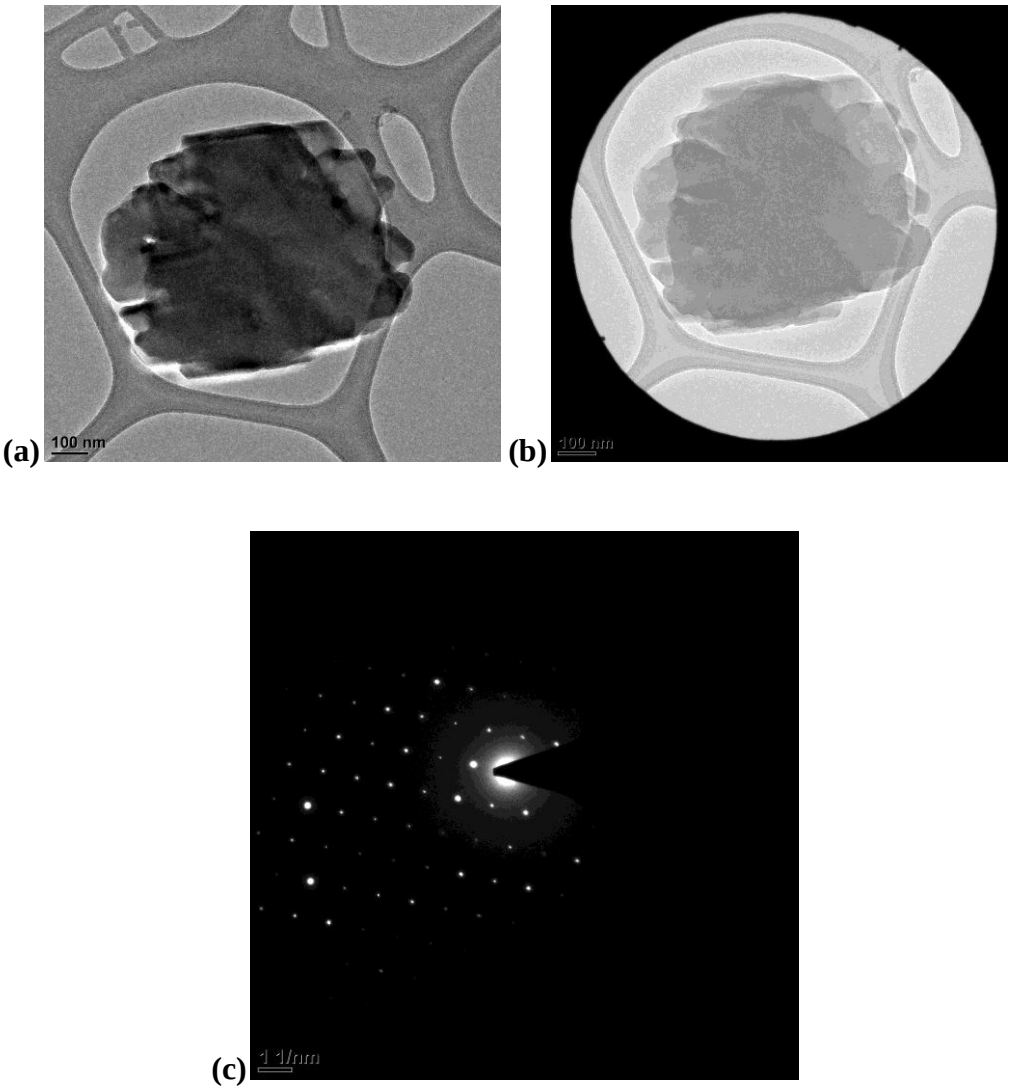

Figure 76: (a)A crystal of Silicalite-1 grown in LPE50 (b) Aperture over the crystal (c) Electron diffraction pattern from a crystal shows that this is a b-oriented single crystal of Silicalite-1.

In conclusion, the templated Silicalite-1 crystals have mesoporosity as confirmed by the nitrogen adsorption data and BJH pore size distribution for the LPE50 sample. The average mesopore size corresponds to the size of the LPE domains in the template, which can be determined by SAXS. Visually, the crystals tend towards the typical coffin shape of MFI but are irregular and don't have smooth facets because they are comprised of smaller crystalline domains grown in the LPE pores. The TEM images allow us to visualize the mesoporosity of these crystals. The single crystallinity of the product crystals has also been confirmed by the electron diffraction pattern.

3.3 Conclusions

The steam assisted crystallization method to grow mesoporous Silicalite-1 in a polymer template of controllable pore size has been presented. The method produces roughly uniformly sized crystals of zeolite with a mesoporosity which is dictated by the polymer template. These mesoporous Silicalite-1 crystals could be useful for catalysis and catalytic testing could be done after incorporation of alumina into the MFI framework. The LPE template has been shown to be stable under severe hydrothermal steaming conditions required for zeolite synthesis. This property could be exploited to grow other materials by the steaming technique. Metal organic frameworks (MOFs) could be an interesting class of materials to template using linear polyethylene.

4. Solvothermal synthesis of zeolites in nanoporous polymer templates

4.1 Introduction and Motivation

Steam assisted crystallization has been used so far for confined synthesis in polymer templates. The main reason for selection of this technique is that conventional bulk solution synthesis methods are based in an aqueous medium. The porous polymers that were used so far were hydrophobic and could not be modified to make them hydrophilic. Because of this compatibility issue, hydrothermal methods could not be used to grow zeolite inside the polymer monoliths. Solution based methods are an alternative route to steaming. Solution based methods are faster and usually more effective at crystallization than vapour phase transport methods. Instead of water based zeolite synthesis solution, if an organic solvent can be used, it could potentially provide an alternative method for confined synthesis. Such methods do exist and are called solvothermal methods. The problem with them is that they have not been very extensively studied and only a limited number of recipes exist in literature to grow zeolites in organic solvents. We know that all organic solvents cannot act as media for zeolite synthesis: some degree of polarity needed. However, the higher the polarity, the greater the hydrophilicity and the lesser the polymer pore wettability. We need a medium with moderate dielectric constant that is high enough for zeolite synthesis, but at the same time, low enough so that it can wet polymer pores.

4.2 Results and Discussion

4.2.1 Selection of medium and method

A number of organic solvents, mainly diols and triols have been used in the past to synthesize zeolite. However, diols and triols were found to be too viscous and hydrophilic to penetrate polymer (LPE) pores. Hence, ethanol was selected as medium as it wets polymer pores and has been used for solvothermal synthesis in the past. Solvothemal synthesis methods are usually very slow when a conventional oven is used to provide the heat. Traditional methods have long synthesis times at temperatures below 100 ^{o}C (~21 days) and a few days at 150-200 ^{o}C. In order to speed up the synthesis process, a microwave reactor was used to provide heat for the reaction. Microwave synthesis: Takes ~3 hours at 180 ^{o}C. The MARS-5 microwave reactor, (2.45GHz) from CEM Corporation was used. Chen et al. have studied synthesis of Silicalite-1 in a microwave reactor using solvents with different dielectric constants (including ethanol). We propose to modify the existing recipe to synthesize zeolite at lower temperatures (within 100^{o}C) so that the synthesis method is compatible with polymers.

4.2.2 Recipe to grow Silicalite-1 at a low temperature

First, the microwave synthesis reported by Chen et al. in 2009 was reproduced. Synthesis temperature was 180 ^{o}C and synthesis time was 18 hours. Composition of synthesis solution was 1.0 SiO_2: 0.357 TPAOH: 12.0 EtOH: 1 H_2O. The components were mixed under uniform stirring and allowed to age for 1 day, following which the microwave reaction was started. At the end of the reaction, the solution was filtered to recover the zeolite crystals and washed with ethanol and DI water. SEM and WAXS confirmed that Silicalite-1 had been synthesized by this method. Then, the synthesis

temperature was reduced and synthesis time for growth of zeolite was experimentally determined. It was found that at 100^{o}C, microwave synthesis for 18 hours resulted in crystallization of Silicalite-1. The characterization results are summarized below.

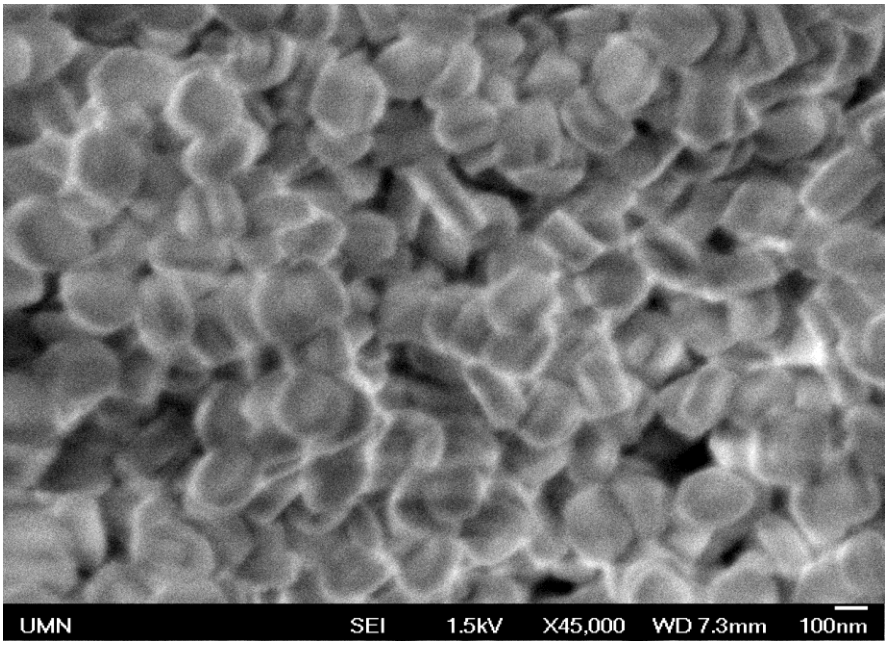

Figure 77: Silicalite-1 crystals synthesized in bulk solution at 180^{o}C

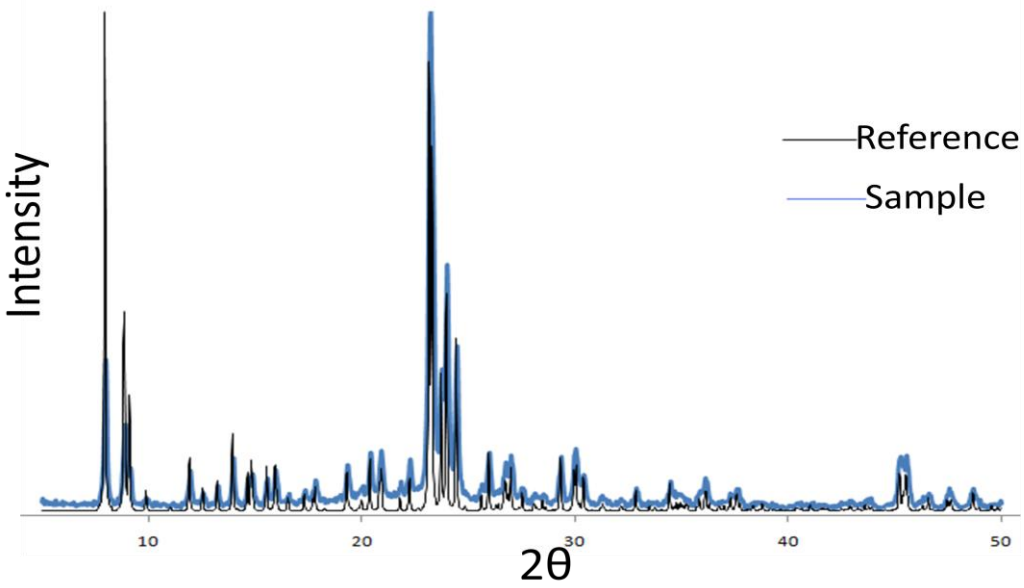

Figure 78: WAXS pattern of Silicalite-1 crystals synthesized in bulk solution

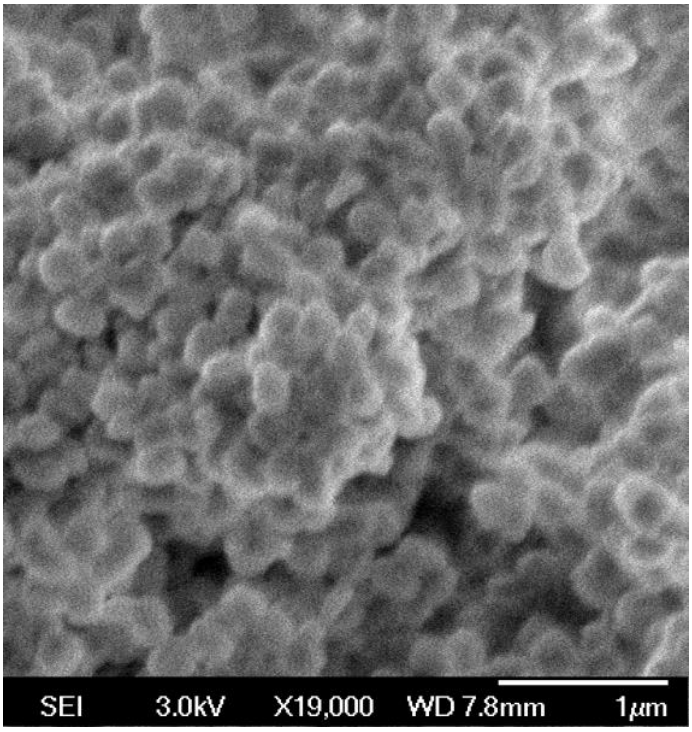

Figure 79: Silicalite-1 crystals synthesized in bulk solution at 100^{o}C for 18 hours

4.2.3 Preliminary results of confined synthesis in LPE by solvothermal method

The synthesis recipe developed at 100^{o}C was used to synthesize Silicalite-1 in a linear polyethylene monolith. The monolith was dipped in the ethanol based synthesis solution at the start of the reaction. After the reaction was completed, the monolith was recovered, washed with ethanol and DI water and then its surface and cross section were viewed by SEM and TEM. Large Silicalite-1 crystals are seen on the surface of the monolith. On viewing the microtomed cross section of the monolith after zeolite synthesis, templated crystals can be seen inside the pores. This data has been presented below as preliminary evidence for confined synthesis by a solvothermal method.

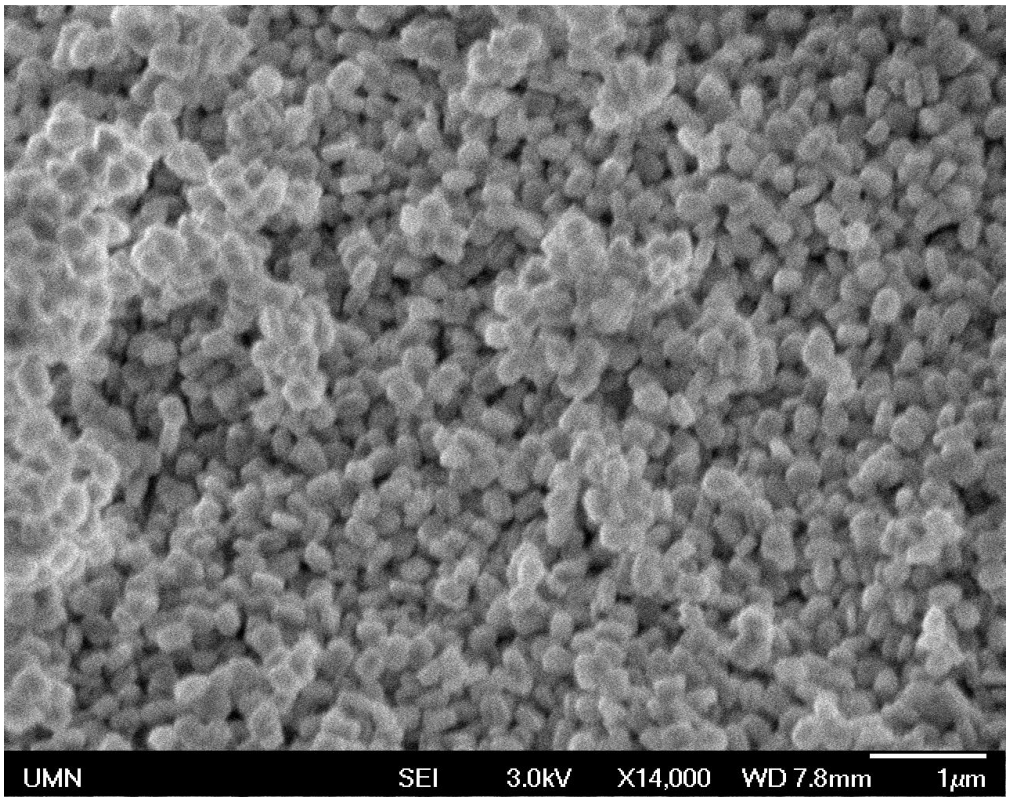

Figure 80: Silicalite-1 crystals synthesized in bulk solution

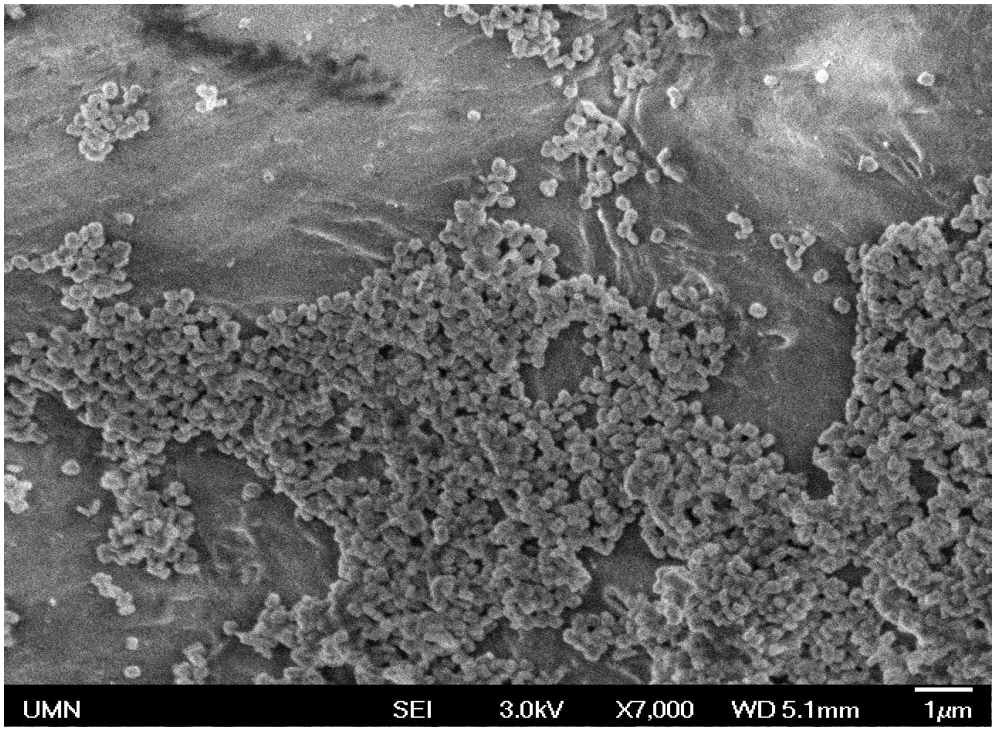

Figure 81: Silicalite-1 crystals on surface of polymer monolith

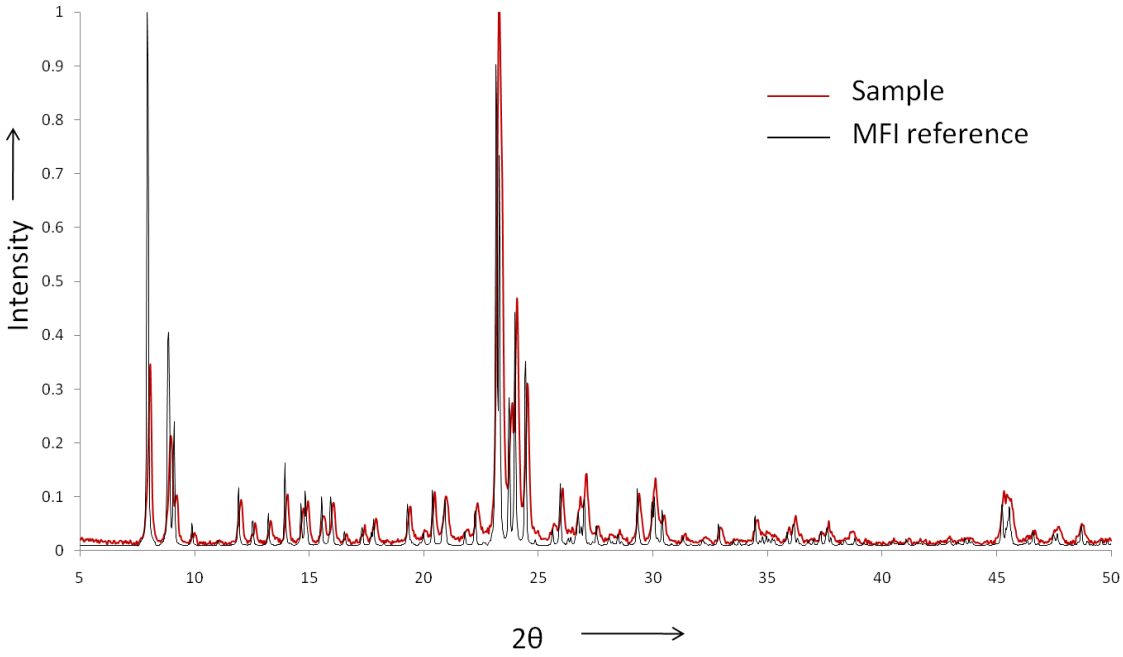

Figure 82: WAXS pattern of Silicalite-1 crystals synthesized in bulk solution

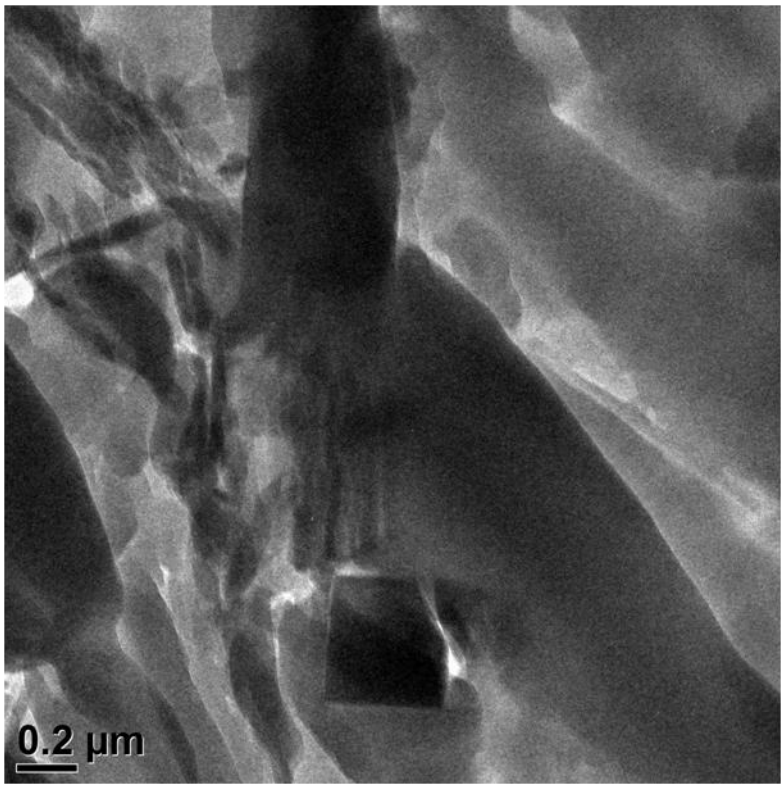

Figure 83: TEM image of microtomed monolith after zeolite synthesis showing confined growth of crystals in pores

(a)

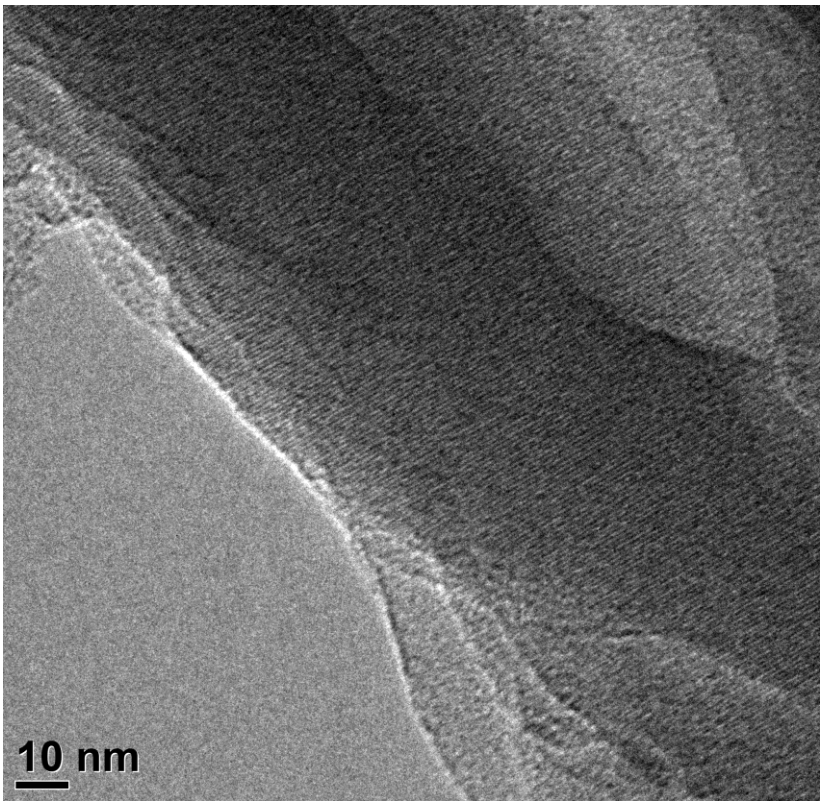

(b)

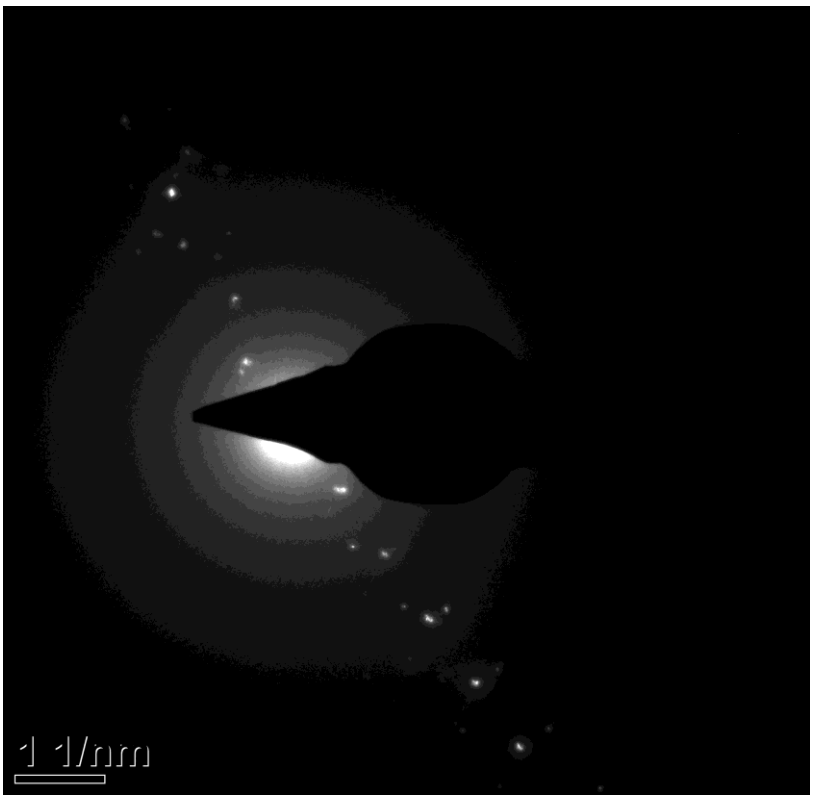

Figure 84: (a) Confined growth of Silicalite-1 inside LPE pore and (b) Corresponding electron diffraction pattern

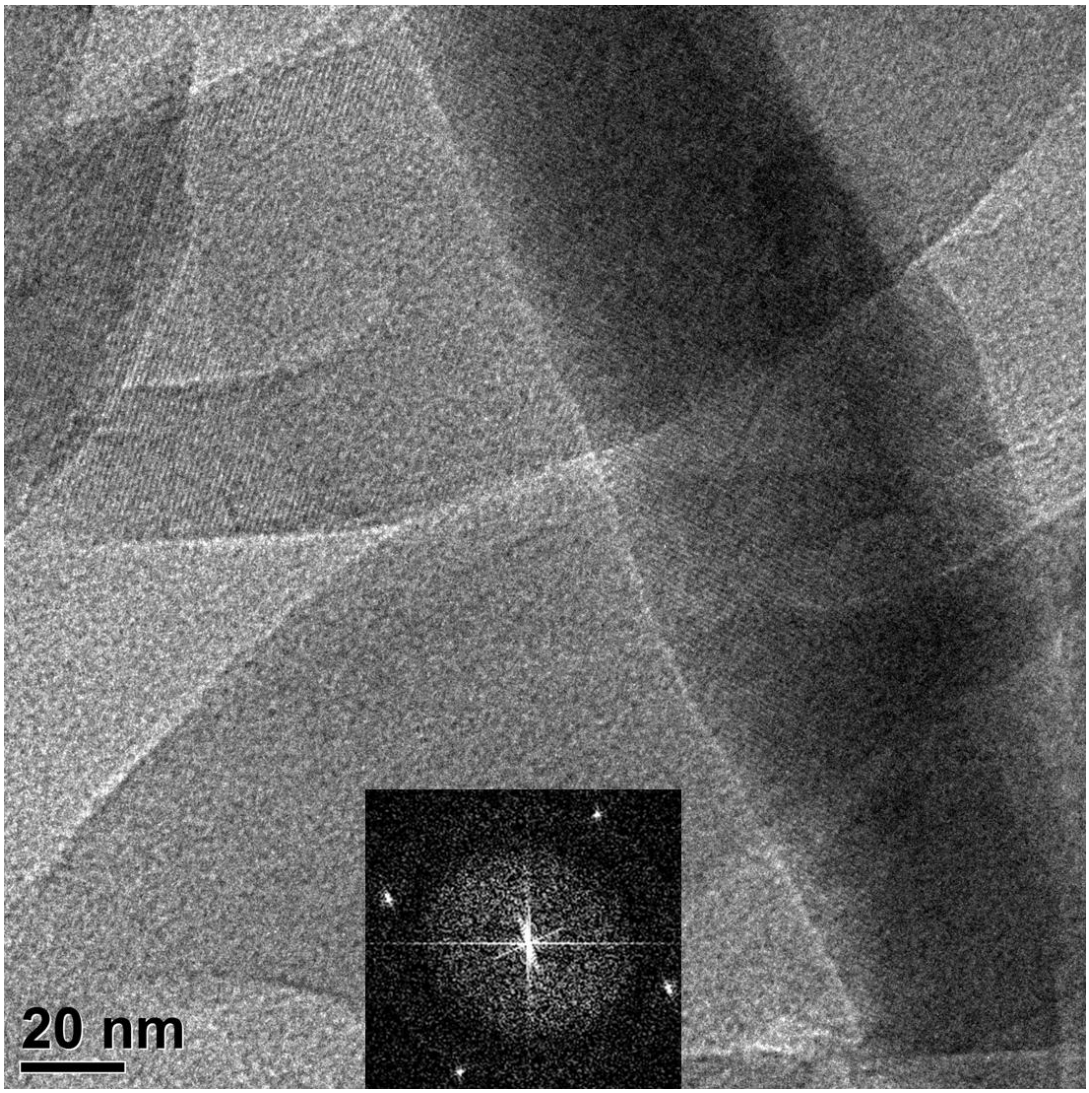

Figure 85: Lattice fringes of Silicalite-1 crystal grown inside LPE pore and (inset) corresponding fourier transform showing spots from the crystal

4.3 Conclusions

The results presented in this chapter provide preliminary evidence that it is possible to carry out confined synthesis of Silicalite-1 inside LPE by solvothermal synthesis based in an ethanol medium. It would be worthwhile to explore this in further detail, explore other organic solvents, other polymer templates, use other recipes and try

to grow different zeolites to convert this into a generic method for confined synthesis of zeolites in polymers.

5. Conclusions and Future Work

It has been successfully demonstrated for the first time that it is possible to synthesize zeolite (specifically, Silicalite-1) by a templating method using nanoporous polymers. Further, it has been shown that that mesoporous zeolite with disordered mesopores can be synthesized. The mesoporosity is controllable by changing the molecular weights and volume fractions of the original triblock copolymer from which the linear polyethylene template is derived. Other zeolite frameworks can also potentially be grown in LPE, for example Zeolite Beta, Zeolite A, etc. Mesoporous zeolites thus synthesized can be tested for catalytic activity for appropriate chemical reactions.

One of the highlights of this work is the discovery that the thermal stability of the template plays a very important role in successful templating of zeolite crystals within its nanopores. The synthesis temperature needs to be significantly below the melting temperature of the polymer template (at least thirty degrees less), which was not obvious earlier.

Another scientific contribution of this work is the discovery that polymer (PCHE) films are capable of nucleating a thin zeolite sub-monolayer on their surface in zeolite synthesis solutions. It would be worthwhile to investigate this phenomenon in more detail because it can be useful for creating seed layers of zeolites for membranes. Different polymers and zeolites can be explored.

Solvothermal synthesis methods can also be explored because they provide a convenient alternative route to confined synthesis in various templates. Recipes for

growing zeolites in different organic solvents can be developed. Solvothermal methods can also be used to grow other zeotypes like Metal Organic Frameworks (MOFs). Mesoporous MOFs could potentially be useful for catalysis.

REFERENCES

1. Pérez-Ramírez, J., Christensen, C.H., Egeblad, K., Christensen, C.H. & Groen, J.C. Hierarchical zeolites: enhanced utilisation of microporous crystals in catalysis by advances in materials design. *Chem. Soc. Rev.* **37**, 2530 (2008).
2. Kärger, J. & Freude, D. Mass Transfer in Micro- and Mesoporous Materials. *Chem. Eng. Technol.* **25**, 769 (2002).
3. Egeblad, K., Christensen, C.H., Kustova, M. & Christensen, C.H. Templating Mesoporous Zeolites. *Chem. Mater.* **20**, 946-960 (2008).
4. Janssen, A.H., Koster, A.J. & de Jong, K.P. Three-Dimensional Transmission Electron Microscopic Observations of Mesopores in Dealuminated Zeolite Y. *Angew. Chem. Int. Ed.* **40**, 1102-1104 (2001).
5. Jacobsen, C.J.H., Madsen, C., Houzvicka, J., Schmidt, I. & Carlsson, A. Mesoporous Zeolite Single Crystals. *J. Am. Chem. Soc.* **122**, 7116-7117 (2000).
6. Groen, J.C., Peffer, L.A.A., Moulijn, J.A. & Pérez-Ram\'ırez, J. On the introduction of intracrystalline mesoporosity in zeolites upon desilication in alkaline medium. *Microporous and Mesoporous Materials* **69**, 29–34 (2004).
7. Xiao, F. et al. Catalytic Properties of Hierarchical Mesoporous Zeolites Templated with a Mixture of Small Organic Ammonium Salts and Mesoscale Cationic Polymers. *Angew. Chem. Int. Ed.* **45**, 3090-3093 (2006).
8. Perez-Ramırez, J., Christensen, C.H., Egeblad, K., Christensend, C.H. & Groenef, J.C. Hierarchical zeolites: enhanced utilisation of microporous crystals in catalysis by advances in materials design. *Chem. Soc. Rev* **37**, 2530–2542 (2008).
9. Davis, M.E. Ordered porous materials for emerging applications. *Nature* **417**, 813-821 (2002).
10. Bein, T. Synthesis and Applications of Molecular Sieve Layers and Membranes. *Chem. Mater.* **8**, 1636-1653 (1996).
11. Kondo, M. Tubular-type pervaporation module with zeolite NaA membrane. *Journal of Membrane Science* **133**, 133-141 (1997).
12. Tosheva, L. & Valtchev, V.P. Nanozeolites: Synthesis, Crystallization Mechanism, and Applications. *Chem. Mater.* **17**, 2494-2513 (2005).
13. Fan, W. et al. Hierarchical nanofabrication of microporous crystals with ordered mesoporosity. *Nat Mater* **7**, 984-991 (2008).
14. Yoo, W. et al. Nanoscale Reactor Engineering: Hydrothermal Synthesis of Uniform Zeolite Particles in Massively Parallel Reaction Chambers. *Angew. Chem.* **120**, 9236-9239 (2008).
15. Budd, P.M. et al. Polymers of intrinsic microporosity (PIMs): robust, solution-processable, organic nanoporous materials. *Chem. Commun.* 230 (2004).doi:10.1039/b311764b
16. Meynen, V., Cool, P. & Vansant, E.F. Verified syntheses of mesoporous materials. *Microporous and Mesoporous Materials* **125**, 170-223 (2009).
17. Li, Q., Restch, M., Wang, J., Knoll, W. & Jonas, U. Porous Networks Through Colloidal Templates. *Templates in Chemistry III* Volume **287** (2009).
18. Stein, A., Li, F. & Denny, N.R. Morphological Control in Colloidal Crystal Templating of Inverse Opals, Hierarchical Structures, and Shaped Particles. *Chem. Mater.* **20**, 649-666 (2008).
19. Budd, P.M. et al. Polymers of intrinsic microporosity (PIMs): robust, solution-processable, organic nanoporous materials. *Chem. Commun.* 230 (2004).doi:10.1039/b311764b
20. Olson, D.A., Chen, L. & Hillmyer, M.A. Templating Nanoporous Polymers with Ordered Block Copolymers. *Chem. Mater.* **20**, 869-890 (2008).
21. Ndoni, S., Vigild, M.E. & Berg, R.H. Nanoporous Materials with Spherical and Gyroid Cavities Created by Quantitative Etching of Polydimethylsiloxane in

Polystyrene−Polydimethylsiloxane Block Copolymers. *J. Am. Chem. Soc.* **125**, 13366-13367 (2003).
22. Tao, Y., Kanoh, H. & Kaneko, K. Synthesis of Mesoporous Zeolite A by Resorcinol−Formaldehyde Aerogel Templating. *Langmuir* **21**, 504-507 (2005).
23. Lai, Z., Bonilla, G., Diaz, I., Nery, J.G. & Sujaoti, K. Microstructural Optimization of a Zeolite Membrane for Organic Vapor Separation. *Science* **300**, 456-460 (2003).
24. Choi, J., Ghosh, S., Lai, Z. & Tsapatsis, M. Uniformly a-Oriented MFI Zeolite Films by Secondary Growth. *Angew. Chem.* **118**, 1172-1176 (2006).
25. Wang, H., Holmberg, B.A. & Yan, Y. Synthesis of Template-Free Zeolite Nanocrystals by Using in Situ Thermoreversible Polymer Hydrogels. *J. Am. Chem. Soc.* **125**, 9928-9929 (2003).
26. Jansen, J. & Vanrosmalen, G. Oriented growth of silica molecular sieve crystals as supported films. *Journal of Crystal Growth* **128**, 1150-1156 (1993).
27. Castro, L.B.R., Almeida, A.T. & Petri, D.F.S. The Effect of Water or Salt Solution on Thin Hydrophobic Films. *Langmuir* **20**, 7610-7615 (2004).
28. Stober, W. Controlled growth of monodisperse silica spheres in the micron size range. *Journal of Colloid and Interface Science* **26**, 62-69 (1968).
29. Chen, L., Phillip, W.A., Cussler, E.L. & Hillmyer, M.A. Robust Nanoporous Membranes Templated by a Doubly Reactive Block Copolymer. *J. Am. Chem. Soc* **129**, 13786–13787 (2007).
30. Schmidt, I., Madsen, C. & Jacobsen, C.J.H. Confined Space Synthesis. A Novel Route to Nanosized Zeolites. *Inorg. Chem.* **39**, 2279-2283 (2000).
31. Mao, H. & Hillmyer, M.A. Nanoporous Polystyrene by Chemical Etching of Poly(ethylene oxide) from Ordered Block Copolymers. *Macromolecules* **38**, 4038-4039 (2005).
32. Zalusky, A.S., Olayo-Valles, R., Wolf, J.H. & Hillmyer, M.A. Ordered Nanoporous Polymers from Polystyrene−Polylactide Block Copolymers. *J. Am. Chem. Soc.* **124**, 12761-12773 (2002).
33. Zalusky, A.S., Olayo-Valles, R., Wolf, J.H. & Hillmyer, M.A. Ordered Nanoporous Polymers from Polystyrene−Polylactide Block Copolymers. *J. Am. Chem. Soc.* **124**, 12761-12773 (2002).
34. Rzayev, J. & Hillmyer, M.A. Nanochannel Array Plastics with Tailored Surface Chemistry. *J. Am. Chem. Soc.* **127**, 13373-13379 (2005).
35. Cochran, E.W., Garcia-Cervera, C.J. & Fredrickson, G.H. Stability of the Gyroid Phase in Diblock Copolymers at Strong Segregation. *Macromolecules* **39**, 2449-2451 (2006).
36. Matsen, M.W. & Bates, F.S. Origins of Complex Self-Assembly in Block Copolymers. *Macromolecules* **29**, 7641-7644 (1996).
37. Burban, J.H., He, M. & Cussler, E.L. Silica gels made by bicontinuous microemulsion polymerization. *AIChE J.* **41**, 159-165 (1995).
38. Burban, J.H., He, M. & Cussler, E.L. Organic microporous materials made by bicontinuous microemulsion polymerization. *AIChE J.* **41**, 907-914 (1995).
39. Zhou, N., Bates, F.S. & Lodge, T.P. Mesoporous Membrane Templated by a Polymeric Bicontinuous Microemulsion. *Nano Lett.* **6**, 2354-2357 (2006).
40. Jones, B.H. & Lodge, T.P. Nanoporous Materials Derived from Polymeric Bicontinuous Microemulsions. *Chem. Mater.*
41. Pitet, L.M., Amendt, M.A. & Hillmyer, M.A. Nanoporous Linear Polyethylene from a Block Polymer Precursor. *J. Am. Chem. Soc.* **132**, 8230-8231 (2010).

6. APPENDIX

A.1 Ellipsometry data

All PCHE thin films were made with 1, 2 or 3 drops 12k PCHE at 2000 rpm spin speed. The system was modeled as a silica layer about 250 nm thick and a PCHE thin film described by the Cauchy Model (for polymers). Characterization results have been summarized below.

1. 1 Drop PCHE

Sample 1a: Thickness=67.007 ± 6.18 nm, SiO2 thickness=237.96 ± 6.24, MSE= 4.412

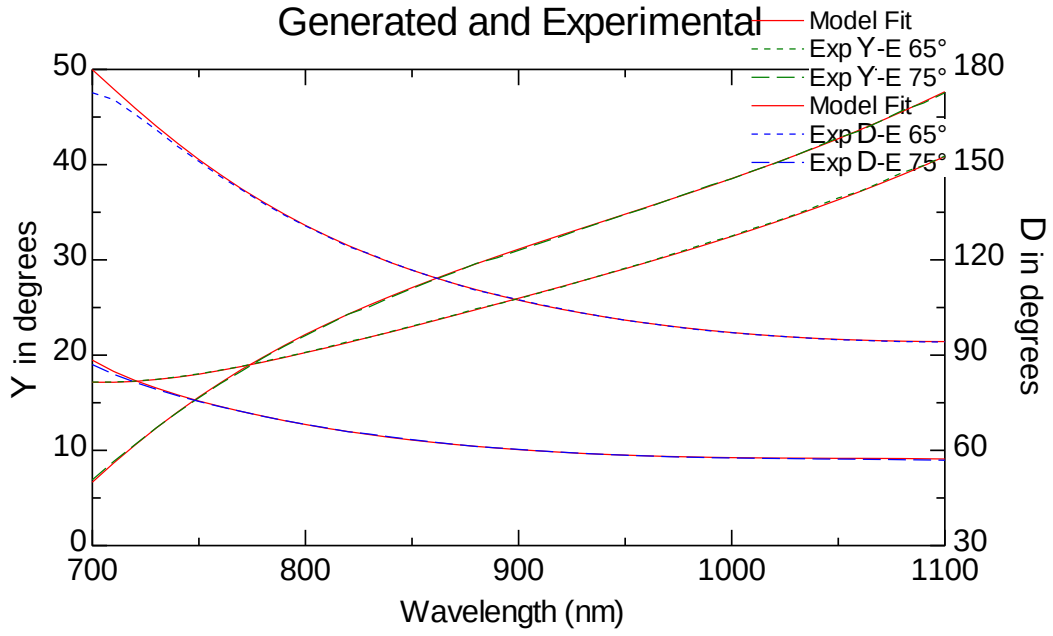

Figure A1.1

Sample 1b: Thickness=59.872 ± 5.09, SiO2 thickness=246.204 ± 5.12, MSE= 4.225

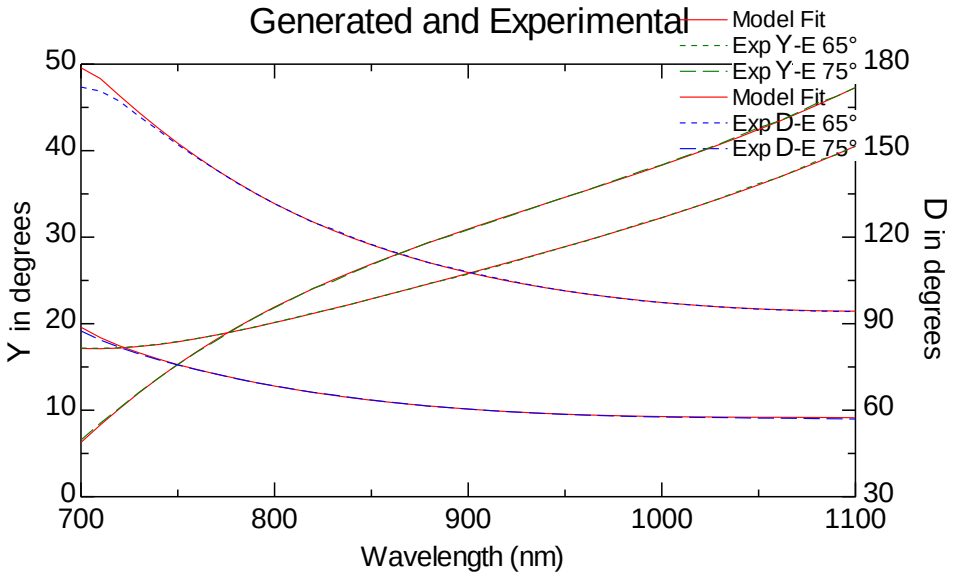

Figure A1.2

Sample 1c: Thickness=62.925 ± 6.37 nm, SiO2 thickness=241.812 ± 6.43, MSE= 3.903

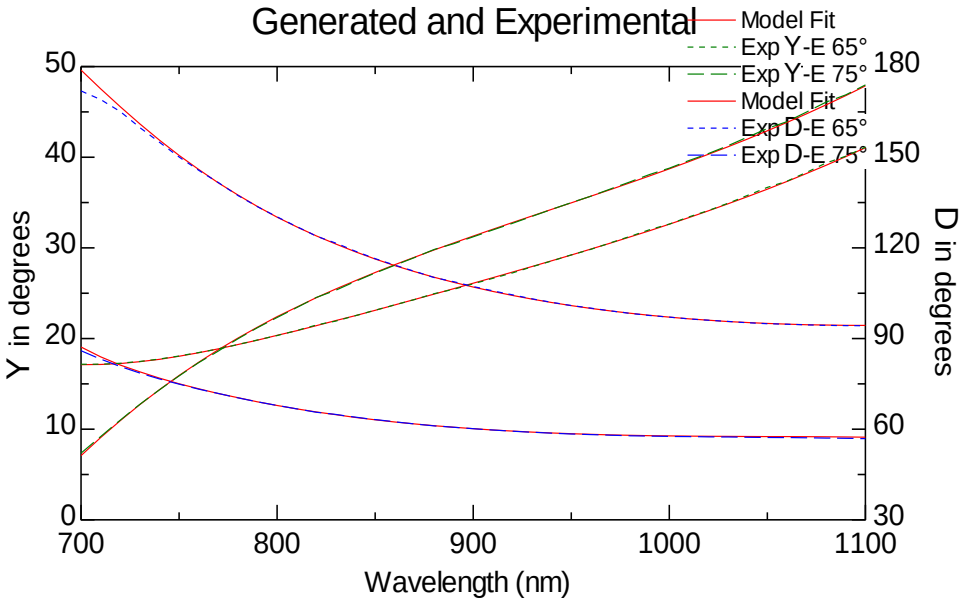

Figure A1.3

2. 2 Drops PCHE

Sample 2a: Thickness=68.068 ± 6.18 nm, SiO2 thickness=240, MSE= 10.07

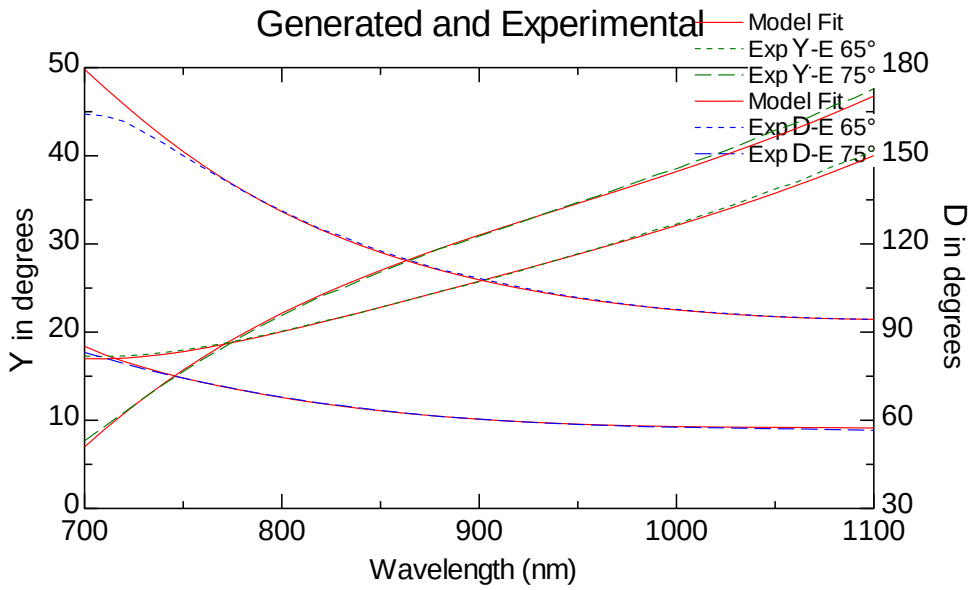

Figure A1.4

Sample 2b: Thickness=2.702 ± 1.04 , SiO2 thickness=307.861 ± 0.809, MSE=7.234

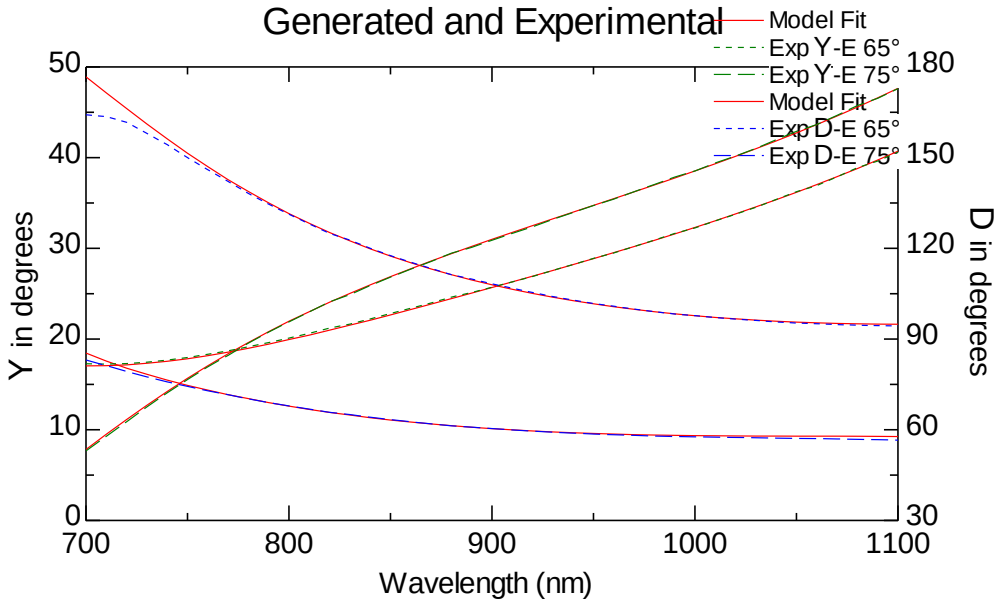

Figure A1.5

Sample 2c: Thickness=55.105 ± 5.83 , SiO2 thickness=247.534 ± 5.92,

MSE=4.418

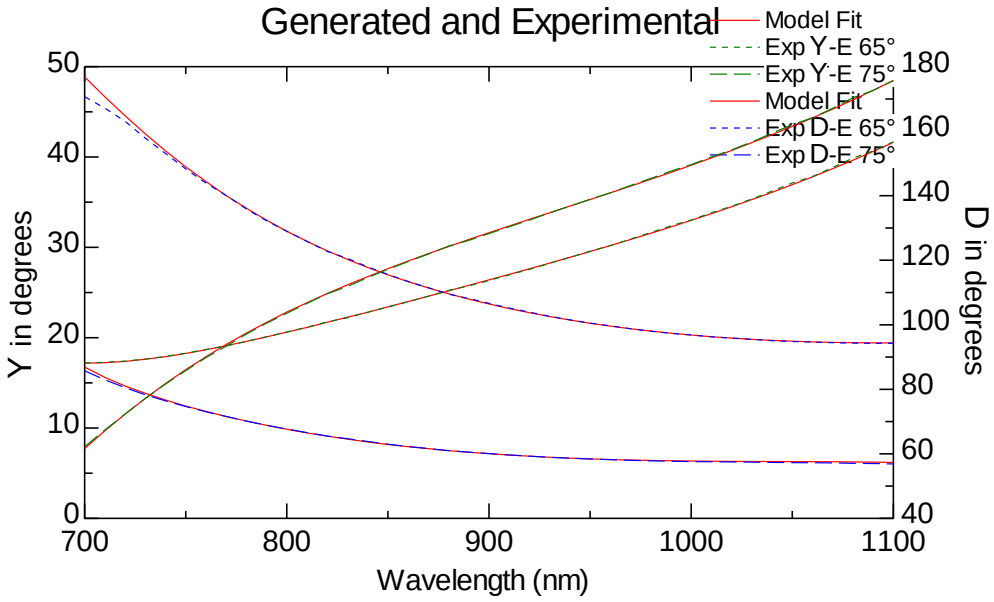

Figure A1.6

3. 3 drops PCHE:

Sample 1: Thickness=74.803 ± 1.26 , SiO2 thickness=240, MSE=15.18

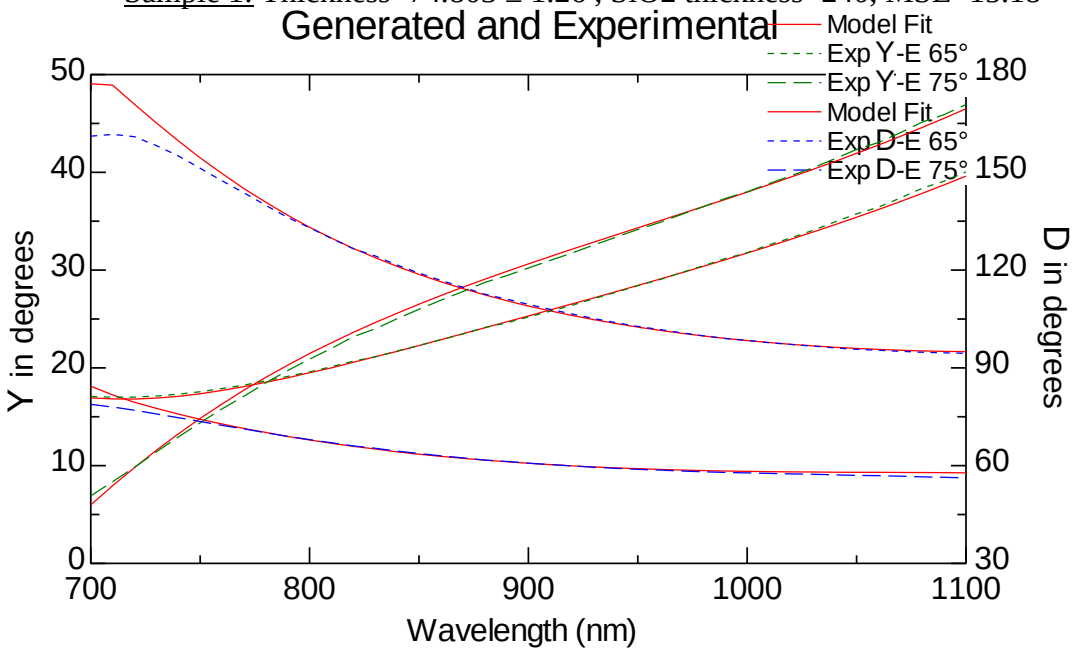

Figure A1.7

A.2 Demonstration of confined synthesis of Silicalite-1 in 3DOm Carbon

3DOm Carbon (Three dimensionally oriented mesoporous carbon) is a bicontinuous mesoporous matrix that has been used for the confined synthesis of zeolite (specifically, Silicalite-1) in the past. In literature, confined synthesis of Silicalite-1 in 3DOm Carbon has been done by an incipient wetness technique. The composition of the impregnated synthesis gel was 9 TPA_2O/50 SiO_2/390 H_2O/180 ethanol. The same method was followed and the protocol and results have been summarized (See figure A2.1).

Synthesis Protocol:

1. Overnight drying of weighed amount of 3DOm Carbon (synthesized by Dr. Wei Fan) in a glass vial at 150 ^oC. This is done to remove moisture from the pores.
2. Impregnation of Carbon with calculated volume of Structure Directing Agent (TPAOH) solution (Ethanol + DI water + Tetrapropylammonium hydroxide or TPAOH) equaling pore volume, followed by thorough mixing to ensure uniform distribution of solution throughout the pores.
3. Evaporation of EtOH overnight, freeing up about 50% of the pore volume.
4. Impregnation of Carbon with calculated amount of TeOS (just enough to fill pores again) which is followed by hydrolysis of TeOS at room temperature for about 3 hours.
5. Synthesis of zeolite by steaming (while avoiding direct contact with water) at 135 ^oC.
6. Calcination of the carbon template to yield pure Silicalite-1.

7. Washing of zeolite with DI water followed by filtration.

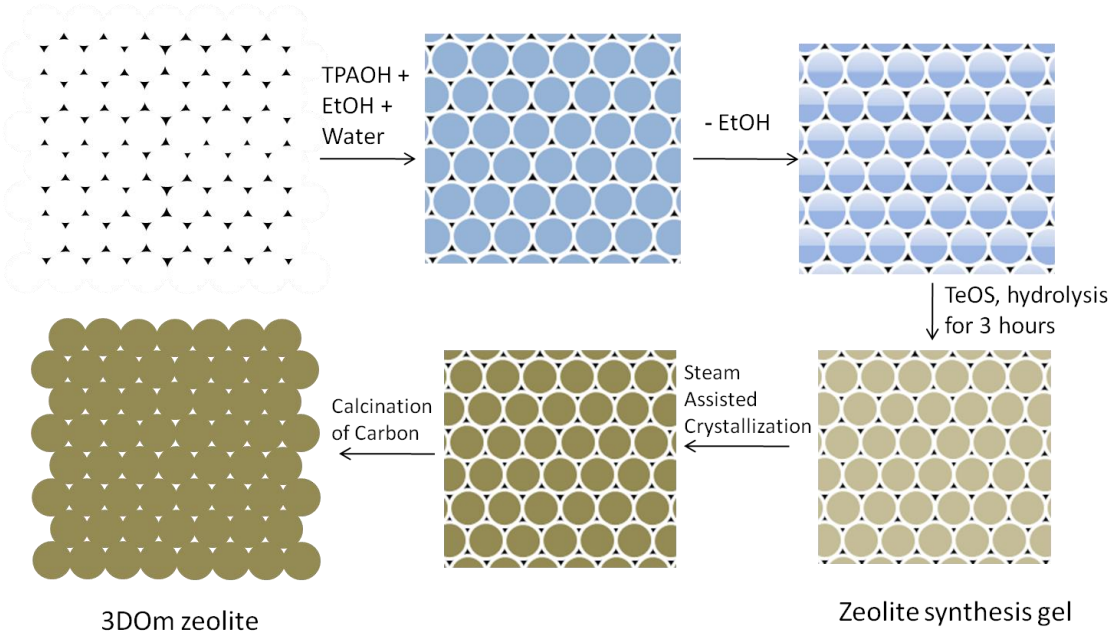

Figure A2.1: Schematic for confined synthesis of zeolite in 3DOm Carbon

Characterization Results:

The following characterizations have been performed:

1. Scanning electron microscopy (SEM) of empty 3DOm Carbon template to visualize empty cages. ~40nm cages can be seen. (Figure A2.2)
2. Small angle x-ray scattering (SAXS) on empty 3DOm Carbon template to determine long range order (FCC) of mesopores. Indexing of the peaks indeed shows an ~FCC arrangement of 3DOm cages. (Figure A2.3)
3. SEM of the 3DOm Carbon + Silicalite-1 after steam assisted crystallization (SAC) was performed. (Figure A2.4)
4. After calcination of the carbon, the 3DOm-imprinted mesoporous Silicalite-1 crystals were visualized by SEM. Large crystals, about 1 micron long, were seen.

They were comprised of ordered domains of smaller crystals, about 40 nm in size (same size as the 3DOm cages). (Figure A2.5)

5. Wide Angle X-ray Scattering (WAXS) was performed on the 3DOm imprinted Silicalite-1 powder to check that the crystals belonged to the MFI framework. This was confirmed by comparing the WAXS pattern obtained to a simulated xrd pattern of MFI (from the International Zeolite Association website). (Figure A2.6)
6. SAXS was performed on the 3DOm-imprinted Silicalite-1 to check for long range order and indeed, the peaks closely matched the empty carbon template, giving proof of templating. (Figure A2.7)
7. TEM of the 3DOm-imprinted Silicalite was done to visualize mesoporosity and to obtain electron diffraction patterns which suggested that the large crystals were single crystals. (Figure A2.8)

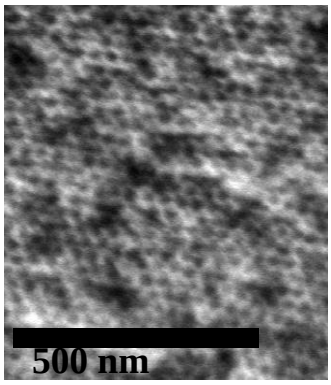

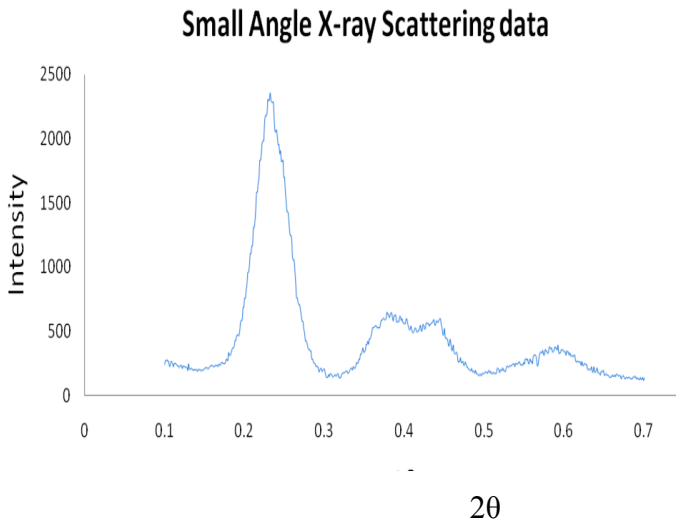

Figure A2.2: SEM of empty 3DOm Carbon template **Figure A2.3: SAXS of empty 3DOm Carbon template**

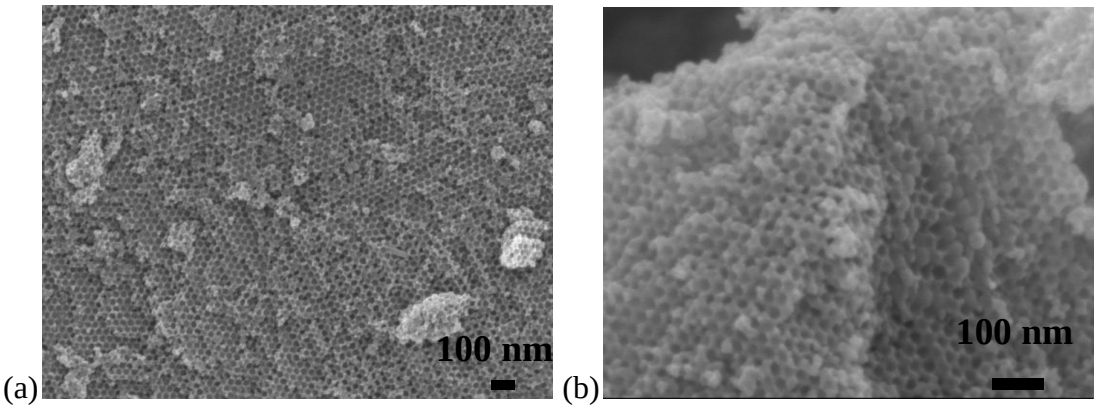

Figure A2.4:(a), (b): Silicalite-1 grown in 3DOm Carbon

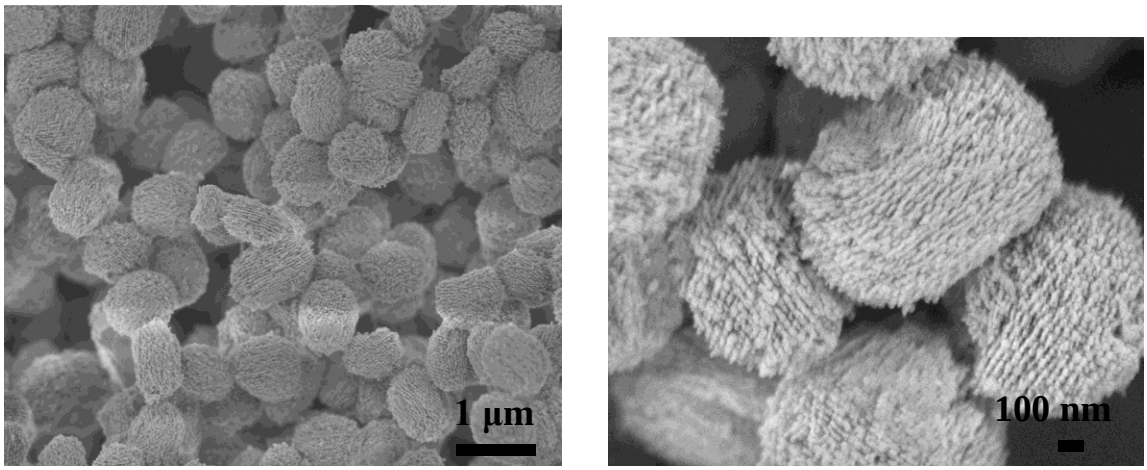

Figure A2.5: SEM of calcined Silicalite-1

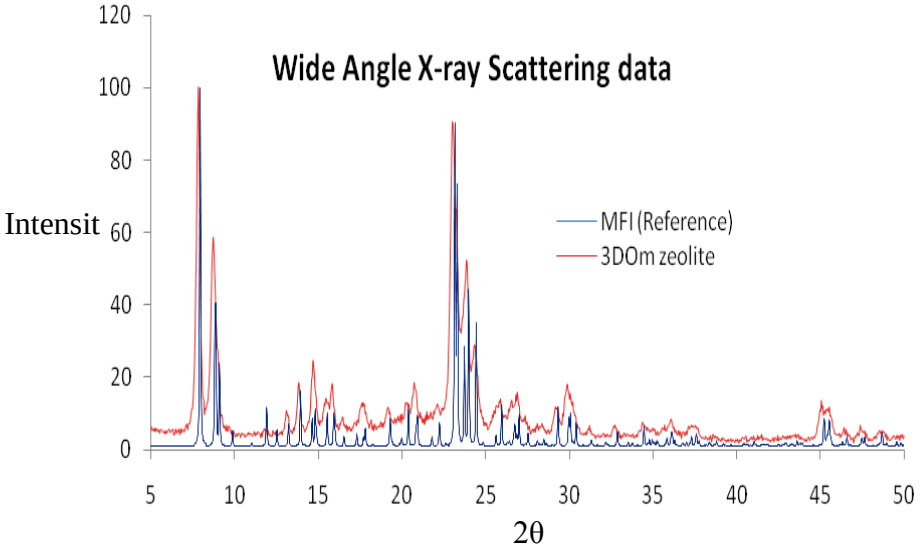

Figure A2.6: WAXS of Silicalite-1 powder compared with a reference (simulated) pattern

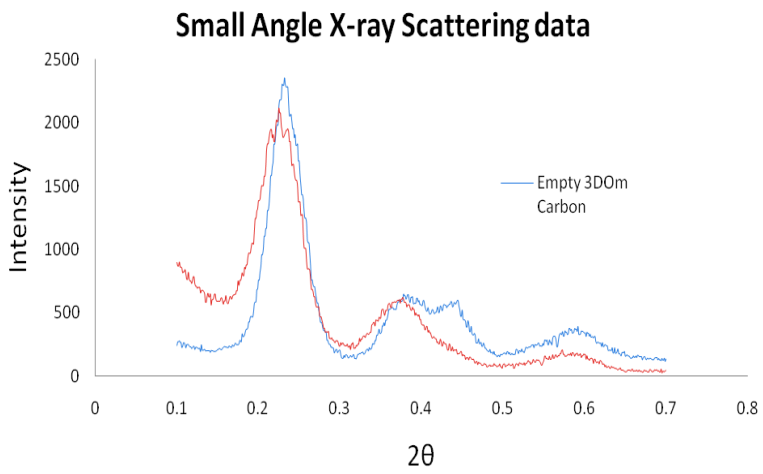

Figure A2.7: SAXS of Silicalite-1 powder compared with empty 3DOm template

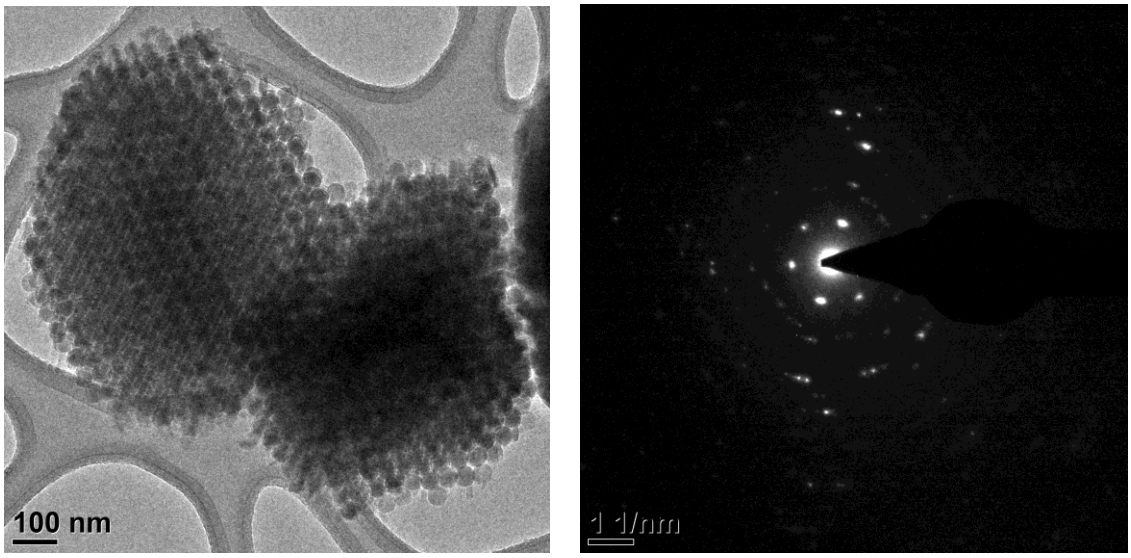

Figure A2.8: TEM image of 3DOm imprinted Silicalite-1 along with electron diffraction pattern corresponding to b-oriented MFI. (Imaging by Xueyi Zhang)

Conclusions:

From the data presented above, one can conclude that 40nm 3DOm imprinted Silicalite-1 has successfully been templated from 3DOm Carbon. Characterizations show that long range order has been preserved in Silicalite-1 as expected. Thus, steam assisted crystallization has successfully been implemented in 3DOm Carbon.